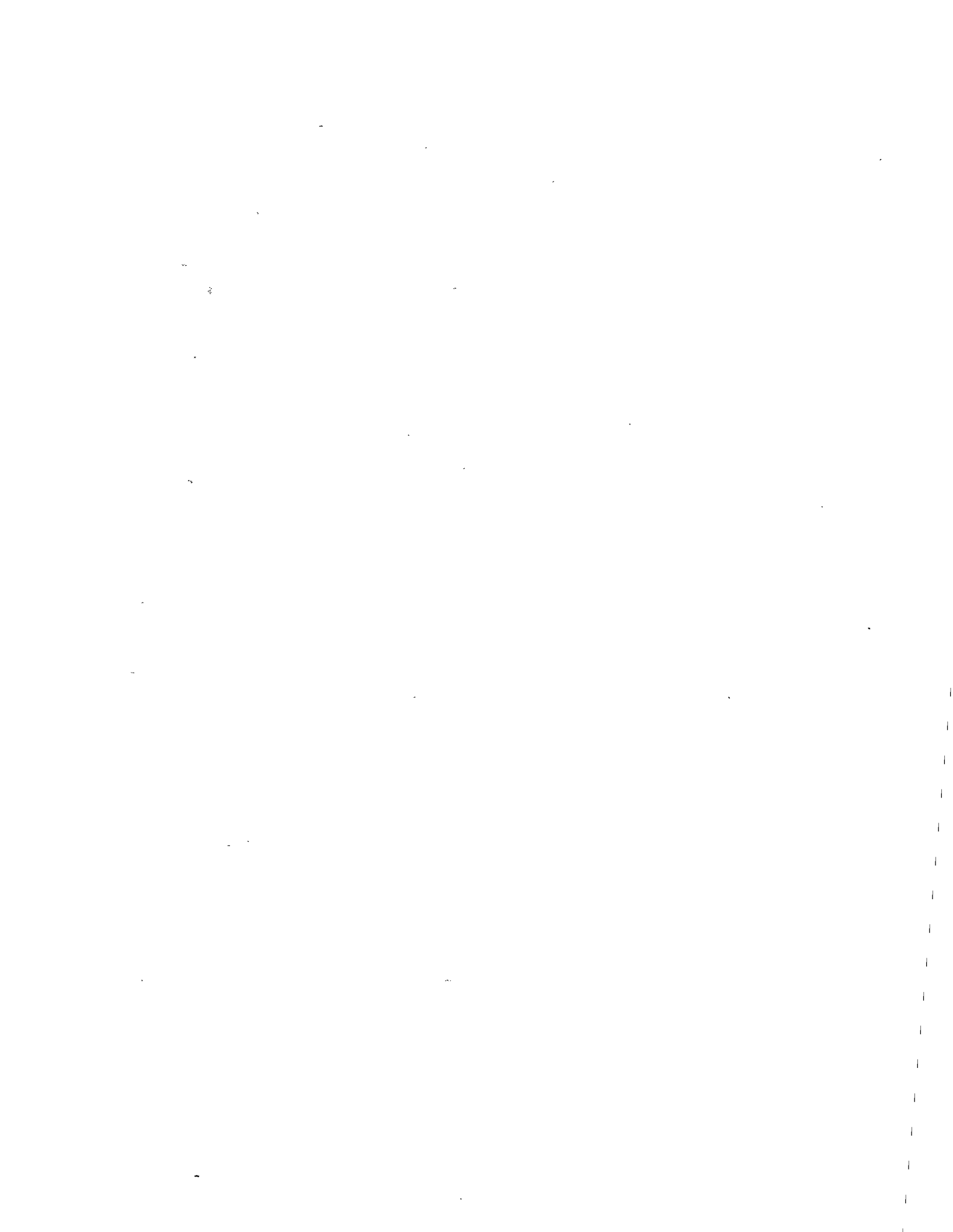


1. Report No. FHWA/TX-82/19+284-3	2. Government Accession No.	3. Recipient's Catalog No.	
4. Title and Subtitle Layer Equivalency Factors and Deformation Characteristics of Flexible Pavements		5. Report Date January 1982	
		6. Performing Organization Code	
7. Author(s) J. T. Hung, J-L. Briaud, and R. L. Lytton		8. Performing Organization Report No. Research Report 284-3	
9. Performing Organization Name and Address Texas Transportation Institute The Texas A&M University System College Station, Texas 77843		10. Work Unit No.	
		11. Contract or Grant No. Research Study 2-8-80-284	
12. Sponsoring Agency Name and Address State Department of Highways and Public Transportation 11th and Brazos Streets Austin, Texas 78701		13. Type of Report and Period Covered September 1979 Interim - October 1981	
		14. Sponsoring Agency Code	
15. Supplementary Notes Research performed in cooperation with DOT and FHWA Research Study Title: "Flexible Pavement Data Base and Design"			
16. Abstract In this report, a method is developed for determining the equivalent thicknesses for different base courses, which will give the same pavement life expectancy.  This study shows how the layer equivalents can be obtained from Texas Triaxial tests or from pavement pressuremeter tests or from Dynaflect tests. The procedures were developed after testing 11 pavement sections having four different types of base courses and subbase courses in the Beaumont District (District 20) in Southeastern Texas. Taking the sand and oyster shell base course as reference (layer equivalent of 1), it was found that the lime treated crushed sandstone had a layer equivalent of 0.68, the iron ore 1.17, and the select sand 1.29.  This study permitted moduli of deformation to be obtained from the pressuremeter test, the Texas Triaxial test and the Dynaflect test coupled with the Russian equation. Comparisons between the various moduli are presented. This study used the cyclic pressuremeter test to determine the stress and strain level dependency of soil moduli and permanent deformation characteristics of the layers.  This report includes the presentation of a procedure to determine the layer equivalents of base courses on the basis of Texas Triaxial tests. Examples of calculations are included.			
17. Key Words Texas Triaxial Test, Pressuremeter Test, Dynaflect Test, Base Course Layer equivalent, Flexible Pavement		18. Distribution Statement No restrictions. This document is available to the public through the National Technical Information Service, Springfield, Virginia 22161	
19. Security Classif. (of this report) Unclassified	20. Security Classif. (of this page) Unclassified	21. No. of Pages 148	22. Price



LAYER EQUIVALENCY FACTORS AND DEFORMATION  
CHARACTERISTICS OF FLEXIBLE PAVEMENTS

by

J. T. Hung, J-L. Briaud, and R. L. Lytton

Research Report Number 284-3

Flexible Pavement Data Base and Design

Research Study 2-8-80-284

conducted for

The Texas State Department of Highways and  
Public Transportation

in cooperation with the  
U. S. Department of Transportation  
Federal Highway Administration

by the

Texas Transportation Institute  
Texas A&M University  
College Station, Texas

January 1982



## ABSTRACT

In this report, a method is developed for determining the equivalent thicknesses for different base courses, which will give the same pavement life expectancy.

This study shows how the layer equivalents can be obtained from Texas Triaxial tests or from pavement pressuremeter tests or from Dynaflect tests. The procedures were developed after testing 11 pavement sections having four different types of base courses and subbase courses in the Beaumont District (District 20) in Southeastern Texas. Taking the sand and oyster shell base course as reference (layer equivalent of 1), it was found that the lime treated crushed sandstone had a layer equivalent of 0.68, the iron ore 1.17, and the select sand 1.29.

This study permitted moduli of deformation to be obtained from the pressuremeter test, the Texas Triaxial test and the Dynaflect test coupled with the Russian equation. Comparisons between the various moduli are presented. This study used the cyclic pressuremeter test to determine the stress and strain level dependency of soil moduli and permanent deformation characteristics of the layers.

This report includes the presentation of a procedure to determine the layer equivalents of base courses on the basis of Texas Triaxial tests. Examples of calculations are included.

## SUMMARY

In this report, a method is developed for determining the equivalent thicknesses of different base courses which will give the same pavement life expectancy. The method was developed from the results of a field and laboratory study carried out to determine layer equivalents of base course materials that are commonly used in the Texas Gulf coast region. The objective of the study was to develop a simple but reliable means based upon field measurements of determining the equivalent thickness of alternative candidate materials for a pavement project so that alternate bids may be taken on several locally available base course aggregates.

The report explains that there are several different types of layer equivalent that can be used, some of which are based upon pavement deflections or curvature under load and others are based upon calculated strains at critical locations in the pavement structure. Different thicknesses of two candidate materials are regarded as equivalent if they produce the same calculated value of pavement criterion, e.g., deflection, curvature, or strain.

Pavement surface deflection was selected as the criterion to be used in this study. It was found that a general version of Odemark's assumption could be used for this purpose, as given in the following equation.

$$h_1 E_1^n = h_2 E_2^n$$

Whereas Odemark assumed that  $n$  is 0.33, field measurements showed that  $n$  actually varies from 0.10 to 0.60. The layer equivalent is the number by which you multiply  $h_1$ , the thickness of one material

to get  $h_2$ , the equivalent thickness of the other material. In this case, the layer equivalent (L.E.) is

$$\text{L.E.} = \left(\frac{E_1}{E_2}\right)^n$$

where  $E_1$  and  $E_2$  are the elastic moduli of the two materials under traffic loading conditions. Odemark's  $n$ -value of 0.33 appears to be a good mean value for unstabilized base course materials.

In order to determine field values of elastic modulus of base courses, a number of measurements were carried out in the Beaumont District (District 20) on a variety of State and Farm-to-Market pavements with base courses that were composed of sand shell, iron ore gravel, lime stabilized crushed sandstone, select sand and others on subgrades that ranged from sandy to clayey. Taking the sand shell base course as reference (layer equivalent of 1), it was found that lime treated crushed sandstone had a layer equivalent of 0.68, the iron ore gravel, 1.17, and select sand, 1.29. The measurements were made with a small aperture pavement pressuremeter and with a Dynaflect. The pressuremeter measured the moduli of the layers directly and the moduli were also calculated indirectly from the measured Dynaflect basin using the Russian equations method which is described in TTI Research Report 207-7F. There was a reasonably good correspondence between the moduli that were measured by the two independent means. The study also used cyclic pressuremeter measurements to determine the stress and strain level dependency of soil moduli and permanent deformation characteristics.

A supplement to this report is Research Report 284-3a, "Layer

Equivalency Factors and Deformation Characteristics of Flexible Pavements Test Data." It contains the collection of graphs of the pressure-meter test and the corresponding regression curves for the hyperbolic stress strain model performed during the course of the study reported in this report.

Cores were taken of the materials in each layer and standard tests were made on them to determine Atterberg limits, water contents, and gradation. Texas Triaxial test data on each of the materials were obtained from the District laboratory.

Correlations were found between the elastic moduli that were measured in the field and the laboratory test data. These correlations, which involve Texas Triaxial test data, Atterberg limits, water content, and gradation are the basis of the new layer equivalent method that is proposed in this report.

The modulus of the material in the field is stiffer than the secant modulus measured in the Texas Triaxial test and the ratio between the two depends upon the plasticity, water content, and gradation of the base course material. The ratio,  $f$ , is given by

$$f = 22.08 C_u^{0.689} I_p^{-1.632} w^{-0.282},$$

where  $w$  = water content, percent,  
 $I_p$  = plasticity index, and  
 $C_u$  = uniformity coefficient.

The method of determining layer equivalents permits them to be calculated from laboratory test data with the assurance that they are based upon the actual moduli of the materials as they exist in the field.

The report gives the details of a procedure for determining layer equivalents based on Texas Triaxial tests and shows several example calculations.

## IMPLEMENTATION STATEMENT

This report gives the details of a method of determining equivalency factors of base courses which should be immediately applicable to design practice in the State of Texas. This procedure does not require the development of new equipment or new materials since it uses a test and equipment which are available in the various district laboratories

However, because the findings and the proposed procedure are based on a limited amount of information, it would be advisable to delay writing a standard until the procedure has been used by the SDHPT on actual projects, and thus verified in practice.

## ACKNOWLEDGEMENTS

The authors are grateful for the help provided by the following people:

Mr. Chester H. Michalak of the Texas Transportation Institute for his assistance in the computer analysis of the test data.

Mr. Franklin Young and the District 20 Personnel of the Texas State Department of Highways and Public Transportation for their most cooperative assistance with the field data.

Mr. Robert Mikulin of the Texas State Department of Highways and Public Transportation for his continued support and encouragement.

## DISCLAIMER

The contents of this report reflect the views of the authors who are responsible for the facts and the accuracy of the data presented within. The contents do not necessarily reflect the official views or policies of the Federal Highway Administration. This report does not constitute a standard, a specification, or regulation.

## TABLE OF CONTENTS

	Page
INTRODUCTION . . . . .	1
Objectives . . . . .	1
Research Plan . . . . .	1
Organization of the Report . . . . .	2
BACKGROUND . . . . .	4
Equivalency Factors . . . . .	4
The Pavement Pressuremeter Test . . . . .	7
Other Tests . . . . .	11
Russian Equation . . . . .	18
THE TEST PROGRAM . . . . .	26
The Test Site and The Soils . . . . .	26
Pavement Pressuremeter Test . . . . .	26
The Dynaflect Test . . . . .	43
Penetration Test as a Reference . . . . .	43
The Texas Triaxial Test . . . . .	46
ANALYSIS OF THE RESULTS . . . . .	47
The Pressuremeter Tests . . . . .	47
The Texas Triaxial Test Modulus . . . . .	62
Dynaflect Modulus . . . . .	69
Correlations and Analysis . . . . .	70
The Equivalency Factors . . . . .	81
New Standard Procedure for Cyclic Pressuremeter Test . . . . .	89

TABLE OF CONTENTS (Continued)

	Page
PROCEDURE FOR DETERMINING THE EQUIVALENCY FACTOR . . . . .	91
Determination of In-Situ Modulus from Texas Triaxial Test Modulus . . . . .	91
Determination of the Equivalency Factor . . . . .	93
Examples . . . . .	94
CONCLUSIONS AND RECOMMENDATIONS . . . . .	97
APPENDIX I. - REFERENCES . . . . .	100
APPENDIX II. - NOTATION . . . . .	102
APPENDIX III. - CALIBRATION CURVES FOR PRESSUREMETER TESTS . . . .	108
APPENDIX IV. - MEASURED DEFLECTIONS FROM DYNAFLECT TEST . . . . .	113
APPENDIX V. - THE CALCULATED RESULTS OF THE PRESSUREMETER TEST DATA . . . . .	118
APPENDIX VI. - TEXAS TRIAXIAL TEST DATA . . . . .	130

## LIST OF TABLES

Table		Page
1	Profiles of Test Sections and Test Data . . . . .	27
2	The Moduli and Index Properties of Soils . . . . .	38
3	The Corrected Strain Values for Pressure- meter Test . . . . .	52
4	Parameters (Zero Strain Moduli) of Mem- brane Resistance . . . . .	57
5	Parameters (Zero Strain Moduli) of Volume Losses . . . . .	58
6	List of Exponents n . . . . .	70
7	Iterated Moduli of Dynaflect/Russian Equation . . . . .	71
8	Equivalency Factors . . . . .	84

## LIST OF FIGURES

Figure		Page
1	Definition of Equivalency Factor . . . . .	5
2	Pavement Pressuremeter . . . . .	8
3	Pressuremeter Test Curve and Corrections . . . . .	10
4	Sensor Array of the Dynaflect Test . . . . .	12
5	Deflection Basin of Pavement under Dynamic Load . . . . .	12
6	Stress versus Strain Chart . . . . .	14
7	Mohr's Diagram of Texas Triaxial Test . . . . .	15
8	Texas Classification of Subgrade and Flexible Base Materials . . . . .	16
9	Vlasov Model Subjected to a Distributed Load . . . . .	21
10	Vlasov Model Subjected to a Rigid Circular Plate . . . . .	21
11	Testing Layout of Dynaflect, Pressuremeter, and Sampling . . . . .	41
12	Pressuremeter Test Curve (a) Reload at Proper Level . . . . .	44
	(b) Reload at Improper Level . . . . .	45
13	Secant Moduli of Cycling Pressuremeter . . . . .	48
14	Model of Inelastic Modulus for Strain-Dependent Soils . . . . .	50
15	Corrections of Pressuremeter Test . . . . .	53
16	TTT Modulus Versus Confining Pressure (a) Section 1 . . . . .	63
	(b) Section 2 . . . . .	64
	(c) Section 3 . . . . .	65
	(d) Section 7 . . . . .	66
	(e) Section 9 . . . . .	67
	(f) Section 11 . . . . .	68
17	Pressuremeter Initial Modulus $E_{oi}$ Versus Pressuremeter Unloading Modulus $E_{U}$ . . . . .	74

LIST OF FIGURES (Continued)

Figure		Page
18	Pressuremeter Unloading Modulus $E_U$ Versus TTT Modulus $E_T$ . . . . .	75
19	Pressuremeter Unloading Modulus $E_U$ Versus Dynalect/Russian Equation Modulus $E_D$ . . . . .	76
20	The Calculated Deflections Versus The Measured Deflections . . . . .	78
21	The Limit Pressure $P_1$ Versus Blow Count $N$ . . . . .	79
22	Water Content $w$ Versus Pressuremeter Unloading Modulus $E_U$ . . . . .	80
23	The Limit Pressure $P_1$ Versus Texas Classification TC . . . . .	82
24	The $n_p$ Versus the $n_T$ . . . . .	83
25	Comparisons Among Three Sets of Equivalency Factors . . . . .	87
26	Soil Stress in Pavement Due to Wheel Load . . . . .	92



## INTRODUCTION

### Objectives of the Report

Escalating costs of base course material and depletion of formerly reliable sources of base course aggregate has made it desirable to establish a simple but accurate method of determining layer equivalencies. This will allow new sources of aggregate to be evaluated conveniently and reliably. The first objective of this report is to propose a method for obtaining layer equivalency factors.

There is also a critical need to update the pavement modeling of the Flexible Pavement System (FPS) and to convert it to a layered elastic modeling for 2 reasons: (1) elastic moduli can be measured in the laboratory and in the field, unlike the stiffness of coefficients that are used in the present version of FPS; (2) much of the recent research on overlay design by the U.S. Department of Transportation Federal Highway Administration (FHWA) has used elastic layered theory as a basis. The Texas State Department of Highways and Public Transportation (SDHPT) could capitalize on this work by converting FPS to a layered elastic form.

Recently, an approximate layered elastic approach, called the Russian equation, has been developed at the Texas Transportation Institute (TTI) (11). The second objective of this report is to compare the elastic moduli computed with the Russian equation with elastic moduli measured in situ with a small aperture pavement pressuremeter.

### Research Plan

The research plan for the first objective consisted of the following

steps:

1. Select 12 pavement sections in Texas having different types of base course, subbase, and subgrade.
2. At each location, perform tests from which layer modulus values can be obtained. These tests were the pavement pressuremeter and the Dynaflect.
3. Collect additional data on the sections, specifically, Texas triaxial test and cross section data from SDHPT. Also, collect soil samples for identification tests in the laboratory.
4. Calculate the various modulus values for each section and obtain the equivalency factor (E.F.) for each base course after choosing a reference base course.

The second objective of the project will be achieved within Step 4 of the first objective. Indeed, for Step 4 the moduli are calculated from (1) the pavement pressuremeter test results, (2) the Dynaflect tests using the Russian equation, and (3) the Texas triaxial test data.

#### Organization of The Report

First, the reader is provided with a background on the different topics involved in the research.

Second, the test program is described including the sites, the soil tested, and the testing procedures followed.

Third, the data reduction is explained together with the calculation of moduli and equivalency factors. Different correlations between the parameters obtained are presented and analyzed.

Fourth, a procedure for determining the equivalency factors is de-

scribed.

The conclusions and recommendations are given, including suggestions for implementation of the results and possible improvements to existing procedures.



## BACKGROUND

### Equivalency Factors

If two different base-course materials A and B are available to build a pavement, different thicknesses  $H_A$  and  $H_B$  of base course will be required for obtaining two equivalent pavement cross sections. Considering material A as the reference for all other base course materials (for example B), the ratio  $\frac{H_B}{H_A}$  is then called the equivalency factor (Fig. 1).

There are several types of layer equivalency factors (12), each of which is based on the kind of role the layer is supposed to play. However, the equivalent thicknesses which are calculated from the equivalency factors of two materials should produce either:

1. The same deflection of the pavement under a given load, or
2. The same vertical strain in the subgrade under a given load, or
3. The same horizontal strain at the bottom of the surface course under a given load, or
4. The same curvature of the surface of the pavement under a given load.

The critical strains in a pavement are the horizontal tensile strain at the bottom of the asphalt layer, the controlling criterion for fatigue cracking, and the vertical compressive strain at the surface of the subgrade, the controlling criterion for pavement surface deformation. Kuo (9) has established a series of thickness equivalency charts for the base layer of a flexible pavement based on (1) elastic layer theory, and (2) limiting strains at critical locations in the pavement. Therefore, the thickness equivalency charts developed by Kuo are based on the combination of Types 2 and 3 criteria mentioned earlier. Kuo's thickness equivalency charts cover

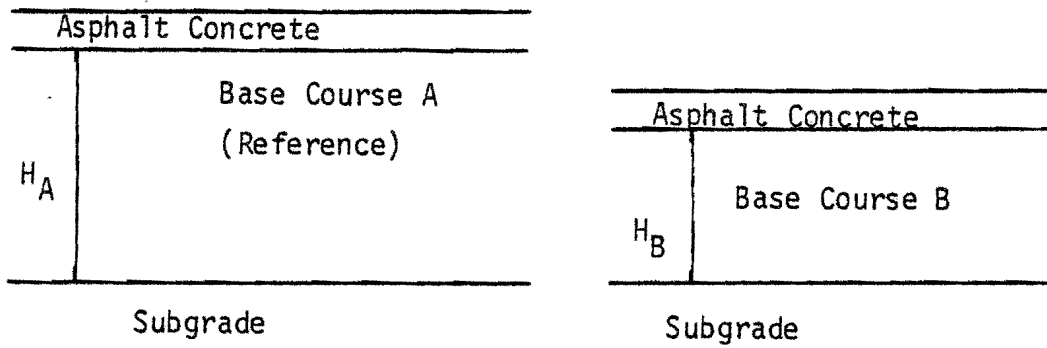


FIG. 1. — Definition of Equivalency Factor

the following cases: 2.5 in.(6.35 cm) and 4.5 in.(11.4 cm) for the thickness of the bituminous concrete, and base courses of different strengths. In the procedure, a reasonable thickness of base course is assumed and the thickness equivalency charts are used to determine the base course modulus that would be required for the chosen base course thickness to be adequate; the engineer can look for a base course which has the required modulus. If on the other hand, the base course material and its modulus are known, the thickness equivalency charts can be entered with a modulus in order to determine the base course thickness.

The equivalency factor adopted in this report is of Type 1, imposing the condition that different base course materials will produce the same deflection under load. Lytton and Michalak (11) have developed such equivalency factors by using the moduli obtained from wave propagation measurements. And by introducing Odemark's assumption, where  $n = 0.33$ , the equivalency factor, E.F., is

$$E.F. = \frac{H_B}{H_A} = \left(\frac{E_A}{E_B}\right)^n. \quad (1)$$

Therefore, only the moduli of available base course materials need to be measured in order to find E.F. values according to this assumption.

By using the Russian equation (see the section on the Russian equation in this report) and a pattern search non-linear regression analysis, Lytton and Michalak (11) calculated the value of  $n$  from measured Dynaflect deflection basins. They found that  $n$  varied from 0.087 to 0.57. The E.F., for their study, depends on (1) the modulus of the subgrade material chosen as the reference material and the modulus of the layer to be considered, and on (2) the value of the exponent  $n$ .

Kuo's charts (9) give E.F. values which range essentially between 0.33 and 3. The n values of Eq. 1 back calculated from Kuo's charts range essentially from 0.1 to 0.4. However, for certain loading conditions and modulus profiles, the n and E.F. numbers can reach extreme values.

Later Lytton (12) wrote Eq. 1 as

$$H_A E_A^{n_A} = H_B E_B^{n_B}, \quad (2)$$

with  $n_A$  and  $n_B$  varying from 0.08 to 0.57, depending on the type and thickness of base course and type of pavement. From Eq. 2, the E.F. is

$$\text{E.F.} = \frac{H_B}{H_A} = \frac{(E_A)^{n_A}}{(E_B)^{n_B}}, \quad (3)$$

and according to Lytton's research, this E.F. varies between 0.5 and 3.5. The base courses involved in the study were crushed limestone, cement-stabilized limestone, lime-stabilized limestone, and gravel.

#### The Pavement Pressuremeter Test

The pavement pressuremeter (Fig. 2) is a pressuremeter specially designed for the problem of pavement evaluation and design (1, 2, 3). The pavement pressuremeter consists of a probe, tubing, and a control unit. The expandable probe is a cylinder 9.1 in. (230 mm) long, 1.28 in. (32.5 mm) in diameter which can be inflated to a diameter of 1.56 in. (39.5 mm). The tubing through which water flows connects the control unit to the probe; this nylon tubing is 0.24 in. (6 mm) outside diameter, 0.08 in. (2 mm) inside diameter; and about 15 ft. (457.2 mm) long. The control unit is equipped with a pressure gauge, a volumeter, a hand pump and control valves in a wooden box.

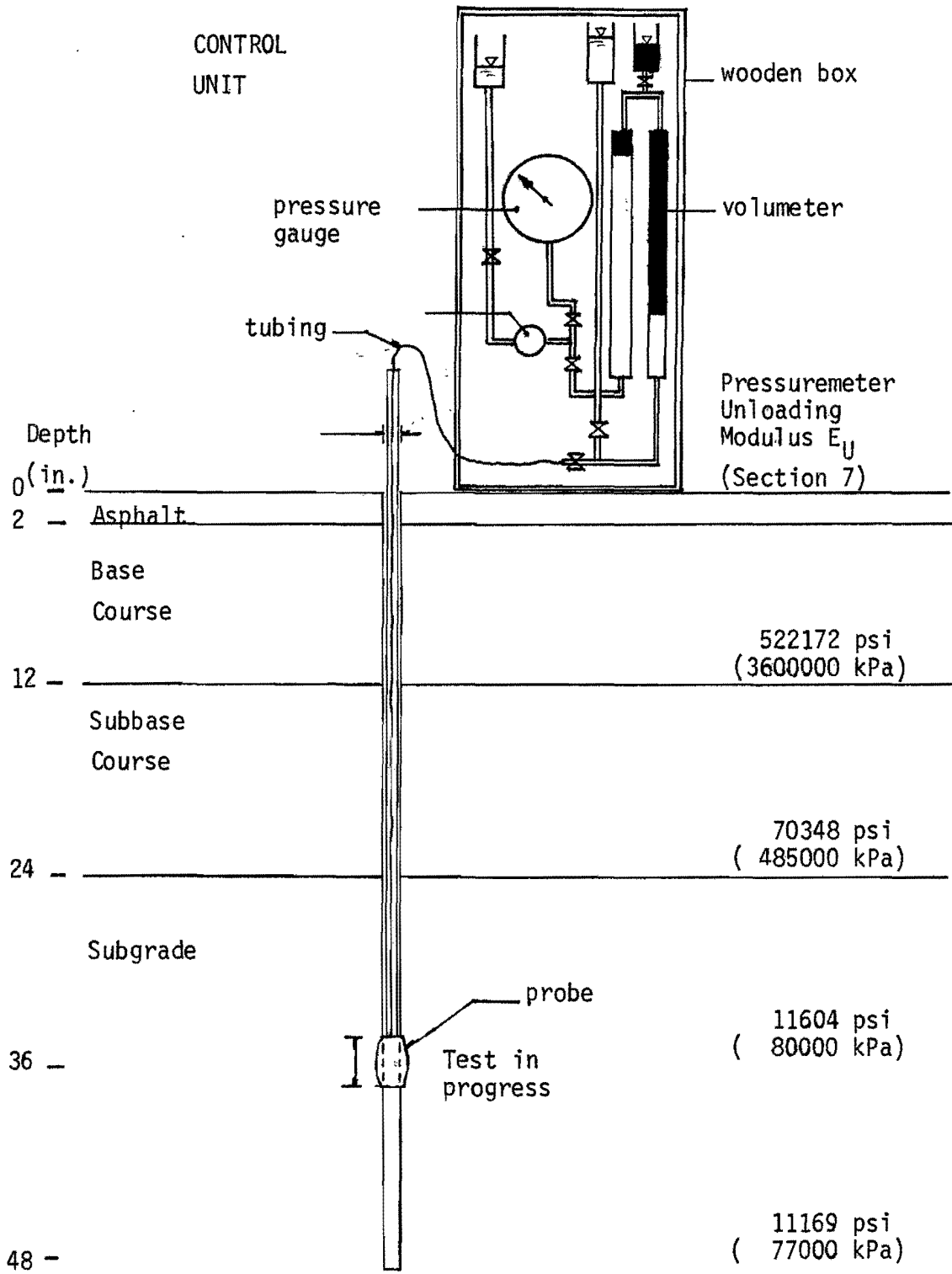


FIG. 2. — Pavement Pressuremeter (in testing)

The function of the control unit is to inflate and deflate the probe in a strain controlled test. The box is also used to transport the probe, tubing, and necessary accessories.

The measurements taken during the tests are the volume of water sent to the probe and the pressure necessary to inflate the probe; this leads to a raw data P-V curve.

During a test, there is a need for two corrections due to the effects of tubing expansion and compression of the rubber membrane and sheath. A volume calibration is needed to correct for the volume loss in the expansion of the tubing. A membrane calibration is also necessary, because when the probe is inflated in the borehole, the pressure against the wall of the borehole is less than the pressure inside the probe. This difference is due to the resistance to expansion of the membrane. The P-V raw data are corrected for volume losses and membrane resistance, and the corrected P-V curve is obtained (Fig. 3). From this curve, the modulus E between points A and B of the P-V curve is computed from the slope of AB by using the linear elastic, cylindrical expansion theory of Lamé' and a Poisson's ratio of 0.33 (1):

$$E = 2.66V_m \frac{\Delta P_{AB}}{\Delta V_{AB}}, \quad (4)$$

where

$$V_m = V_C + \frac{V_A + V_B}{2}, \quad (4a)$$

$V_C$  = initial volume of the probe,

$V_A$  = volume injected at A, and

$V_B$  = volume injected at B.

This theory assumes that the pressuremeter is infinitely long; this approxi-

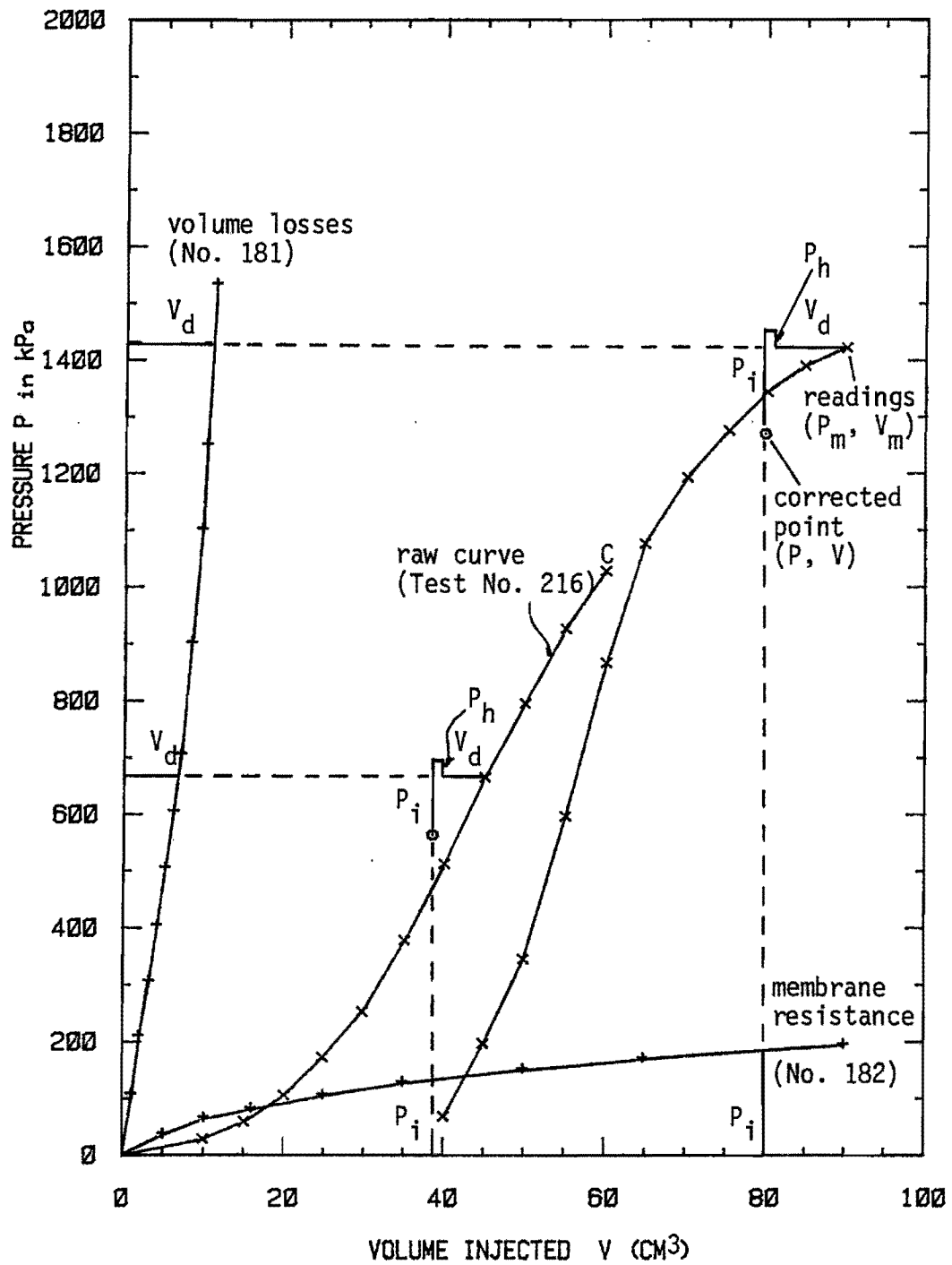


FIG. 3. — Pressuremeter Test Curve and Corrections  
(From Ref. 3)

mation seems to make a difference of 5% on the modulus E if the length to diameter ratio of the probe is 8 or more (2).

The procedure chosen to prepare the borehole in which to insert the pavement pressuremeter probe is to drive a solid rod having the same outside diameter as the probe. This procedure disturbs the soil, but, nevertheless, was retained for the detailed reasons described in Ref. 2. The main reasons are that 1) it is up to now the only economical and practical technique, 2) the unload-reload moduli which are used are obtained at large strain levels where the disturbance effect is lessened, and 3) a good correlation was obtained between such moduli and a test that involves no disturbance to the soil: the plate test.

#### Other Tests

Besides the pavement pressuremeter test, the Dynaflect test, and the Texas Triaxial Test data were used in this research.

The Dynaflect system consists of a dynamic force generator mounted on a small two-wheel trailer, a control unit, a sensor assembly, and a sensor (geophone) calibration unit. Its purpose is to permit rapid and precise measurement of pavement deflections. The generator generates a peak-to-peak dynamic force of 1000 lbs. (4.447 KN) at a fixed frequency of 8 Hz. The force is applied to the pavement through two 4 in. (10.2 cm) wide, 16 in. (40.6 cm) OD, rubber-coated wheels which are spaced 20 in. (50.8 cm) center to center (Fig. 4). Deflections are measured with 5 geophones, each 1 ft. (30.5 cm) apart, on the symmetry axis which passes between the load wheels (Figs. 4, 5) (10). Tests are run by stopping the trailer briefly at successive test locations.

The deflections measured with the Dynaflect were used together with an

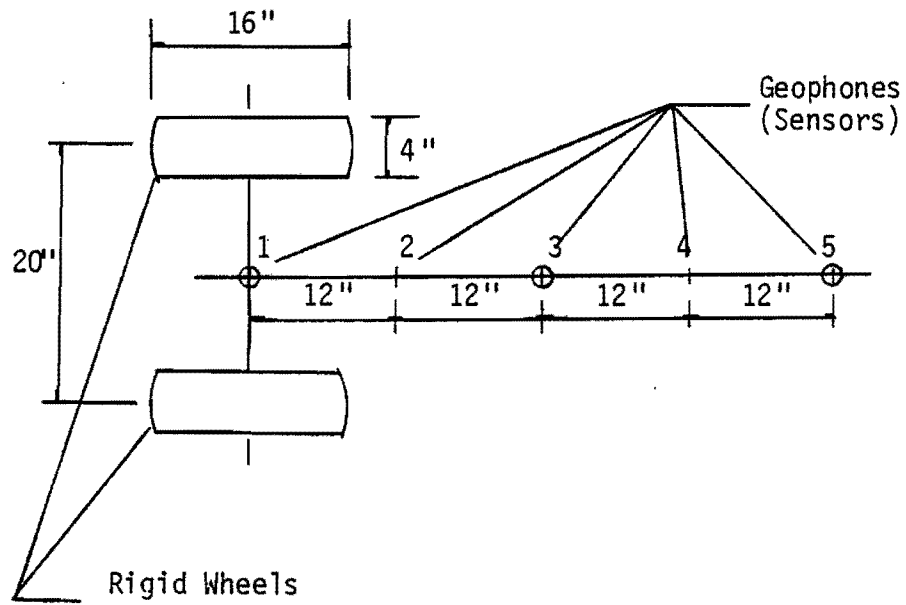


FIG. 4. — Sensor Array of The Dynaflect Test

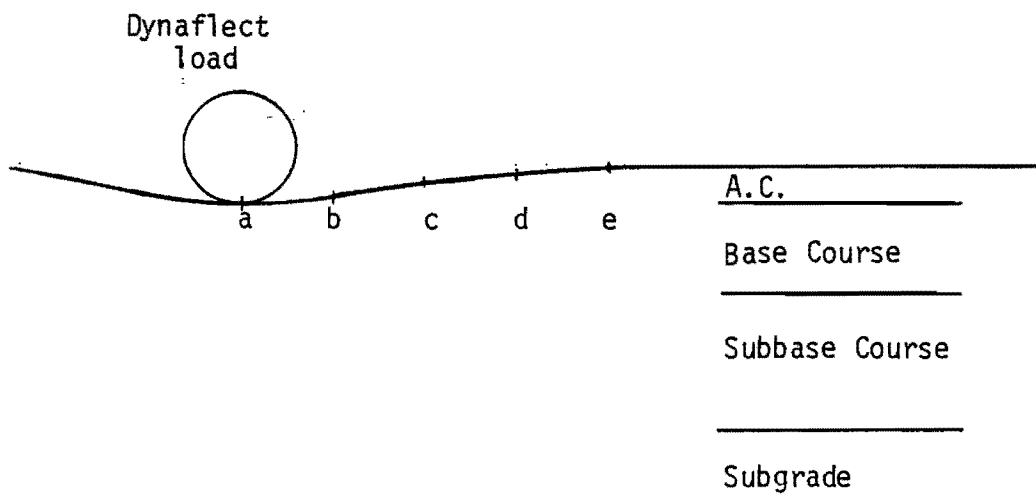


FIG. 5. — Deflection Basin of Pavement Under Dynamic Load

equation for predicting the surface deflections of a pavement subjected to a known load (11). Using this deflection equation, Michalak, et al. (14) presented several methods to calculate the elastic moduli of pavement materials and in-situ stiffness coefficients which are adopted as major input factors in the Flexible Pavement System (FPS) in Texas (20).

The Texas Triaxial Test (TTT) (13) was also used in this study; it is basically an unconsolidated undrained test and differs from the standard triaxial test in that

- (1) the confining pressure is applied laterally only (therefore, the vertical stress  $\sigma_1$  is equal to the value of the applied vertical stress), and
- (2) lateral pressures are applied by compressed air between the tube and the rubber membrane.

By performing a series of two or more tests at different lateral confining pressures (Fig. 6), a failure envelope (Fig. 7) is obtained. By drawing the failure envelope on to the chart for classification of subgrade and flexible base materials (Fig. 8), the material can be classified to the nearest class. This strength classification chart offers a means of evaluating granular base materials (13).

There are several existing test methods that can be used to measure soil modulus but are not used in this research. Among these test methods, the most widely used methods are:

- (1) Plate-load test: In this test, the following equations are used to compute the  $k$  value and soil modulus (19, 23),

$$k = \frac{P}{\Delta} \text{ and} \quad (5a)$$

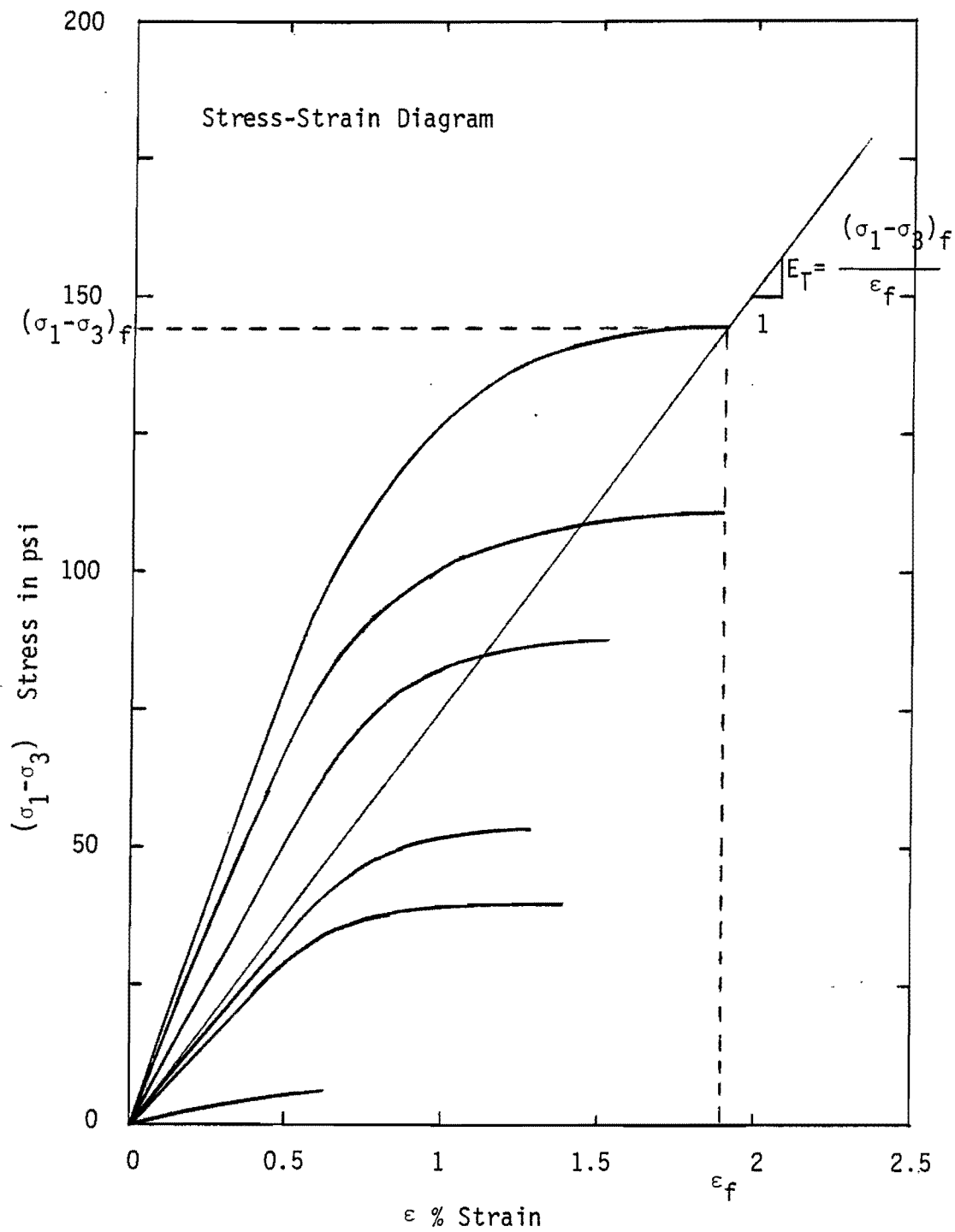


FIG. 6. — Stress versus Strain Chart (From Ref. 13)

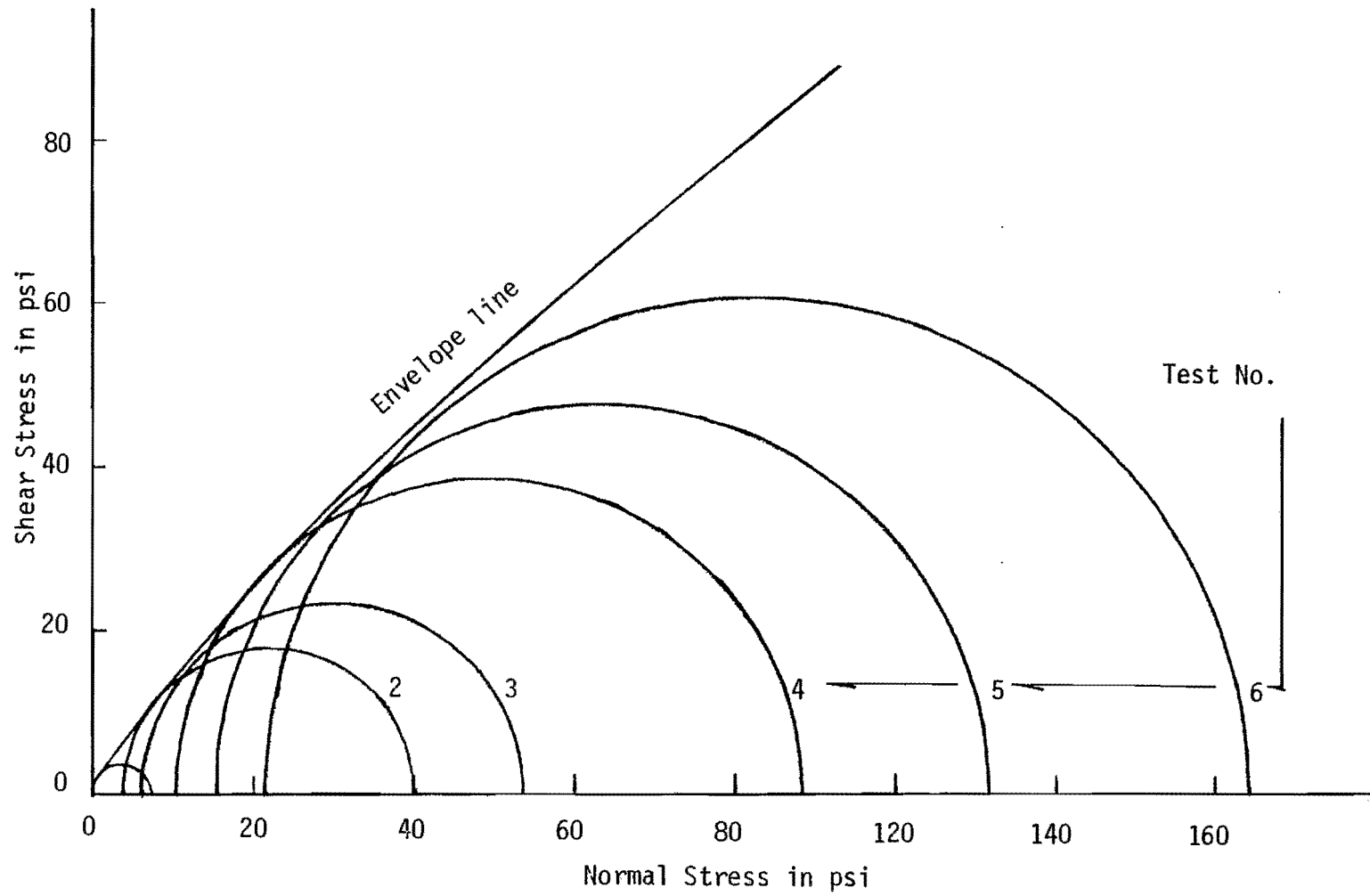


FIG. 7. — Mohr's Diagram of Texas Triaxial Test (From Ref. 13)

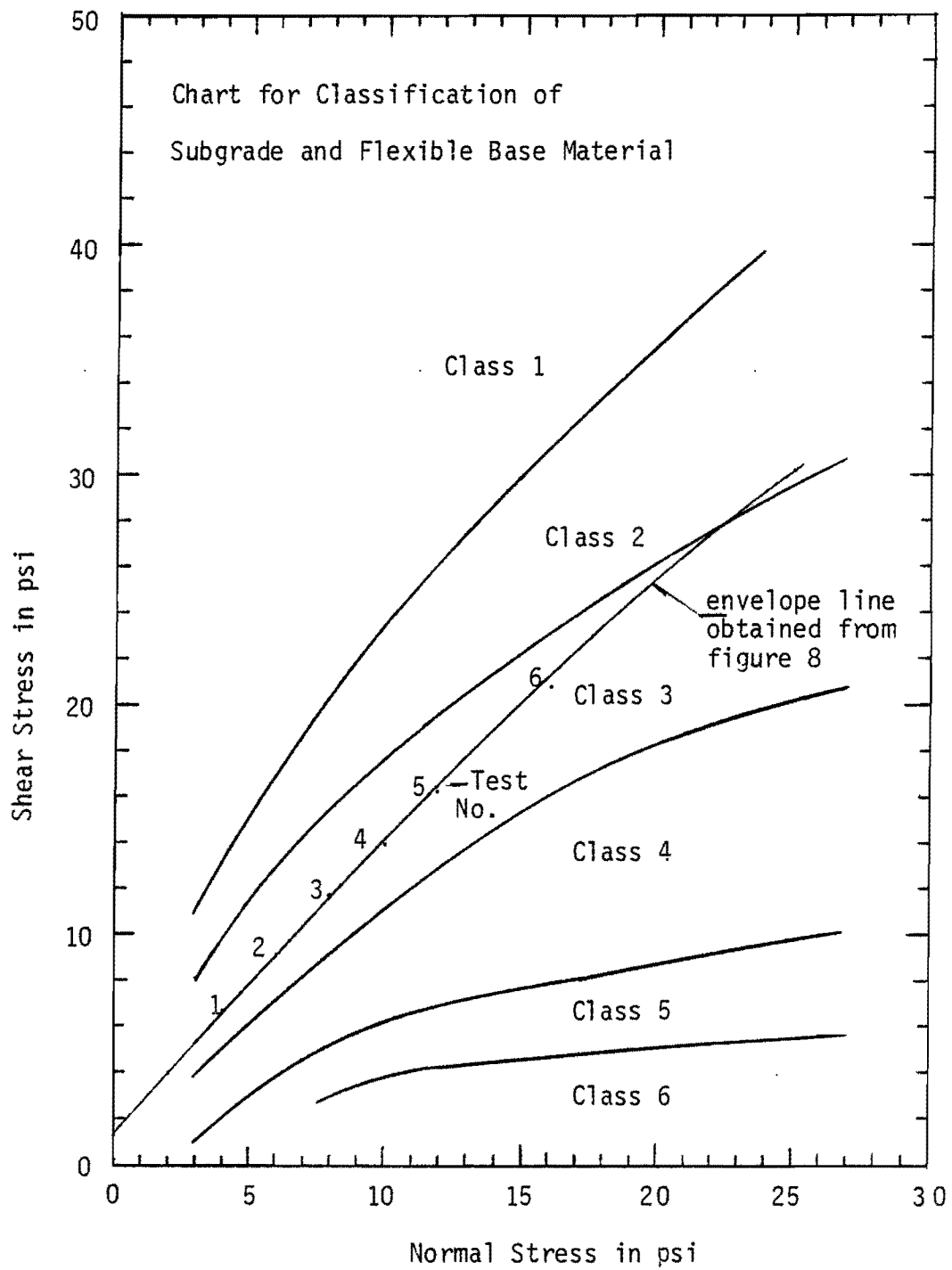


FIG. 8. — Texas Classification of Subgrade and Flexible Base Materials (From Ref. 13)

$$E = \frac{\pi}{4} (1 - \nu^2) \frac{qD}{s}, \quad (5b)$$

where

$p$  = unit load on the plate (psi),

$\Delta$  = deflection of the plate (in.),

$k$  = modulus of subgrade reaction,

$E$  = soil modulus,

$q$  = distributed load acting on the rigid plate,

$D$  = diameter of the rigid plate,

$s$  = settlement of the rigid plate under the distributed circular load, and

$\nu$  = Poisson's ratio of the soil.

A study of the results of many tests indicate that the most representative value for  $k$  for subgrades may be obtained using a load intensity of 10 psi (68.9 kPa) (23) with a 30 in. (76.2 cm) bearing plate (which is stacked in series of 24-, 18-, and 12-in. plates).

(2) Triaxial Compression Test: The modulus is calculated from the straight portion of the stress-strain curve. In most cases, however, the stress-strain curve of the soil will not be straight. The modulus of deformation is then calculated as a secant modulus between the origin, and a stress value equal to the stress condition which will exist in the pavement.

(3) California Bearing Ratio Test (CBR Test): The soil modulus can be correlated to the CBR value in the following relationship (23):

$$E = 1500 \times (\text{CBR}) \text{ psi}, \quad (6)$$

(4) Resilient modulus Test: This is a dynamic test conducted in a triaxial device equipped for repetitive load conditions (23). The resilient modulus  $M_R$  is defined as the ratio of the repeated axial deviator stress  $\sigma_d$  to the recoverable axial strain  $\epsilon_a$ ;

$$M_R = \frac{\sigma_d}{\epsilon_a} \quad (7)$$

For granular subgrade, subbase, and base courses, the resilient modulus tests have demonstrated the significant effect of confining pressure  $\sigma_3$  upon the modulus values. The following equations account for this stress dependency;

$$M_R = K_1 \sigma_1^{K'_1} \quad (8)$$

or

$$M_R = K_2 \theta^{K'_2}, \quad (9)$$

where

$M_R$  = resilient modulus (psi),

$\sigma_3$  = confining pressure (psi),

$\theta$  = bulk stress of first stress invariant ( $\theta = \sigma_1 + \sigma_2 + \sigma_3$ ),  
psi,

$K_1, K_2, K'_1, K'_2$  = experimental test constants.

### Russian Equation

The Russian equation is the nickname of a deflection equation which is based on an approximate elastic theory. This theory uses a

two-parameter elastic Vlasov model derived by introducing displacement constraints to simplify the basic equation for a linear elastic isotropic continuum.

When a homogeneous isotropic elastic half space is subjected to a limited distributed load, the displacement components in the X, Z-directions are  $u$ ,  $w'$  respectively (Fig. 9), and it is assumed that

$$u(x,z) = 0 \text{ and} \quad (10)$$

$$w'(x,z) = w'(x)h(z), \quad (11)$$

where the function  $h(z)$  describes the variation of displacement  $w'(x,z)$  in the Z-direction. One such function was proposed by Vlasov and Leont'ev (22) for an elastic layer of depth H:

$$h(z) = 1 - \left(\frac{z}{H}\right). \quad (12)$$

By using the stress-strain relations for plane strain conditions (21) and Lagrange's principles of virtual work, Vlasov and Leont'ev obtained the distributed load function (Fig. 9) as

$$q(x) = k_v w'(x) - 2t \frac{d^2 w'(x)}{dx^2}, \quad (13)$$

where,  $k_v$  and  $t$  are two parameters which depend on soil properties and layer thickness, i.e.

$$k_v = \frac{E_t}{(1-\nu_t)^2} \int_0^H \left(\frac{dh}{dz}\right)^2 dz = \frac{E_t}{H(1-\nu_t)^2}, \text{ and} \quad (14a)$$

$$t = \frac{E_t}{4(1+\nu_t)} \int_0^H (h)^2 dz = \frac{E_t H}{12(1+\nu_t)}, \quad (14b)$$

where

$$E_t = \frac{E_e}{(1-\nu_e)^2}, \quad (15)$$

$$\nu_t = \nu_e(1-\nu_e), \quad (16)$$

and  $E_e$ ,  $\nu_e$  are respectively the elastic modulus and Poisson's ratio for the elastic material (18).

For the concentrated force problem, Eq. 13 is reduced to the form of

$$2t \frac{d^2 w'}{dx^2} - k_v w' = 0, \quad (17)$$

and the general equation for the displacement  $w'(x,z)$  of the elastic layer is

$$w'(x,z) = \frac{P}{4t\alpha} h(0)h(z)e^{-\alpha x}, \quad (18)$$

where

$$\alpha = \sqrt{\frac{k_v}{2t}}. \quad (19)$$

If we assume the linear variation of transverse displacement with Eq. 12, then Eq. 18 is reduced to the form of

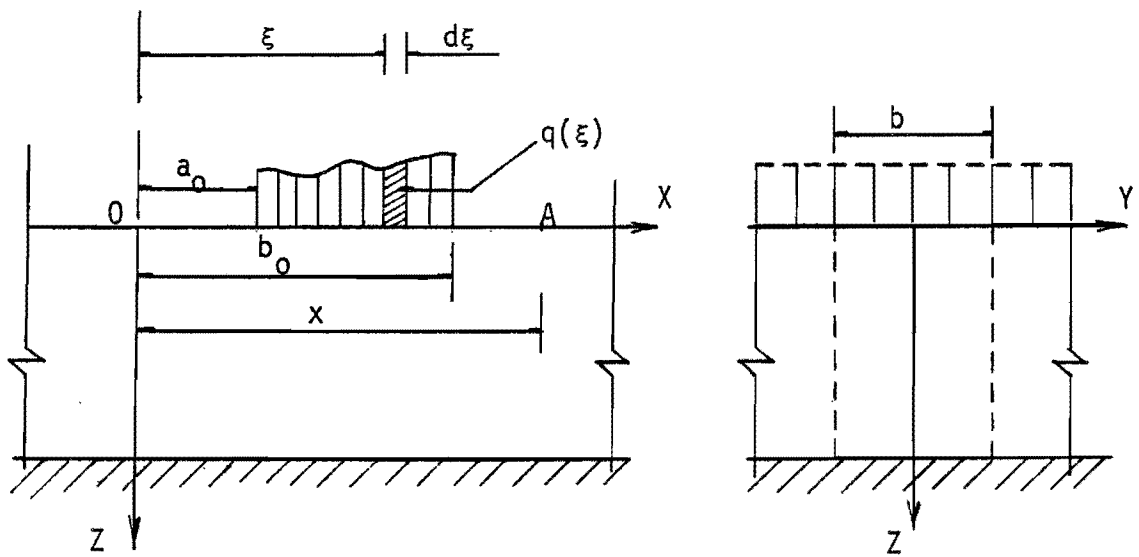


FIG. 9. — Vlasov Model Subjected to a Distributed Load

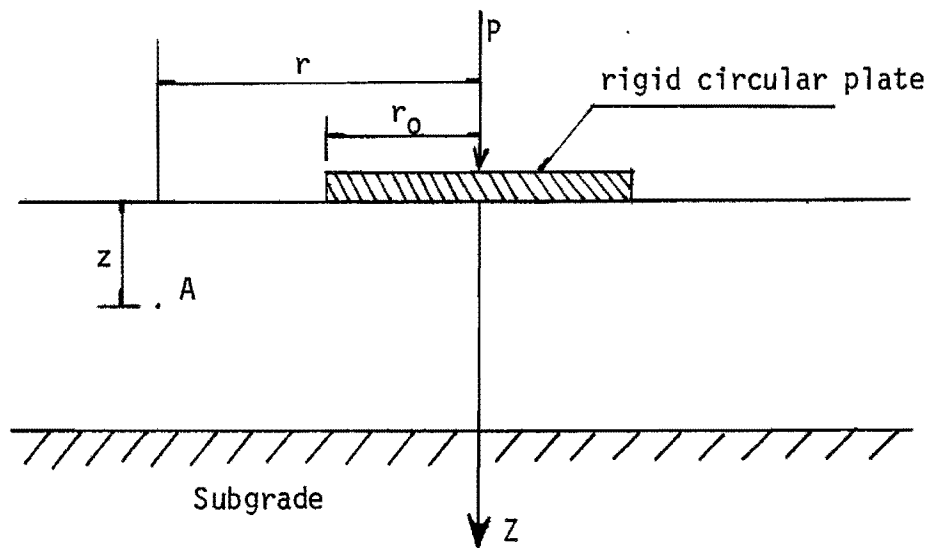


FIG. 10. — Vlasov Model Subjected to a Rigid Circular Plate

$$w'(x,z) = \frac{3(1-\nu_t^2)}{[6(1-\nu_t)]^{\frac{1}{2}}} \frac{P}{E_0} e^{-\alpha x} \left[ 1 - \frac{z}{H} \right] \quad (20)$$

$$\text{and } w'(x,0) = w'(x). \quad (21)$$

By using the result for the displacement in Eq. 18 for the concentrated force as influence functions, it is possible to evaluate the displacements in the elastic layer subjected to a distributed surface load, and then, the displacements of a point A of coordinates  $x$  and  $z$  in the elastic layer subjected to a distributed load  $q(\xi)$  applied at some distance from the origin 0, as shown in Fig. 9, can be expressed as follows.

(1) In  $a_0 \leq x \leq b_0$  region,

$$w'(x,z) = \frac{h(0)}{4\alpha t} \left[ \int_{a_0}^x q(\xi) e^{-\alpha(x-\xi)} d\xi + \int_0^{b_0} q(\xi) e^{\alpha(x-\xi)} d\xi \right] h(z). \quad (22)$$

(2) In  $x > b_0$  region,

$$w'(x,z) = \frac{h(0)}{4\alpha t} \left[ \int_{a_0}^{b_0} q(\xi) e^{-\alpha(x-\xi)} d\xi \right] h(z). \quad (23)$$

(3) In  $x < a_0$  region,

$$w'(x,z) = \frac{h(0)}{4\alpha t} \left[ \int_{a_0}^{b_0} q(\xi) e^{\alpha(x-\xi)} d\xi \right] h(z). \quad (24)$$

If the distributed load is uniform ( $q_0$ ), then the surface deflection is

$$w'(x,0) = \frac{q_0}{2k_v} [2 - e^{-\alpha(x-a_0)} - e^{\alpha(x-b_0)}] \quad (25)$$

Lytton and Michalak (11) assumed the variation of displacement in the Z-direction to be

$$h(z) = \left[ \frac{H-z}{H} \right]^m, \quad (26)$$

and then introducing into Eq. 20, the deflection equation turns out to be

$$w'(x,z) = \frac{3(1-\nu_0^2)}{[6(1-\nu_0)]^{\frac{1}{2}}} \frac{1}{\psi_t \psi_\alpha} \frac{P}{E_0} e^{-\alpha x} \left( \frac{H-z}{H} \right)^m, \quad (27)$$

where

$$\psi_\alpha = \left( \frac{\psi_k}{\psi_t} \right)^{\frac{1}{2}}, \quad \alpha = \frac{1}{H} \frac{[6(1-\nu_0)]^{\frac{1}{2}}}{(1-\nu_0)} \psi_\alpha, \quad (28)$$

$$\psi_k = H \int_0^H \left[ \left( -\frac{m}{H} \right) \left( 1 - \frac{z}{H} \right)^{m-1} \right]^2 dz, \quad (29)$$

and

$$\psi_t = \frac{3}{H} \int_0^H \left[ 1 - \frac{z}{H} \right]^{2m} dz. \quad (30)$$

For the Dynaflect test, the pavement is modeled as an elastic layer of depth  $H$  above a rigid layer; a load  $P$  is applied to a rigid circular plate of radius  $r_0$ . Then for all points where the distance  $r$  is greater than  $r_0$  (Fig. 10), the deflection equation is

$$w(r,z) = \frac{3P(1+\nu_0)}{\pi E_0 H \psi_t} K_0(\alpha r) \left[ \frac{H-z}{H} \right]^m, \quad (31)$$

where

$r$  = the horizontal radius ,

$z$  = the depth below the surface ,

$K_0(\alpha r) = K_0$  the modified Bessel function with argument  $\alpha r$   
and the other parameters are as defined before.

By using a generalized form of Odemark's assumption (15), the thickness of all component layers are transformed into an equivalent thickness of a material with single modulus; the transformed total thickness of all layers is

$$H' = \sum_{i=1}^{k'} h_i \left( \frac{E_i}{E_0} \right)^n, \quad (32)$$

where

$k'$  = the number of layers ,

$n$  = 0.333 in Odemark's assumption, but is found by analysis of  
field measurements in their study ,

$H'$  = the transformed depth of all layers ,

$h_i$  = the thickness of layer  $i$  ,

$E_i$  = the elastic modulus of layer  $i$  , and

$E_0$  = the modulus of the datum layer which is chosen to be the  
subgrade .

Therefore, Eq. 31 is revised for a multilayer system as

$$w(r,z) = \frac{C}{\pi} P \frac{1+\nu_0}{E_0} \frac{2m+1}{H'} K_0(\alpha r) \left[ \frac{H'-z}{H'} \right]^m, \quad (33)$$

where

$\bar{z}$  = the transformed depth to the point at depth  $z$  below the surface; i.e.,

$$\bar{z} = \sum_{i=1}^{l-1} h_i \left( \frac{E_i}{E_0} \right)^n + \left( z - \sum_{i=1}^{l-1} h_i \right) \left( \frac{E_l}{E_0} \right)^n, \quad (34)$$

$l$  = the number of the layer in which  $z$  falls, and

$$\alpha = \frac{mB}{H'} \left[ \frac{2(2mB+1)}{(2mB-1)(1-\nu_0)} \right]^{\frac{1}{2}}. \quad (35)$$

From the field measurement data and by using Eq. 26, the constants  $m$ ,  $n$ , and  $H$  are determined through non-linear regression analysis by combining Eq. 32 and the variation equation of vertical displacement (11),

$$w'(r, \bar{z}) = w'(r, 0) \left[ \frac{H' - \bar{z}}{H'} \right], \quad (36)$$

and then, Eq. 33 is used to find the constants  $B$ ,  $C$ , by following non-linear regression analysis procedures developed at TTI. In dealing with the above iterations, the initial values of  $m=1.0$ ,  $n=0.333$ ,  $B=1.0$ ,  $C=1.0$ , and  $H=70$  inches were used.

## THE TEST PROGRAM

### The Test Sites and The Soils

The selected test sites are located in Texas within an 80 mile radius from Beaumont. The subgrades encountered were clay, sandy clay, clayey sand, and silty sand. The subbase materials were selected sand, lime stabilized clay, and sand and shell. The base course materials were iron ore, sand and shell, crushed siltstone, cemented treated crushed stone, and limestone. The surface course was generally asphalt concrete. Tables 1(a) - 1(k) list the profile for each tested section. And Tables 2(a) - 2(k) present the index properties of the various soils tested. At each section, tests were performed in the outside wheel path. Five Dynaflect tests were run first, 5 ft. (152.4 cm) apart; then two holes were made for pressuremeter testing, with 4 tests being performed in each hole; one hole was used for soil sampling (Fig. 11).

### Pavement Pressuremeter Test

For each pressuremeter test, two calibrations must be done. These are the membrane calibration and the volume calibration. In other words, three test components constitute a whole pressuremeter test: the pressuremeter tests performed in the soil and two correction tests performed with the probe at the ground surface.

On the average, one set of calibration curves was obtained after each working day, during which an average of 15 pressuremeter tests

TABLE 1. — Profiles of Test Sections and Test Data

(a) Section 1 -- (1947-1-1) on FM 1293, 1 mile West of FM 1003 (direction West)

Layers and Thickness Depth (ft)	Thickness (in.)	Test No.	Pressuremeter Modulus* (kPa)		Pressuremeter Limit Pressure* $P_1$ (kPa)	N** blows/ft	Water Content w %	Texas Triaxial Test Classification
			$E_0$	$E_U$ & ( $E_R$ )				
0	Seal Coat  0.75							
	Iron Ore 7.25	121	21900	961000( 132000)	1700	20	6.94 <sup>†</sup>	3.1***
1	Select Sand 4.00	125	36700	1130000( 123000)	≥ 2500			
		126	34700	713000( 109000)	> 2500		11.73 <sup>†</sup>	
2	Silty Sand	120	37200	786000( 110000)	> 2500	26		4.3
		124	32700	1010000( 127000)	> 2500			
3	Subgrade					20		
		123	8500	203000( 42000)	840			4.3
		119	10200	359000( 76000)	1080	16		
4								
		122	12300	237000( 81000)	990			4.3
		118	10500	344000( 83000)	1050	19		

\* : Modulus at zero strain = initial tangent modulus on the reloading part of the first cycle

\*\* : Blow count for driving an  $1\frac{3}{8}$  inches (3.49 cm) solid rod with the SPT hammer

\*\*\*: Detailed Texas triaxial test data available.

†: measured data.

TABLE 1 -- (Continued)

(b) Section 2 -- (932-1-1) on FM 365, 0.6 miles East of Port Arthur Road (direction)

Layers and Thickness Depth (ft)      Thickness (in.)	Test No.	Pressuremeter Modulus* (kPa)		Pressuremeter Limit Pressure* P <sub>1</sub> (kPa)	N** blows/ft	Water Content w %	Texas Triaxial Test Classification
		E <sub>0</sub>	E <sub>U</sub> & (E <sub>R</sub> )				
0 <u>H.M.A.C.</u> 2.00							
Sand & Shell      12.00	71	27100	2160000( 221000)	≥ 2500	42	5.62 <sup>+</sup>	1.0*** (at w=7.00)
1 <u>        </u>	70	26000	1470000( 138000)	2500			
Select Sand 6.00	66	25200	944000( 81000)	2500			
2 <u>        </u>	69	11800	130000( 61000)	1060	10	12.9	3.0*** (at w=11.0)
Clay	65	12400	162000( 92000)	980			
3 <u>Subgrade</u>	68	4500	53000( 32000)	280	8	21.0 <sup>+</sup> 25.9	4.4*** (at w=25.0)
	64	6200	53000( 36000)	350			
	67	4000	35000( 24000)	260			
4 <u>        </u>	63	4100	40000( 15000)	300	9	33.16 <sup>+</sup>	
					11	35.86 <sup>+</sup> 35.78 <sup>+</sup>	

TABLE 1. — (Continued)

(c) Section 3 -- (305-7-1) on SH 87, 3 miles South of Newton County Line (direction North)

Layers and Thickness Depth (ft)      Thickness (in.)	Test No.	Pressuremeter Modulus* (kPa)			Pressuremeter Limit Pressure* P <sub>1</sub> (kPa)	N** blows/ft	Water Content w %	Texas Triaxial Test Classification
		E <sub>0</sub>	E <sub>U</sub>	& (E <sub>R</sub> )				
0  S.C. 1.5	34	26100	870000	( 77000)	> 2500	18	5.0	1*** (at w=8.3)
Sand & Shell 12.0	32				loss press.		12.57 <sup>+</sup>	
1  Select Sand 12.0	28	15500	510000	( 42000)	2000		11.1	3.0*** (at w=11.0)
	33	7900	242000	( 39000)	1375			
	31	8800	223000	( 45000)	1125			
2  Clay 12.0	27				1575		23.8	5.0*** (at w=22.6)
	30	11300	152000	( 90000)	1300		19.13 <sup>+</sup>	
3  Subgrade	26	14200	196000	( 65000)	1325		19.65 <sup>+</sup>	4.6
	29	7200	60000	( 34000)	525			4.6
4 	25	6500	135000	( 52000)	575		29.31 <sup>+</sup>	

TABLE 1. — (Continued)

(d) Section 4 -- (601-1-1) on SH 326, 1.6 miles South of SH 105 (direction South)

Layers and Thickness Depth (ft)      Thickness (in.)	Test No.	Pressuremeter Modulus* (kPa)		Pressuremeter Limit Pressure* P <sub>1</sub> (kPa)	N** blows/ft	Water Content w %	Texas Triaxial Test Classification
		E <sub>0</sub>	E <sub>U</sub> & (E <sub>R</sub> )				
0  H.M.A.C. 2.5							
Sand & Shell 8.0	86	41400	1450000( 165000)	≥ 2500	40	6.22 <sup>+</sup>	
	88	41000	1680000( 418000)	> 2500			
1  Select Sand 9.0	82	43200	1270000( 219000)	> 2500	12	18.52 <sup>+</sup>	3.6
	85	12300	126000( 97000)	775			
	81	12400	152000( 93000)	815			
2  Clay					20	18.26 <sup>+</sup>	4.8
3  Subgrade	84	18200	423000( 150000)	1165			
	80	18400	536000( 194000)	1385			
4  Clay	87	12800	186000( 100000)	675	19	18.0 <sup>+</sup>	4.8
	83	10600	254000( 108000)	655			
	79	10100	207000( 116000)	615			

TABLE 1. — (Continued)

(e) Section 5 -- (601-2-1) on SH 326, 0.3 miles North of US 90 (direction North)

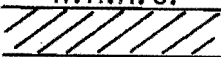
Layers and Thickness Depth (ft)	Thickness (in.)	Test No.	Pressuremeter Modulus* (kPa)		Pressuremeter Limit Pressure* $P_1$ (kPa)	N** blows/ft	Water Content w %	Texas Triaxial Test Classification
			$E_o$	$E_U$ & ( $E_R$ )				
0	H.M.A.C.  4.5							
	Sand & Shell 5.0	97	13900	269000( 101000)	1515		6.16 <sup>+</sup>	
1	Select	95	13700	248000( 56000)	1600	12		
	Sand 7.5	92	13900	352000( 108000)	1460		22.1 <sup>+</sup>	
2		91	10100	104000( 68000)	710	9		
	Clay	94	10100	83000( 60000)	700		28.08 <sup>+</sup>	
3	Subgrade	90	10400	105000( 106000)	1010	13		
4		96	6400	78000( 49000)	530	17		
		93	8800	115000( 53000)	830	16	21.23 <sup>+</sup>	
							23.64 <sup>+</sup>	

TABLE 1. — (Continued)

(f) Section 6 -- (932-1-2) on FM 365, 1 mile West of Port Arthur Road (direction West)

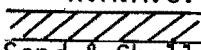
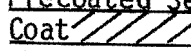
Layers and Thickness Depth (ft)	Thickness (in.)	Test No.	Pressuremeter Modulus* (kPa)		Pressuremeter Limit Pressure* $P_1$ (kPa)	N** blows/ft	Water Content w %	Texas Triaxial Test Classification
			$E_o$	$E_U$ & ( $E_R$ )				
0	H.M.A.C.  3.0 Sand & Shell 4.0	55	43200	1260000 ( 857000)	2200		4.2 <sup>+</sup> 6.11 <sup>+</sup>	
1	Select Sand 10.0	50	20900	338000 ( 179000)	1800	9	14.2	3.0
		57	28900	664000 ( 209000)	2500			
2	— Clay	49	11400	138000 ( 35000)	740	11	26.0 <sup>+</sup> 22.4	4.4
		54	6600	88000 ( 58000)	500			
		56	5300	100000 ( 68000)	580			
3	— Subgrade	48	5900	93000 ( 39000)	500	12	19.2 <sup>+</sup>	5.5
		53	5000	81000 ( 37000)	500			
4	—	52	8600	79000 ( 141000)	500	16	36.7 <sup>+</sup>	
		47	7400	68000 ( 39000)	440			

TABLE 1. — (Continued)

(g) Section 7 -- (244-2-1) on SH 63, 9 miles N.W. of Jasper (direction North)

Layers and Thickness Depth (ft)	Thickness (in.)	Test No.	Pressuremeter Modulus* (kPa)		Pressuremeter Limit Pressure* $P_1$ (kPa)	$N^{**}$ blows/ft	Water Content w %	Texas Triaxial Test Classification
			$E_0$	$E_U$ & ( $E_R$ )				
0	Precoated Seal Coat  2.0							
1	Crushed Stone (Siltstone, cement-treated) 10.0	151	90800	3600000 (186000)	>> 2500	66	25.46 <sup>+</sup> 17.7	1.0***
2	Select Sand 12.0	150	15300	485000 (226000)	1900	43	7.83 <sup>+</sup> 8.9	3.7*** (at w=8.9)
3	Clayey Sand	149	7200	80000 (39000)	525	28		4.1*** (at w=14.8) 3.9
4	Subgrade	148A	6800	77000 (42000)	525	27		3.9

NOTE: No measurements were taken at Section 8.

TABLE 1. — (Continued)

(h) Section 9 -- (367-1-46) on SH 124, 6.8 miles South of FM 1985 (direction South)

Layers and Thickness Depth (ft)	Thickness (in.)	Test No.	Pressuremeter Modulus* (kPa)		Pressuremeter Limit Pressure* $P_1$ (kPa)	N** blows/ft	Water Content w %	Texas Triaxial Test Classification
			$E_0$	$E_U$ & ( $E_R$ )				
0	<del>L.Wt.A.</del> Limestone							
	0.38 5.0							
	Sand & Shell	187	26300	1370000( 129000)	> 2500	40	8.00 <sup>+</sup> 3.86 <sup>+</sup>	2.1***
1	8.6	183	25200	1300000( 126000)	> 2500		7.76 <sup>+</sup>	
	Lime Stabilized Clay					12	16.5 <sup>+</sup>	
2	—	186	8500	55000( 44000)	590			
		182	7200	57000( 45000)	600			
	Clay	185	4100	35000( 28000)	500	8	28.0 <sup>+</sup>	
3	Subgrade	181	4900	58000( 35000)	575			
						9	32.7 <sup>+</sup>	
4	—	184	2400	19000( 12000)	225			
		180	2200	19600( 10000)	200	11	36.0 <sup>+</sup>	

TABLE 1. — (Continued)

(i) Section 10 -- (508-4-84) on SH 73, 0.5 miles West of FM 823 (direction East)

Layers and Thickness Depth (ft)	Thickness (in.)	Test No.	Pressuremeter Modulus* (kPa)		Pressuremeter Limit Pressure* P <sub>1</sub> (kPa)	N** blows/ft	Water Content w %	Texas Triaxial Test Classification
			E <sub>0</sub>	E <sub>U</sub> & (E <sub>R</sub> )				
0	Limestone	6.0					5.71 <sup>+</sup>	
	Sand & Shell	6.0	171	18800 827000( 99000)	2000	28	7.11 <sup>+</sup>	
1	Select Sand	6.0	167	16700 572000(100000)	2000		15.21 <sup>+</sup>	
	Lime Stabilized Clay	6.0	173	31300 478000(196000)	≥ 2500	15	29.01 <sup>+</sup>	
2	Clay		170	41900 1260000(390000)	2500			
			166	38400 626000(174000)	2170	13	21.2 <sup>+</sup>	
3	Subgrade		169	5600 73000( 45000)	800			
			165	7600 103000( 63000)	870			
			172	2600 33000( 16000)	300	14	26.14 <sup>+</sup>	
4			168	3100 38000( 18000)	350			
			164	3900 44000( 27000)	350	12	34.16 <sup>+</sup>	



TABLE 1. — (Continued)

(k) Section 12 -- (214-2-1) on SH 63, 3.8 miles East of Jasper County Line (direction East)

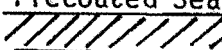
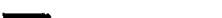
Layers and Thickness Depth (ft)	Thickness (in.)	Test No.	Pressuremeter Modulus* (kPa)		Pressuremeter Limit Pressure* $P_L$ (kpa)	N** blows/ft	Water Content w %	Texas Triaxial Test Classification
			$E_o$	$E_U$ & ( $E_R$ )				
0	Precoated Seal  3.5							
	Iron Ore	202	41200	1100000( 209000)	>> 2500	33	5.2 <sup>+</sup>	
1	 9.0	198	39300	518000( 128000)	>> 2500			
	Select Sand					19	7.54 <sup>+</sup>	
2		201	18400	425000( 114000)	1575			
	Sandy Clay	197	11700	345000( 113000)	1400	31		
3	 Subgrade	200	28800	1090000( 143000)	> 2500			
4		196	23900	724000( 201000)	> 2500			
		199	20500	1030000( 108000)	> 2500	28		

TABLE 2.— The moduli and Index Properties of Soils

(a) Section 1

Material	$E_U(5 \text{ psi})$ (kPa)	$E_T(5 \text{ psi})$ (kPa)	$f$	$I_p$	$w$ (%)	$P_p$	$C_u$	$C_c$
Iron ore	4604	16410	9.28	5.8	6.94	15.6	46.7	2.4
Silty sand	--	--	--	6.1	11.73	11.1	23.1	2.7

(b) Section 2

Sand & shell	15183	23200	9.87	4.7	5.62	6.1	23.0	0.44
Select sand	44415*	12170	2.58	6.6	12.9	--	--	--
clay	18255	4540	6.83	32.0	35.86	--	--	--

(c) Section 3

Sand & shell	15190	20250	5.68	8.1	12.57	11.0	58	3.5
Select sand	15688	3680	15.01	6.2	11.1	--	--	--
Clay	42889	18060	4.18	33.8	19.39	--	--	--

(d) Section 4

Sand & shell	--	--	--	5.2	6.22	12.2	38.3	1.05
--------------	----	----	----	-----	------	------	------	------

Note: Number with \* is mixed value which is measured from the mentioned layer and the beneath layer.

TABLE 2. — (Continued)

(e) Section 5

Material	$E_U(5 \text{ psi})$ (kPa)	$E_T(5 \text{ psi})$ (kPa)	f	$I_p$	w (%)	$P_p$	$C_u$	$C_c$
Sand & shell	--	--	--	--	6.16	1.3	10.5	2.03

(f) Section 6

Sand & shell	--	--	--	2.1	6.11	12.4	35.0	0.97
--------------	----	----	----	-----	------	------	------	------

(g) Section 7

lime treated crushed sandstone	11826	177420	2.77	7.0	25.46	8.0	18.3	0.4
Select sand	55176	14200	5.55	9.2	7.83	11.5	46.0	3.3
Clayey sand	22177	3530	6.42	--	--	--	--	--

(h) Section 9

Limestone	5417*	12490	16.24	4.0	3.86	9.2	30.3	2.7
Sand & shell	--	--	--	8.6	7.76	9.0	19.0	1.9

Note: Number with \* is mixed value which is measured from the mentioned layer and the beneath layer

TABLE 2. — (Continued)

(i) Section 10

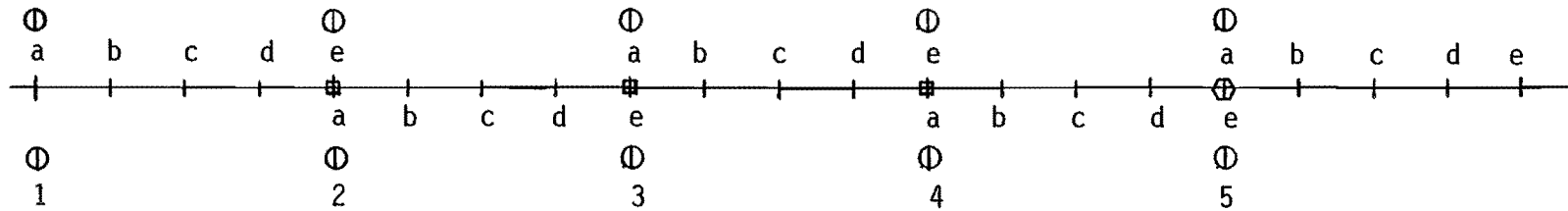
Material	$E_U(5 \text{ psi})$ (kPa)	$E_T(5 \text{ psi})$ (kPa)	f	$I_p$	w (%)	$P_p$	$C_u$	$C_c$
Limestone	--	--	--	--	5.71	14.2	55.0	3.7
Sand & shell	--	--	--	9.5	7.11	6.0	12.5	1.62

(j) Section 11

Iron ore	13118	53480	2.14	11.4	8.27	11.8	30.0	7.8
Select sand	26391	6090	24.12	12.3	6.08	--	--	--
Sandy clay	24194	2700	29.14	31.2	16.2	48.2	--	--

(k) Section 12

Iron ore	--	--	--	12.6	5.2	11.0	30.6	2.1
Select sand	--	--	--	14.6	7.54	12.5	51.2	7.1



+ : positions where geophones were arranged to measure deflections

⊙ : Dynaflect wheel load

⊕ : positions where bore-hole were made to perform pressuremeter test

○ : position where samples were obtained

1, 2, 3, 4, 5 : positions where axis of Dynaflect load located

FIG. 11. — Testing Layout of Dynaflect, Pressuremeter, and Sampling

were run. Tests and calibrations were performed at a probe inflation rate of  $0.020 \text{ in.}^3/\text{sec}$  ( $0.33 \text{ cm}^3/\text{sec}$ ).

The detailed test procedures for membrane and volume calibrations are described in Ref. 3, and were strictly followed during the testing program. The calibration curves are presented in Appendix III.

The borehole was prepared by driving into the ground a solid steel rod, 1.374 in. (3.49 cm) in diameter.

Immediately after the solid steel rod was withdrawn from the ground, the pavement pressuremeter probe was inserted into the hole down to the depth such that the middle of the probe was 4 ft. (122 cm) below the pavement surface. The probe has an outer diameter of 1.28 in. (32.5 mm) and usually can be forced down into the prepared hole by one or two people; sometimes, if the soil around the borehole has yielded inward, the assembly needs to be forced in. In a few cases, the probe could not be inserted to the desired testing depth. Once the probe is 4 ft. (122 cm) deep, a test is run; then the probe is pulled up to 3 ft. (91 cm) depth and another test is run; the sequence is repeated up to the surface.

The pressuremeter tests were performed at positions 2, 3, and 4 (Fig. 11) in each section. The test rate was kept at  $0.020 \text{ in.}^3/\text{sec}$  ( $0.33 \text{ cm}^3/\text{sec}$ ). During the test, one person inflates the probe with the hand pump and reads the volumeter every  $0.305 \text{ in.}^3$  ( $5 \text{ cm}^3$ ) except for the cycles where readings are taken every  $0.061 \text{ in.}^3$  ( $1 \text{ cm}^3$ ). A second person reads the pressure gauge and records the volume and pressure data.

For each test at least one cycle was performed. The unload-

reload cycle started at the end of the straight part of the curve, as shown in Fig. 12(a). The reloading part of the cycle was started when the pressure reading had decreased to 7.2 psi (50 kPa) or the volume reading was 1.22 in.<sup>3</sup> (20 cm<sup>3</sup>) less than the volume reading at the unloading point (E on Fig. 12(a) ). Multicycle tests were usually performed in position 4 at each section (Fig. 11). During these tests, the reloading pressure was varied.

### The Dynaflect Test

Dynaflect tests were run at the location where pavement pressuremeter tests would be performed. The test locations were selected in the outer wheel path of the right lane. The layout of Dynaflect tests and test holes for the pressuremeter tests is shown in Fig. 11.

The Dynaflect trailer was halted at each position in order to perform the test. The geophones a, b, c, d, and e (Fig. 11) measured the deflections. All of these test data are collected in Appendix IV.

### Penetration Test as a Reference

While making the hole for the pressuremeter test, the blow count per 6 in. (15.2 cm) of penetration of the solid steel rod was recorded. This blow count provided an indication of the resistance of the soil with depth. The recorded data are collected in Column 5 of Tables 2(a) - 2(k).

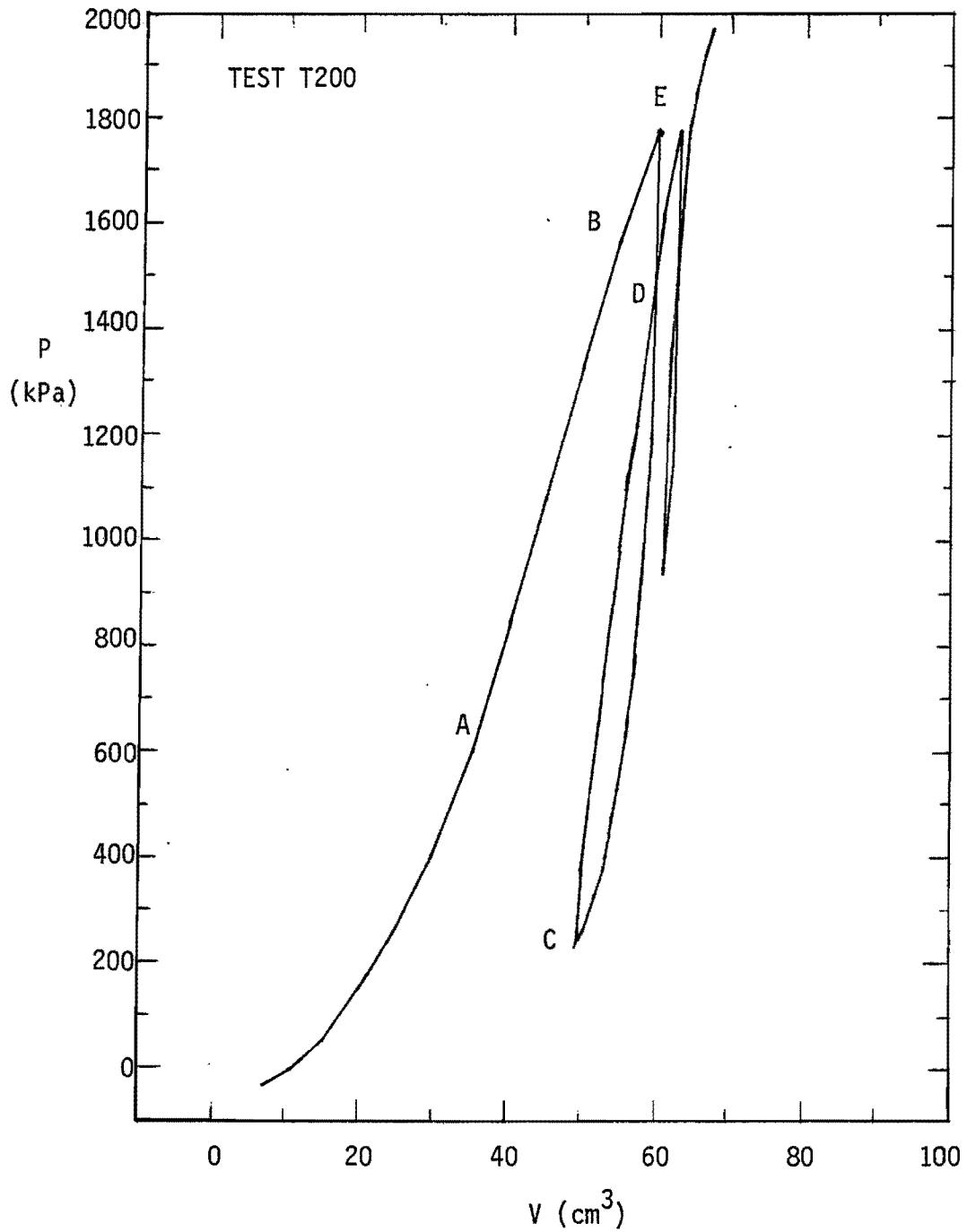


FIG. 12. — Pressuremeter Test Curve  
 (a) reload at proper level

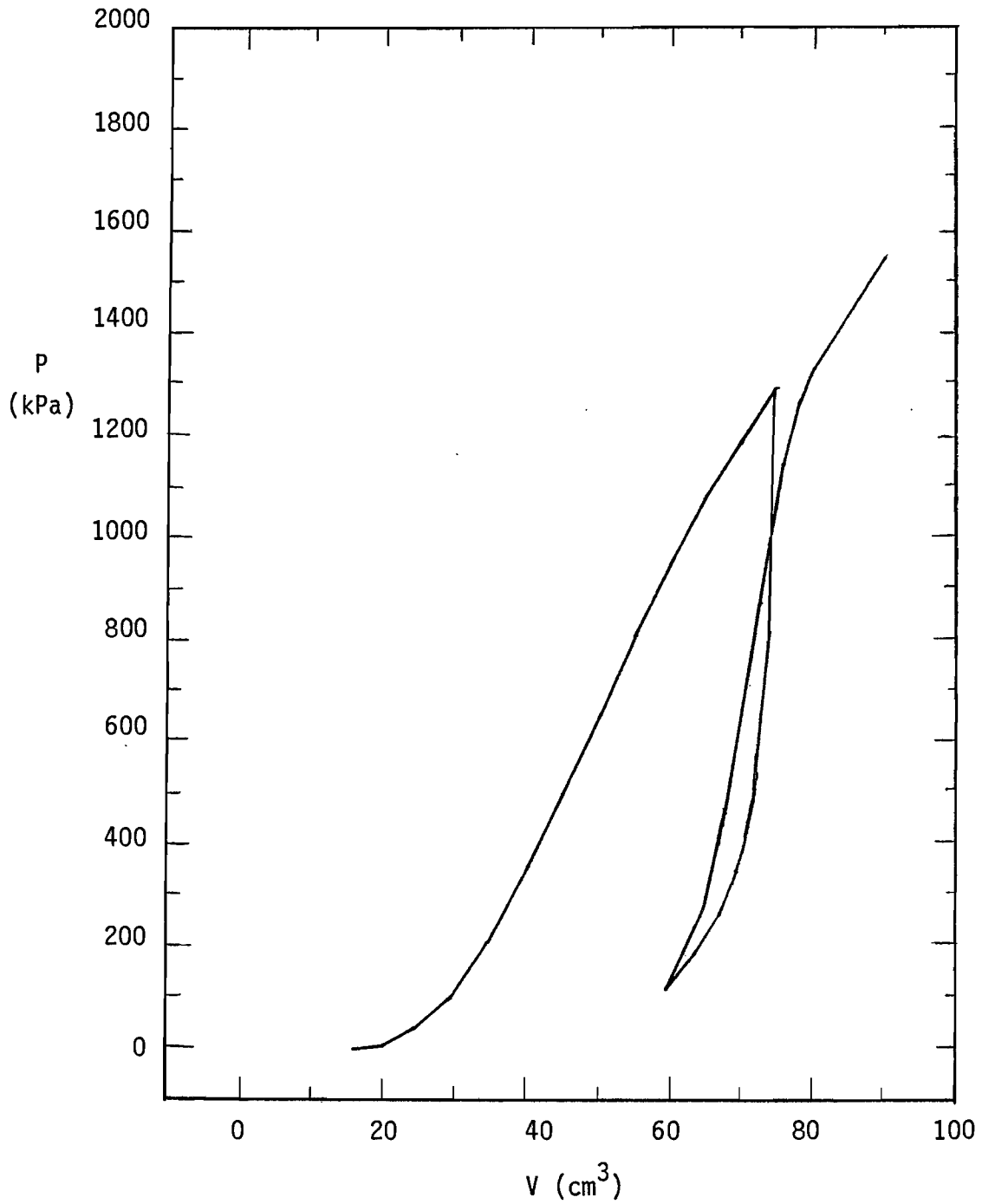


FIG. 12 — Pressuremeter Test Curve  
 (b) reload at improper level

### The Texas Triaxial Test

The Texas Triaxial classification data was obtained from the Texas SDHPT. The Texas classification values are based on Texas triaxial test results by superposing the failure envelope of Mohr circles on the classification chart of Fig. 8.



## ANALYSIS OF THE RESULTS

The analysis of the results is aimed primarily at obtaining moduli of deformation from the tests performed. This analysis of the results describes how the moduli are calculated from the pressuremeter tests, the Texas Triaxial tests, and the Dynaflect tests. Correlations between various moduli and other soil parameters are presented, and equivalency factors are calculated for the different base courses and subbase courses which were tested.

### The Pressuremeter Tests

The conventional way to reduce pressuremeter tests results, as described in Refs. 1, 2, and 3, is to correct the raw data curve point-by-point in order to obtain a corrected curve and then to calculate the soil parameters such as modulus and limit pressure from the corrected curve. In this report, a different approach was chosen--it consisted of calculating the moduli from the raw data curve and then correcting the moduli.

Calculation of the raw moduli. - If soil were linearly elastic, there would be only one Young's modulus for that soil. Because soil is not linearly elastic, many moduli of deformation can be defined depending on such factors as strain level, stress level, first loading, or n-th loading cycle. The following discussion concerns the first unloading portion of the pressuremeter test curve at a strain level equal to zero and the stress level generated by the expanded probe at the unloading point (Fig. 13).

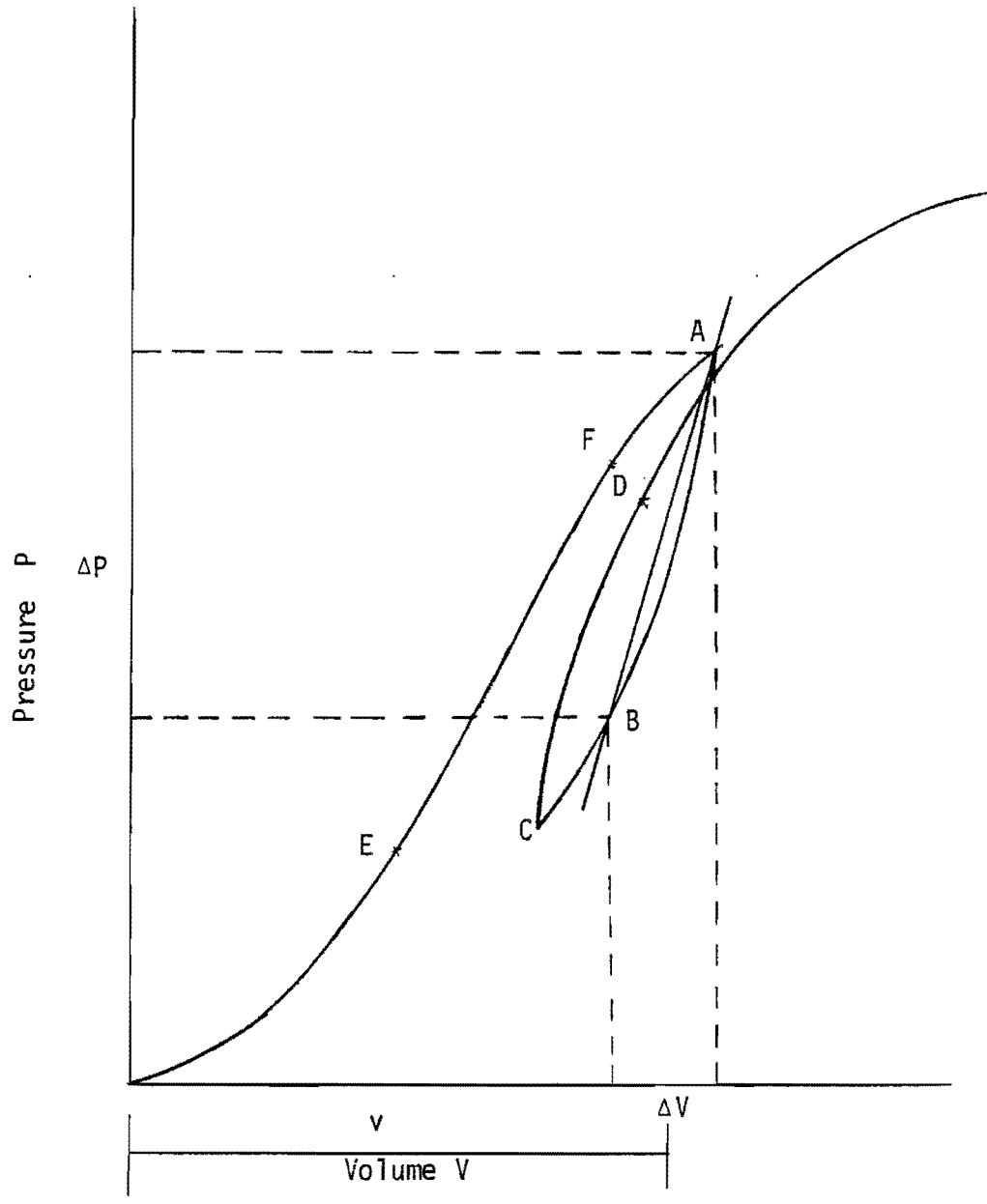


FIG. 13. — Secant Moduli of Cycling Pressuremeter

It has been found (6, 8) that certain stress-strain curves for soils can be modeled reasonably well by a hyperbolic equation, as shown in Fig. 14(a),

$$\sigma = \frac{\epsilon}{a + b\epsilon}, \quad (37a)$$

which can be written

$$\frac{\epsilon}{\sigma} = a + b\epsilon, \quad (37b)$$

The term  $a$  is the inverse of the tangent modulus  $E$ , as shown in Figs. 14(a), 14(b).

According to Eq. 37b, the  $\frac{1}{E}$  versus  $\epsilon$  curve should be a straight line and the adequacy of the hyperbolic model can be judged from the fit between the data points and the straight line obtained by a regression analysis. As seen from Figs. 14(a) and 14(b), the hyperbolic model is very satisfactory.

The  $(\frac{1}{E}, \epsilon)$  data points were obtained as follows: the unloading moduli were the secant moduli with point A as the origin (Fig. 13), and the unloading data points as the point of intersection. The reloading moduli were the secant moduli with the point C as the origin (Fig. 13), and the reloading data points as the point of intersection. The uncorrected strain corresponding to the secant modulus was calculated as

$$\epsilon_{\text{uncorrected}} = \frac{\Delta v}{V_0 + v}, \quad (38)$$

where  $\Delta v$  and  $v$  are defined in Fig. 13, and  $V_0$  is the deflated volume of the probe.

Since for all tests during the unload and reload cycle, the volume readings were taken every cubic centimeter, the  $\Delta v$  values were constant

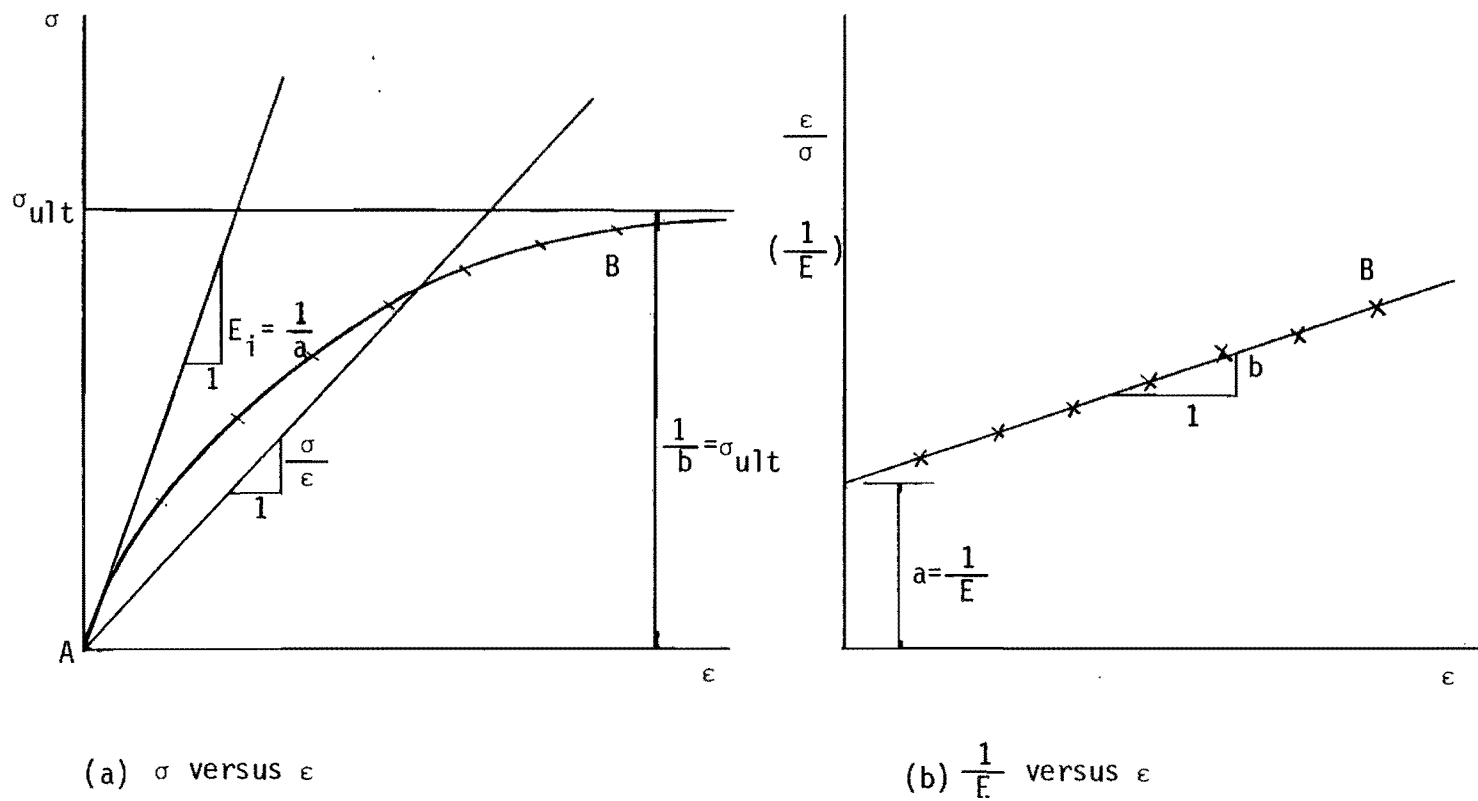


FIG. 14. — Model of Inelastic Modulus for Strain-Dependant Soils

from one test to the next. The uncorrected strains and the corrected strains were therefore reasonably constant for all tests. Using this fact, the corrected strains in Table 3 were calculated for three typical tests and the averages were used for all tests.

Calculation of the corrected moduli. - The standard method of correcting a pressuremeter test curve is described in Refs. 2 and 3. This method does not apply to the case where an unload-reload cycle is performed during the test.

For a pressuremeter test without cycling, the same membrane calibration curve and the same volume calibration curve can be used for a number of tests. In the case of cyclic pressuremeter tests, each test usually has different pressure boundaries and volume boundaries for the cycles; this requires, ideally, that cyclic membrane and volume calibrations be performed for each test at the corresponding volume and pressure boundaries. This is a very cumbersome procedure. Instead, the following correction procedure was chosen for the case of the unload curve.

1. Calculate the raw unload secant moduli (discussed previously in this section under "Calculation of the raw moduli");
2. plot the  $\frac{1}{E}$  versus  $\epsilon$  curve and find the best fit straight line by regression analysis (discussed previously in this section under "Calculation of the raw moduli");
3. extend the straight line to zero strain and read the zero strain unloading modulus as shown in Fig. 14(b); and
4. correct the zero strain unloading modulus for volume losses and membrane resistance.

TABLE 3. — The Corrected Strain Values for Pressuremeter Test

$\Delta v$ ( $\text{cm}^3$ )	Test 34		Test 30		Test 136		Average		
	Rel.	Unl.	Rel.	Unl.	Rel.	Unl.	Rel.	Unl.	Overall
1	.0009	.0000	.0009	.0035	.0031	.0022	.0016	.0019	.0017
2	.0026	.0017	.0031	.0065	.0062	.0053	.0040	.0045	.0042
3	.0051	.0038	.0062	.0091	.0093	.0089	.0069	.0073	.0071
4	.0068	.0060	.0097	.0117	.0133	.0124	.0099	.0100	.0100
5	.0098	.0081	.0133	.0152	.0169	.0160	.0133	.0131	.0132
6	.0128	.0106	.0168	.0183	.0209	.0200	.0168	.0163	.0165
7	.0157	.0140	.0204	.0217	.0249		.0203		.0200
8	.0187	.0157	.0243	.0239	.0289		.0240		.0238
9	.0213	.0187	.0283	.0270	.0331		.0276		.0276
10	.0247	.0217	.0323	.0304	.0379		.0313		.0313
11	.0281		.0358						
12	.0315		.0398						
13	.0349		.0438						
14	.0383		.0482						
15	.0417		.0522						

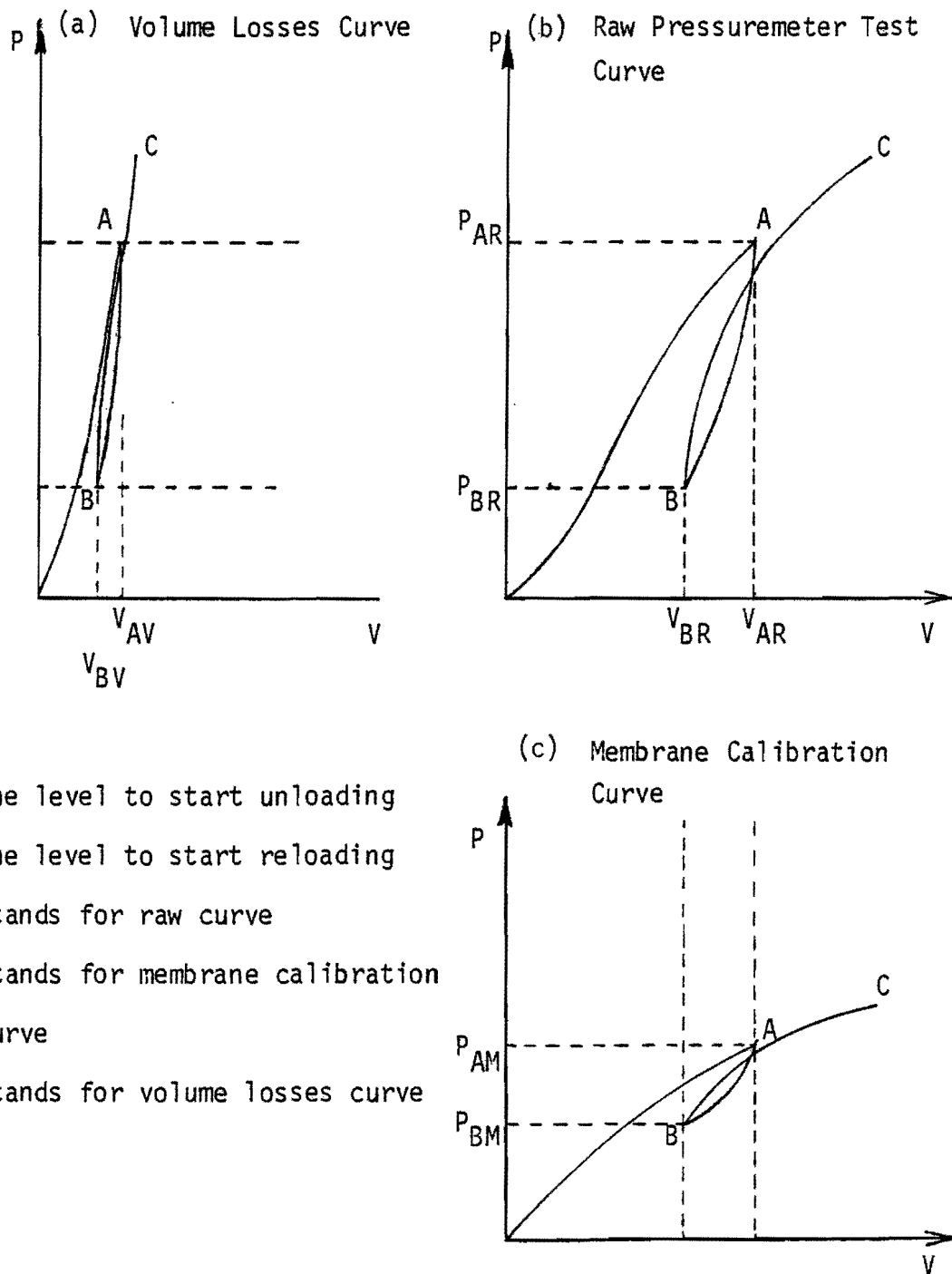


FIG. 15. - Corrections of Pressuremeter Test

The fourth step of this procedure was achieved through the following mathematical derivations, where the subscript R stands for raw values, C for corrected values, M for membrane correction, and V for volume correction.

(1) For the unloading portion of the curve (AB on Fig. 15)

$$E_R = \frac{P_{AR} - P_{BR}}{V_{AR} - V_{BR}} = \frac{1}{a_R}, \text{ and} \quad (39)$$

$$E_C = \frac{(P_{AR} - P_{AM}) - (P_{BR} - P_{BM})}{(V_{AR} - V_{AV}) - (V_{BR} - V_{BV})} = \frac{(P_{AR} - P_{BR}) - (P_{AM} - P_{BM})}{(V_{AR} - V_{BR}) - (V_{AV} - V_{BV})},$$

$$= \frac{\left(\frac{P_{AR} - P_{BR}}{V_{AR} - V_{BR}}\right) - \left(\frac{P_{AM} - P_{BM}}{V_{AR} - V_{BR}}\right)}{\left(\frac{V_{AR} - V_{BR}}{V_{AR} - V_{BR}}\right) - \left(\frac{V_{AV} - V_{BV}}{V_{AR} - V_{BR}}\right)} \cdot \left(\frac{V_{AR} - V_{BR}}{P_{AR} - P_{BR}} \cdot \frac{P_{AR} - P_{BR}}{V_{AR} - V_{BR}}\right), \quad (40)$$

$$E_C = \frac{1}{a_C} \quad (41)$$

but

$$E_M = \frac{P_{AM} - P_{BM}}{V_{AR} - V_{BR}} = \frac{1}{a_M}, \text{ and} \quad (42)$$

$$E_V = \frac{P_{AR} - P_{BR}}{V_{AV} - V_{BV}} = \frac{1}{a_V}. \quad (43)$$

Thus,

$$E_C = \frac{E_R - E_M}{1 - \frac{V_{AV} - V_{BV}}{P_{AR} - P_{BR}} \cdot \frac{V_{AR} - V_{BR}}{V_{AR} - V_{BR}} \cdot \frac{P_{AR} - P_{BR}}{V_{AR} - V_{BR}}} = \frac{E_R - E_M}{1 - \frac{E_R}{E_V}},$$

$$= \frac{E_V(E_R - E_M)}{E_V - E_R}, \text{ or} \quad (44)$$

$$\frac{1}{E_C} = \frac{E_V - E_R}{E_V(E_R - E_M)} = \frac{1}{E_R - E_M} - \frac{E_R}{E_V(E_R - E_M)},$$

$$= \frac{1}{\frac{1}{E_R} - \frac{1}{E_M}} - \frac{\frac{1}{E_R}}{\frac{1}{E_V}(\frac{1}{E_R} - \frac{1}{E_M})} \quad (45)$$

Then

$$a_C = \frac{1}{\frac{1}{a_R} - \frac{1}{a_M}} - \frac{\frac{1}{a_R}}{\frac{1}{a_V}(\frac{1}{a_R} - \frac{1}{a_M})} = \frac{a_R a_M - a_V a_M}{a_M - a_R}, \text{ or}$$

$$a_C = (a_R - a_V) \frac{a_M}{a_M - a_R} \quad (46)$$

(2) For the reloading portion of the curve (BC) on Fig. 15, the following relationship is obtained :

$$a_C = (a_R - a_V) \frac{a_M}{a_M - a_R} \quad (47)$$

Besides the above relationship, the corrected ultimate strength is derived as

$$\begin{aligned}
P_{\text{corrected}} &= (P_{\text{CR}} - P_{\text{CM}}) - (P_{\text{BR}} - P_{\text{BM}}), \\
&= (P_{\text{CR}} - P_{\text{BR}}) - (P_{\text{CM}} - P_{\text{BM}}); \quad (48)
\end{aligned}$$

$$\frac{1}{b_C} = \frac{1}{b_R} - \frac{1}{b_M} = \frac{b_M - b_R}{b_R b_M}, \text{ or}$$

$$b_C = \frac{b_R b_M}{b_M - b_R}, \quad (49)$$

where

$$\frac{1}{b_C} = \sigma_{ult} \text{ after correction,}$$

$$\frac{1}{b_R} = \sigma_{ult} \text{ from the raw data test curve, and}$$

$$\frac{1}{b_M} = \sigma_{ult} \text{ from the membrane calibration curve.}$$

Since the zero strain moduli obtained from the membrane resistance curve (Appendix III-1) and the volume losses curve (Appendix III-2) are reasonably constant, they were calculated from typical tests. Tests 10 and 11 were used for the membrane resistance and Tests 14 and 15 were used for the volume losses. The curves for these tests were considered as regular pressuremeter test curves and the previously described method for calculating the zero strain modulus was applied to each cycle of each test. Tables 4 and 5 summarize the results and give the averages that were used for the correction of all pressuremeter tests. In Tables 4 and 5, the values of  $a_{UM}$  and  $a_{UV}$  are substituted into Eq. 46 for  $a_M$  and  $a_V$  respectively; the values of  $a_{RM}$

TABLE 4. — Parameters (Zero Strain Moduli) of Membrane Resistance

TEST	$a_{UM}(10^{-4} \frac{1}{\text{kPa}})$	$a_{RM}(10^{-4} \frac{1}{\text{kPa}})$	$b_M(10^{-2} \text{kPa})$
10	0.6515	2.6465	2.8790
	1.2904	2.0696	2.4416
	0.9929	2.7082	1.4029
	1.6048	3.3090	0.9303
		2.8792	1.0312
11	1.6288	5.2670	0.9706
	1.4314	2.6283	1.5637
	1.4312	1.4893	2.1373
	1.8304	1.3003	1.9031
	0.9730	2.0790	0.9965
Average	1.3150	2.6400	1.6256

TABLE 5. — Parameters (Zero Strain Moduli) of Volume Losses

TEST	$a_{UV} (10^{-6} \frac{1}{\text{kPa}})$	$a_{RV} (10^{-5} \frac{1}{\text{kPa}})$
14	3.6199	1.0476
	2.5836	1.3172
	1.7021	1.3398
	1.7469	1.5935
15	8.0148	1.4229
	5.4580	0.6481
	2.7755	0.0423
Average	1.70	0.25

and  $a_{RV}$  are substituted into Eq. 47 for  $a_M$  and  $a_V$  respectively; and the  $b_M$  value is substituted into Eq. 49.

The results of all pressuremeter tests are listed in Appendix V, and sample calculations are given below for Test 169.

(1) For the unloading portion:

$$\begin{aligned} a_{CU} &= (a_R - a_V) \frac{a_M}{a_M - a_R} , \\ &= (1.3877 \times 10^{-5} - 1.7 \times 10^{-6}) \frac{1.315 \times 10^{-4}}{1.315 \times 10^{-4} - 1.3877 \times 10^{-5}} , \\ &= 1.3614 \times 10^{-5} \text{ 1/kPa, and} \end{aligned}$$

$$E_{CU} = \frac{1}{a_{CU}} = \frac{1}{1.3614 \times 10^{-5}} = 73400 \text{ kPa .}$$

(2) For the reloading portion:

$$\begin{aligned} a_{CR} &= (a_R - a_V) \frac{1}{a_M - a_R} , \\ &= (2.2738 \times 10^{-5} - 0.25 \times 10^{-5}) \frac{2.64 \times 10^{-4}}{1.315 \times 10^{-4} - 1.3877 \times 10^{-5}} , \\ &= 2.2145 \times 10^{-5} \text{ 1/kPa;} \end{aligned}$$

$$b_{CR} = \frac{b_R b_M}{b_M - b_R} = \frac{9.174 \times 10^{-4} \cdot 1.6256 \times 10^{-2}}{1.6256 \times 10^{-2} - 9.174 \times 10^{-4}} = 9.7227 \times 10^{-4} ;$$

$$E_{CR} = \frac{1}{a_{CR}} = \frac{1}{2.2145 \times 10^{-5}} = 45100 \text{ kPa;}$$

$$\frac{1}{b_{CR}} = \frac{1}{9.7227 \times 10^{-4}} = 1030 \text{ kPa};$$

$$\frac{E_{CU}}{E_{CR}} - 1 = 0.62685.$$

During a pressuremeter test the pressure against the wall of the borehole increases from zero to the limit pressure. The stress level at which the soil is being tested increases accordingly. Since the modulus of deformation of most soils is sensitive to stress level it may be possible to characterize this variation with the pressuremeter. On Fig. 13, the zero strain reload modulus  $E_{CR}$  is obtained at a radial stress  $P_R(C)$ ; the zero strain unload modulus  $E_{CU}$  is obtained at a radial stress  $P_U(A)$ . If at A an infinitely small cycle was performed, the unload and reload modulus would be equal and, therefore, the zero strain reload modulus for the radial stress  $P_U(A)$  is  $E_{CU}$ . Assuming the common power law as characterization of stress sensitivity and the same  $k$  and  $n$  values for unload and reload, then

$$E_{CR} = k(P_R)^{n_p}, \text{ and} \quad (50)$$

$$E_{CU} = k(P_U)^{n_p}. \quad (51)$$

Therefore,

$$\frac{E_{CU}}{E_{CR}} = \left( \frac{P_U}{P_R} \right)^{n_p}, \quad (52)$$

and  $n_p$  can be determined from an unload-reload cycle during a pressuremeter test.

Generally in Eqs. 50 and 51, the stress is the minor stress or sometimes the first stress invariant. For the pressuremeter test this stress is the major principal stress and consequently the value of  $n_p$  obtained from pressuremeter test is likely to be different from the value of  $n$  obtained when using  $\sigma_3$  or  $\frac{\sigma_1 + \sigma_2 + \sigma_3}{3}$ .

Using Test 169 as an example, the calculation of  $n$  is shown below:

$$\frac{E_U}{E_R} = \left( \frac{P_U}{P_R} \right)^{n_p}; \quad (53)$$

therefore,

$$\begin{aligned} n_p &= \frac{\log E_U - \log E_R}{\log P_U - \log P_R} = \frac{\log(73400) - \log(45100)}{\log(478) - \log(124)}, \\ &= \frac{4.8657 - 4.6542}{2.6794 - 2.0934} = \frac{0.21152}{0.58601} = 0.36066. \end{aligned}$$

Various moduli were obtained from each pressuremeter test. The pressuremeter unloading modulus  $E_U$  was chosen as the reference modulus for the pressuremeter test. This is because this modulus is felt to have a higher level of reliability than the other pressuremeter moduli.  $E_U$  is not as influenced by the borehole disturbance as  $E_{oi}$  is;  $E_R$  was not chosen because its value seems to depend significantly on the reloading pressure and the shape of the reloading curve (Figs. 12(a) and 12(b)). The zero strain level was chosen as a reference level. Also resilient moduli are used in pavement design and  $E_U$  can be thought of as a resilient modulus.

### The Texas Triaxial Test Modulus

From the data points of the TTT obtained from SDHPT, the moduli are calculated at different confining pressure levels as follows.

The point which is recorded during the Texas triaxial test is point A as shown in Fig. 16(a). The secant modulus at point A of which the testing soil is at failure level can be calculated as

$$E_T = \frac{(\sigma_1 - \sigma_3)_f}{\epsilon_f}, \quad (54)$$

where

$E_T$  = the secant modulus at failure,

$\sigma_{1f}$  = the applied axial pressure at failure ,

$\sigma_{3f}$  = the confining pressure at failure,

$(\sigma_1 - \sigma_3)_f = \sigma_{1f} - \sigma_{3f}$  , and

$\epsilon_f$  = the vertical strain at failure.

Appendix VI lists the TTT moduli and confining pressure  $\sigma_3$  for several sections where data existed prior to this research project.

Three equations can be written:

$$E = k (\sigma_3)^{n_T}, \quad (55)$$

$$E = k (\sigma_1)^{n_P}, \text{ and} \quad (56)$$

$$E = k \left( \frac{\sigma_1 + \sigma_2 + \sigma_3}{3} \right)^{n_a}. \quad (57)$$

Using Eq. 55,  $n_T$  values were obtained for the TTT. Since the initial tangent modulus is used, the initial stress state should be used in Eqs. 55 to 57. In this case,  $\sigma_3$  is known, and  $\sigma_1$  is zero. Eq. 55 was selected and, as can be seen from Figs. 16(a)-16(f), the  $n_T$  values from the TTT differ from the  $n_P$  values from the pressuremeter test as shown

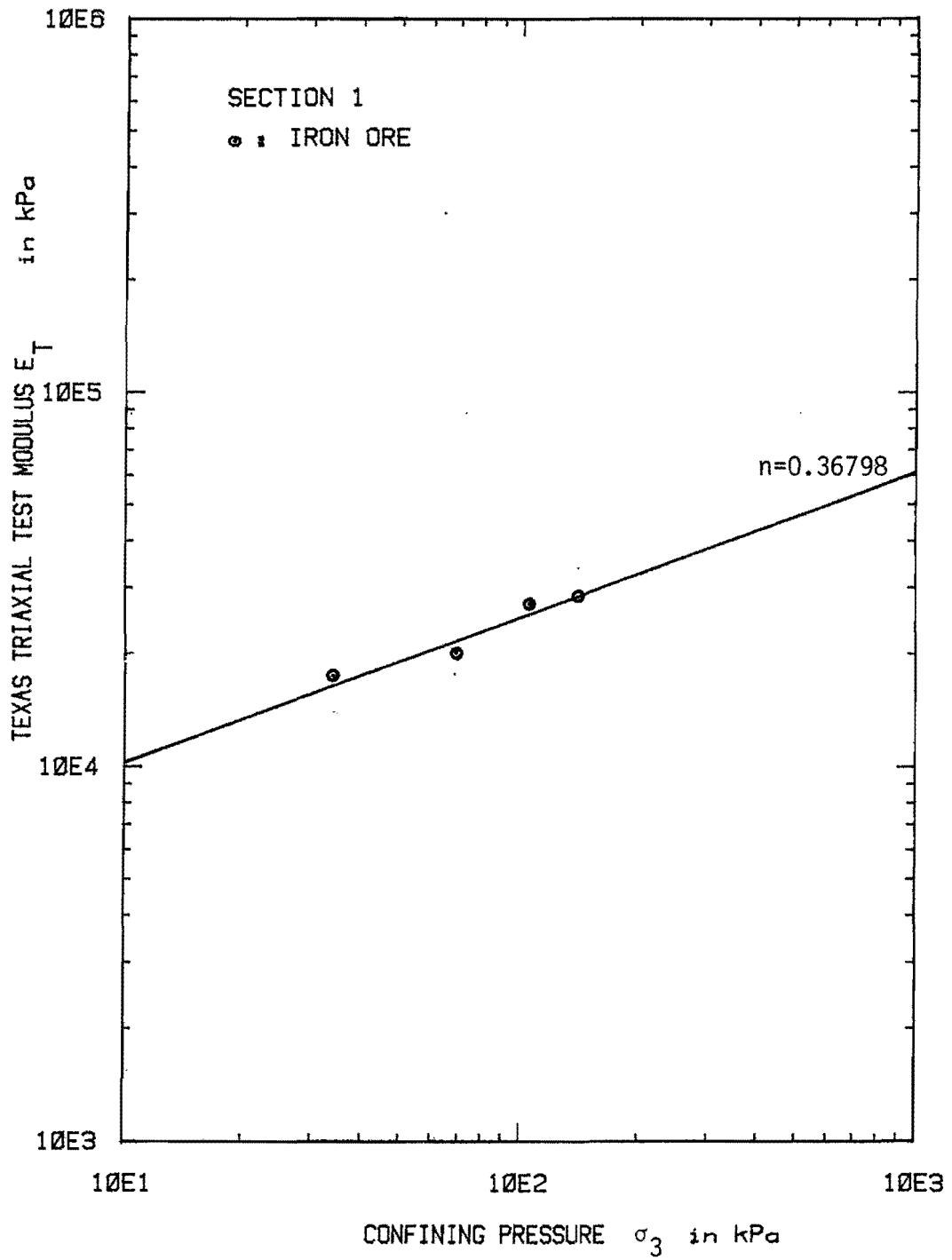


FIG. 16(a) — TTT Modulus versus Confining Pressure -  
 Section 1

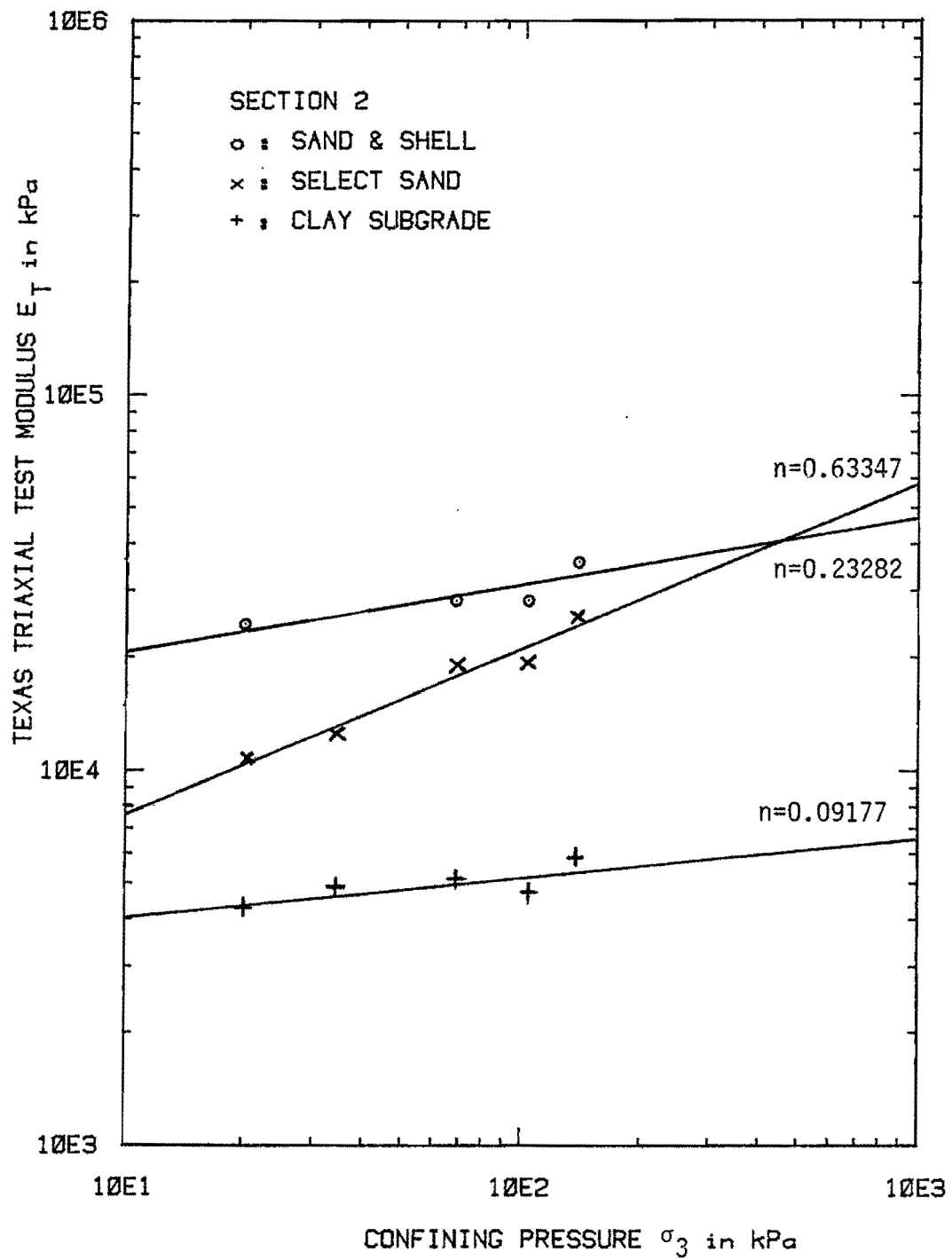


FIG. 16(b) — TTT Modulus versus Confining Pressure -  
Section 2

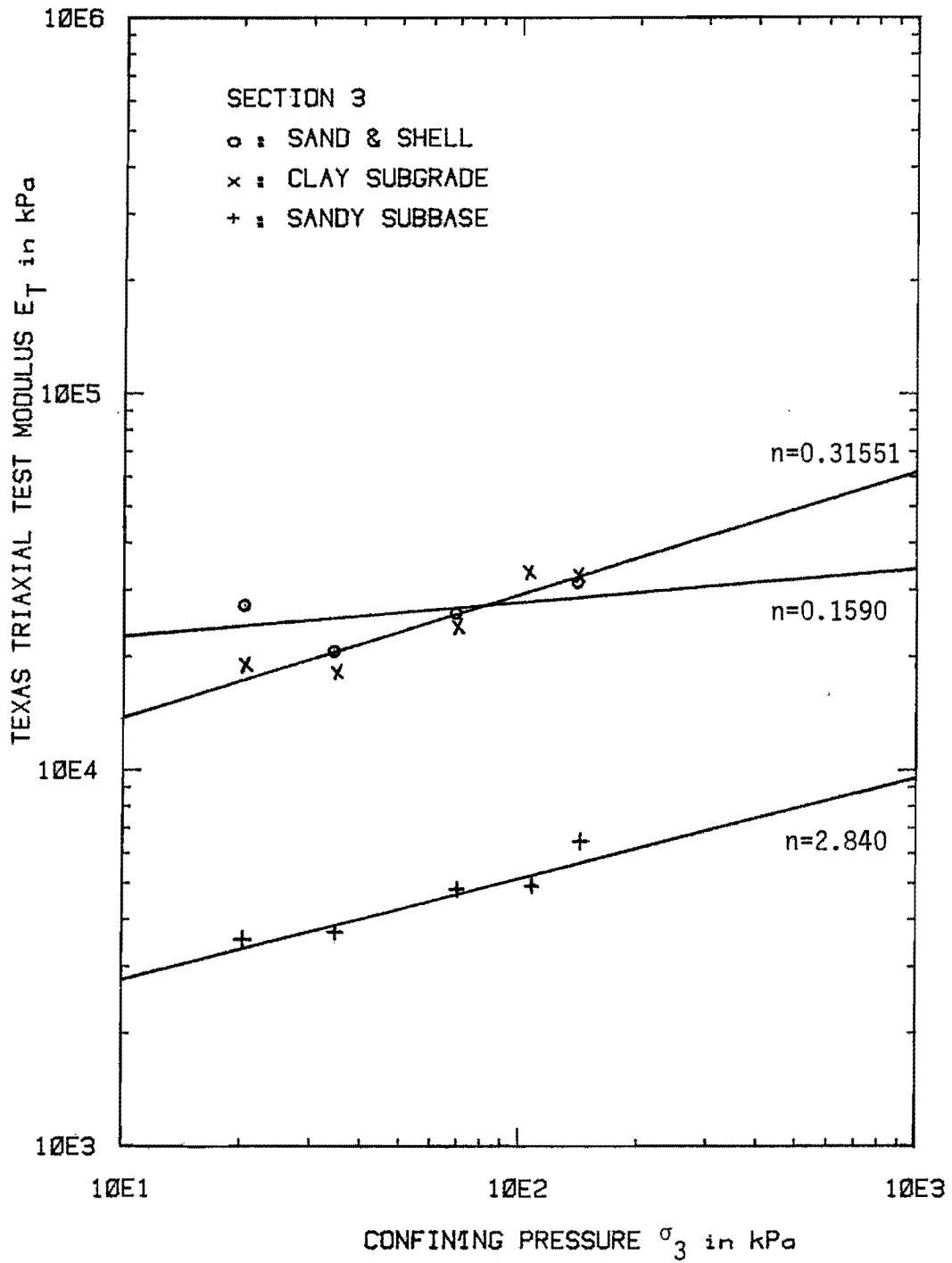


FIG. 16(c) — TTT Modulus versus Confining Pressure -  
Section 3

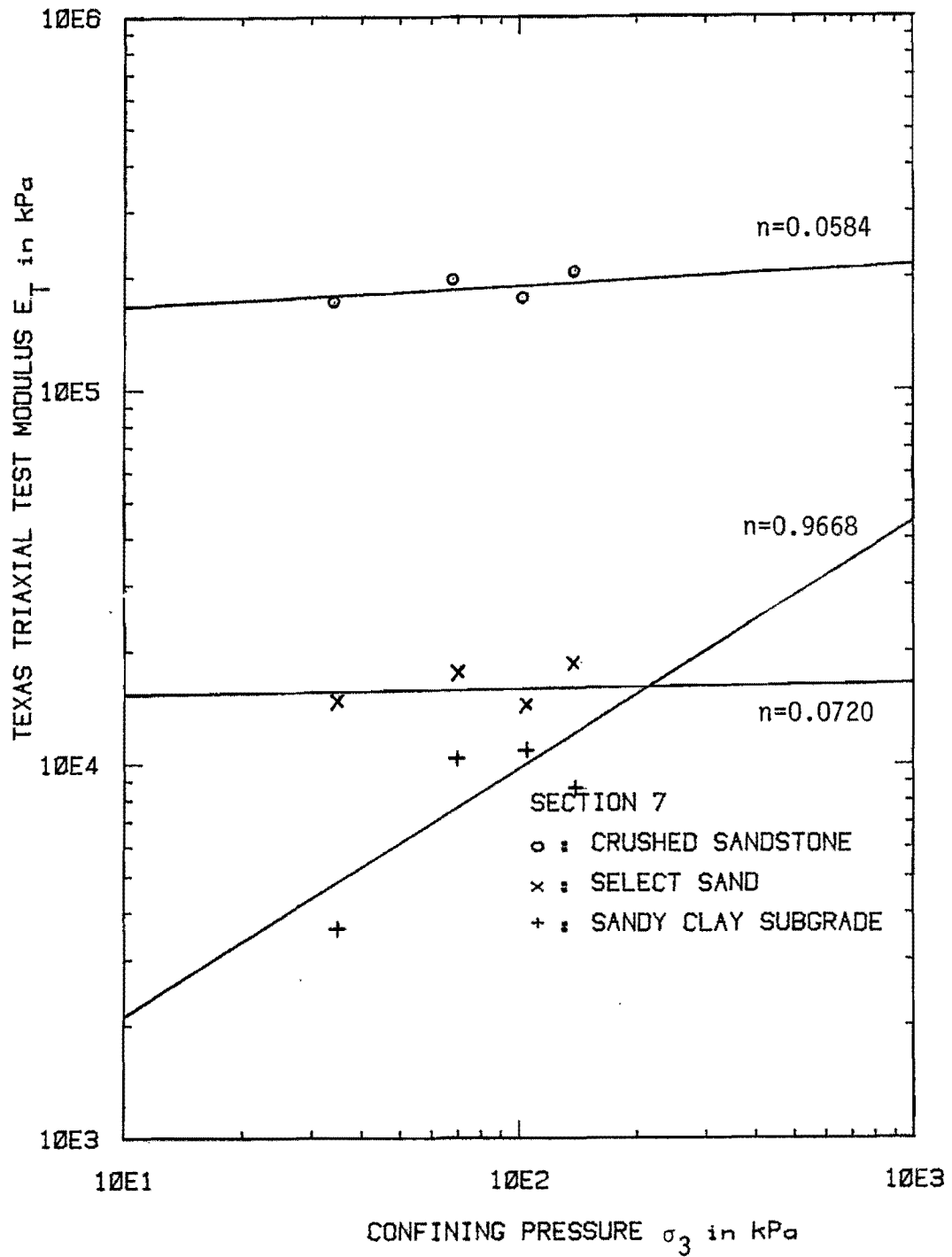


FIG. 16(d) — TTT Modulus versus Confining Pressure -  
Section 7

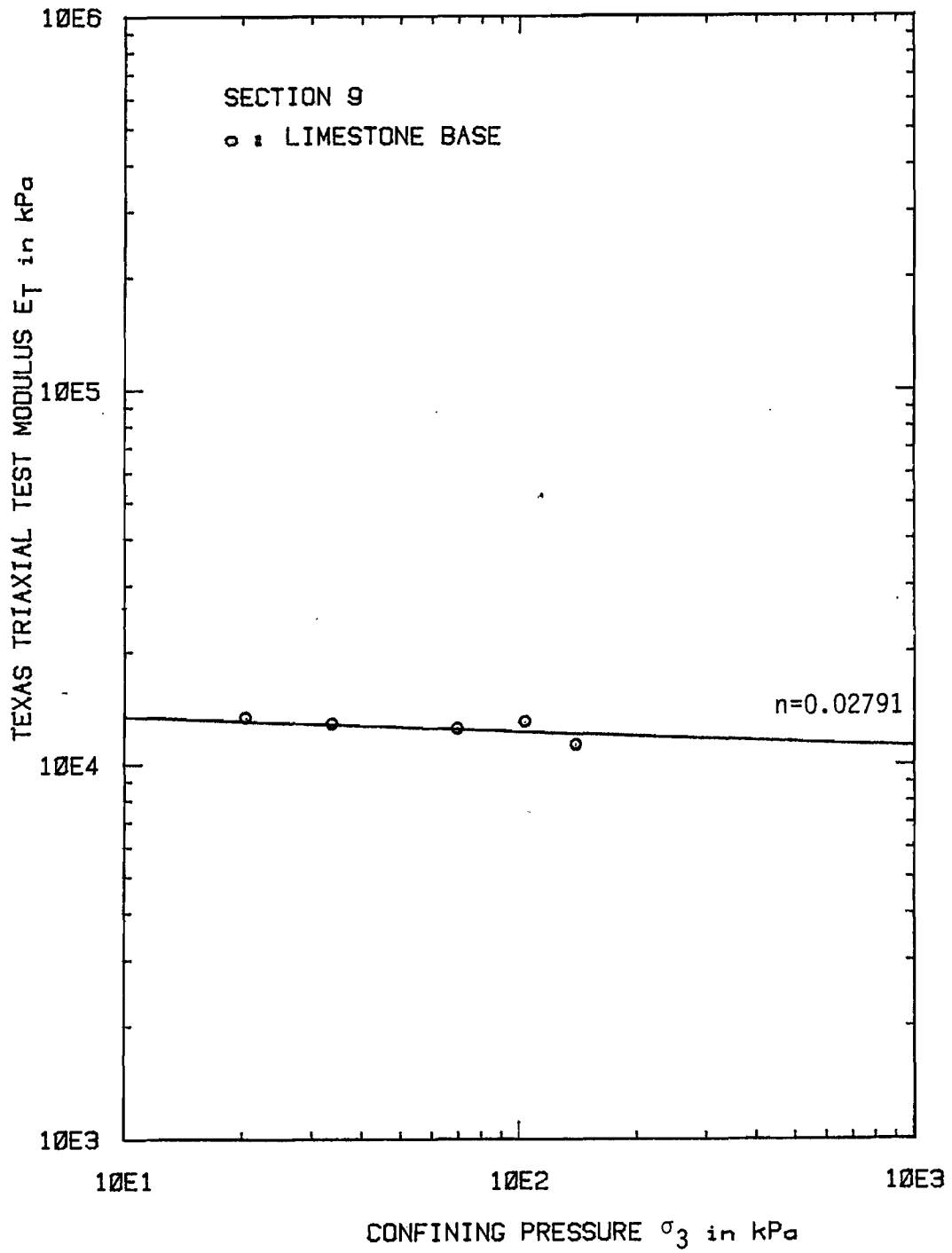


FIG. 16(e) — TTT Modulus versus Confining Pressure -  
 Section 9

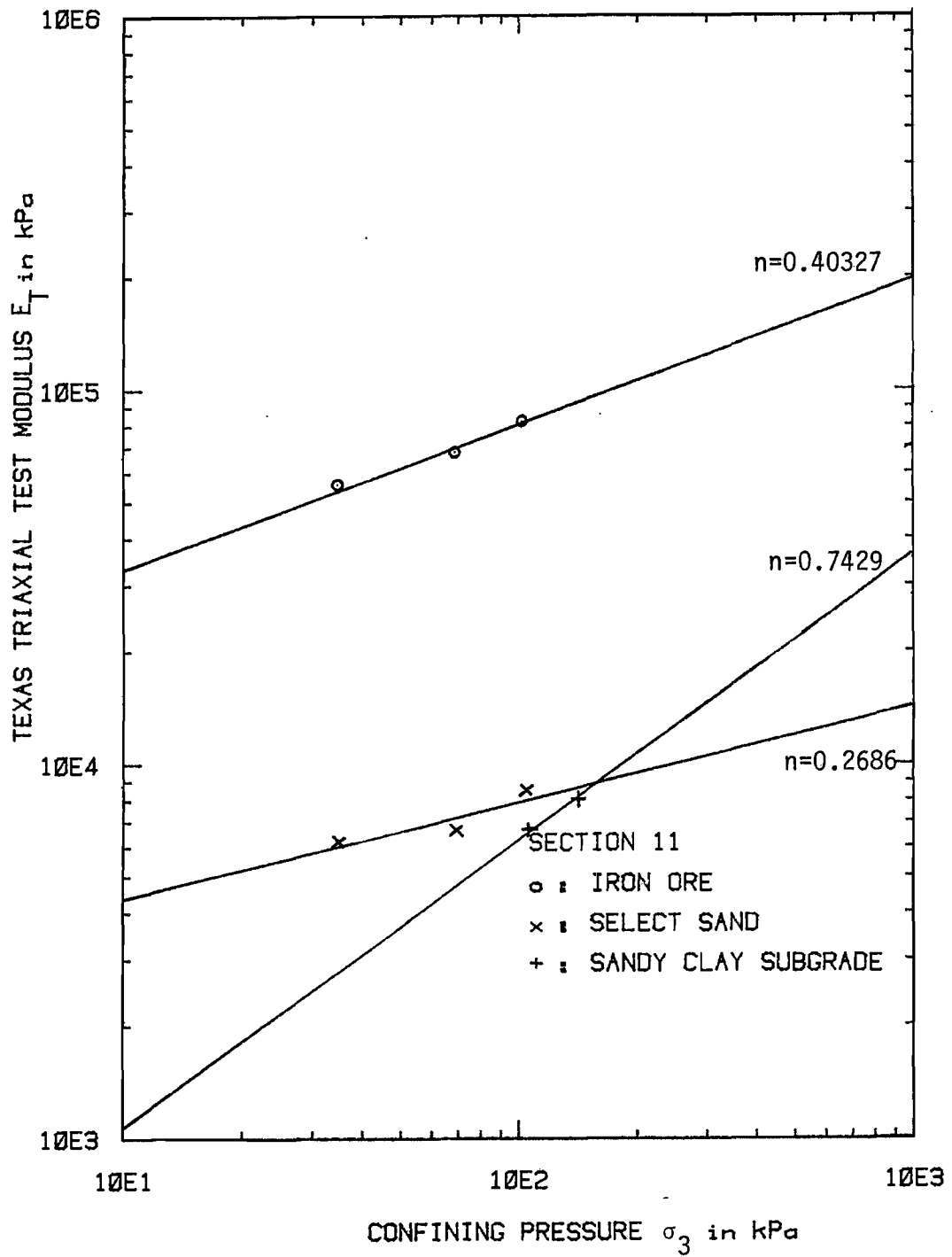


FIG. 16(f) — TTT Modulus versus Confining Pressure -  
Section 11

in Table 6. This is probably due to the fact that Eq. 55 is used for the TTT while Eq. 56 is used for the pressuremeter test, and the fact that the Texas Triaxial test data was not obtained at the same time and at the same location as the pressuremeter data. Instead, the TTT data was obtained from the files of the SDHPT.

### Dynalect Modulus

The Russian equation computer program was used. In this program, a known deflection basin measured under the wheels of the Dynalect is input together with a first guess of the layer moduli and the constants needed in the theory. The program uses an iteration technique and a best-fit method to determine the layer moduli which will give a calculated deflection basin as close to the measured deflection basin as possible with this theory.

The zero strain unload pressuremeter moduli measured in the various pavement and subgrade layers were used as the first guess of the layer moduli; the program calculated the deflection basin under the Dynalect loading with these moduli as layer input. Then the program started the iteration process to zero in on the "best fit" set of moduli. Table 7 collects the iterated moduli of all sections obtained with the Dynalect-Russian equation method.

### Correlations and Analysis

The analysis of the test data led to the determination of a number of parameters. The following correlations have been found between these parameters.

TABLE 6. — List of Exponents n

Section	Layer	$n_p$	$n_T$
1	2	1.45	0.368
	3	1.054	
	4	0.870	
2	2	1.229	0.233
	3		0.633
	4	0.388	0.092
		0.527	
3	2	1.071	0.159
	3	0.938	0.316
	4	0.415	
		0.374	0.284
4	2	1.198	
	3	0.305	
	4	0.582	
	5	0.375	
5	2	0.847	
	4	0.255	
		0.488	
6	2	0.323	
	3	0.635	
	4	0.448	
7	2	1.430	0.058
	3	0.598	0.072
	4	0.532	0.987
9	3	1.329	-0.028
	4	0.243	
		0.662	
10	2	1.180	
	4	0.588	
		0.383	
		0.630	
11	2	1.112	0.403
	3	0.968	0.269
	4	0.708	0.743
12	2	0.869	
	4	0.685	
		0.956	

TABLE 7. - Iterated Moduli of Dynaflect/Russian Equation

Section	Layer	E <sub>p</sub> (psi)	E <sub>D</sub> (E <sub>Russian</sub> (psi))				
1	2	139376	51923	40271	26270	17413	39757
	3	133720	37169	62886	38695	41294	44674
	4	130239	43688	62738	35543	44480	41563
	5	41479	17005	17646	15266	16005	16611
2	2	221900	19001	19568	21241	20014	20730
	3	21174	29921	29713	29117	29148	28742
	4	6526	5115	5157	5209	5183	5227
3	2	100073	8113	5603	10150	11160	11244
	3	33647	30636	29657	31557	34365	34819
	4	25235	22171	21157	24206	30356	25296
	5	14213	7674	7271	7116	7830	7531
4	2	213198	24207	24207	24207	24207	24207
	3	20159	11168	11168	11168	11168	11168
	4	69615	60624	60624	60624	60624	60624
	5	31327	22336	22336	22336	22336	22336
5	2	42059	8726	8726	8726	8726	8726
	3	14068	10734	10734	10734	10734	10734
	4	13923	17256	17256	17256	17256	17256
6	2	182741	43925	43111	50584	48595	50322
	3	72661	21063	21121	21273	21191	21014
	4	13343	5831	5853	5909	5879	5813

TABLE 7. -- (Continued)

Section	Layer	$E_p$ (psi)	$E_D(E_{\text{Russian}}(\text{psi}))$					
7	2	--	--	--	--	--	--	--
	3	70340	11875	12162	12454	11575	11337	9828
	4	11312	10931	10948	10815	11065	11088	11440
9	2	194344	242969	237211	216330	216316	274289	
	3	7496	10190	10176	11815	11815	10190	
	4	2799	4000	4000	4000	4000	4000	
11	2	91950	29205	21991	23005	18029	16511	
	3	131545	71283	57492	62702	57994	56169	
	4	18419	10508	9810	9371	9752	9711	
12	2	117331	34677	63648	30098	36544	33491	
	3	55837	25494	10965	20370	16968	14573	
	4	137491	9287	9262	10547	11751	12551	
10	2	59463	21941	21941	21941	21200	21941	
	3	12762	5241	5241	5241	4870	5241	
	4	5511	4715	4656	4775	4994	4733	

(1) Pressuremeter unloading modulus  $E_U$  versus pressuremeter initial secant modulus  $E_{oi}$ : The first loading pressuremeter modulus was determined from the portion EF of the pressuremeter curve (Fig. 13); the zero strain unloading pressuremeter modulus was determined as explained in the section entitled calculation of the corrected moduli. Fig. 17 shows the correlations between the two moduli. It is likely that the pressure level at which the unloading begins has some influence on the value of  $E_U$ . This pressure level varies from one test to the next and may be the reason for the scatter of Fig. 17. The equation of the straight line on Fig. 17 is

$$E_U = 0.2695 (E_{oi})^{1.4538} . \quad (58)$$

(2) Pressuremeter unloading modulus  $E_U$  versus TTT modulus  $E_T$ : The TTT modulus was obtained as explained in the section entitled "Texas Triaxial test modulus" in this report. Fig. 18 shows the relation between  $E_U$  and  $E_T$ . The TTT modulus  $E_T$  was calculated at a confining pressure ( $\sigma_3$ ) of 5 psi (34.5 kPa). The unloading modulus  $E_U$  was obtained at a pressure  $P_U$  and reduced to a pressure of 5 psi (34.5 kPa) by use of Eq. 52. This pressure of 5 psi (34.5 kPa), however, represents the major principal stress, whereas it is the minor principal stress in the TTT. This difference may account for part of the scatter.

(3) The pressuremeter unloading modulus  $E_U$  versus the Dynaflect/Russian equation modulus  $E_D$ : Fig. 19 presents the graph of  $E_U$  versus  $E_D$ ; some scatter is evident. The scatter could be due to the inaccuracies in the pressuremeter measurements and data reduction, or

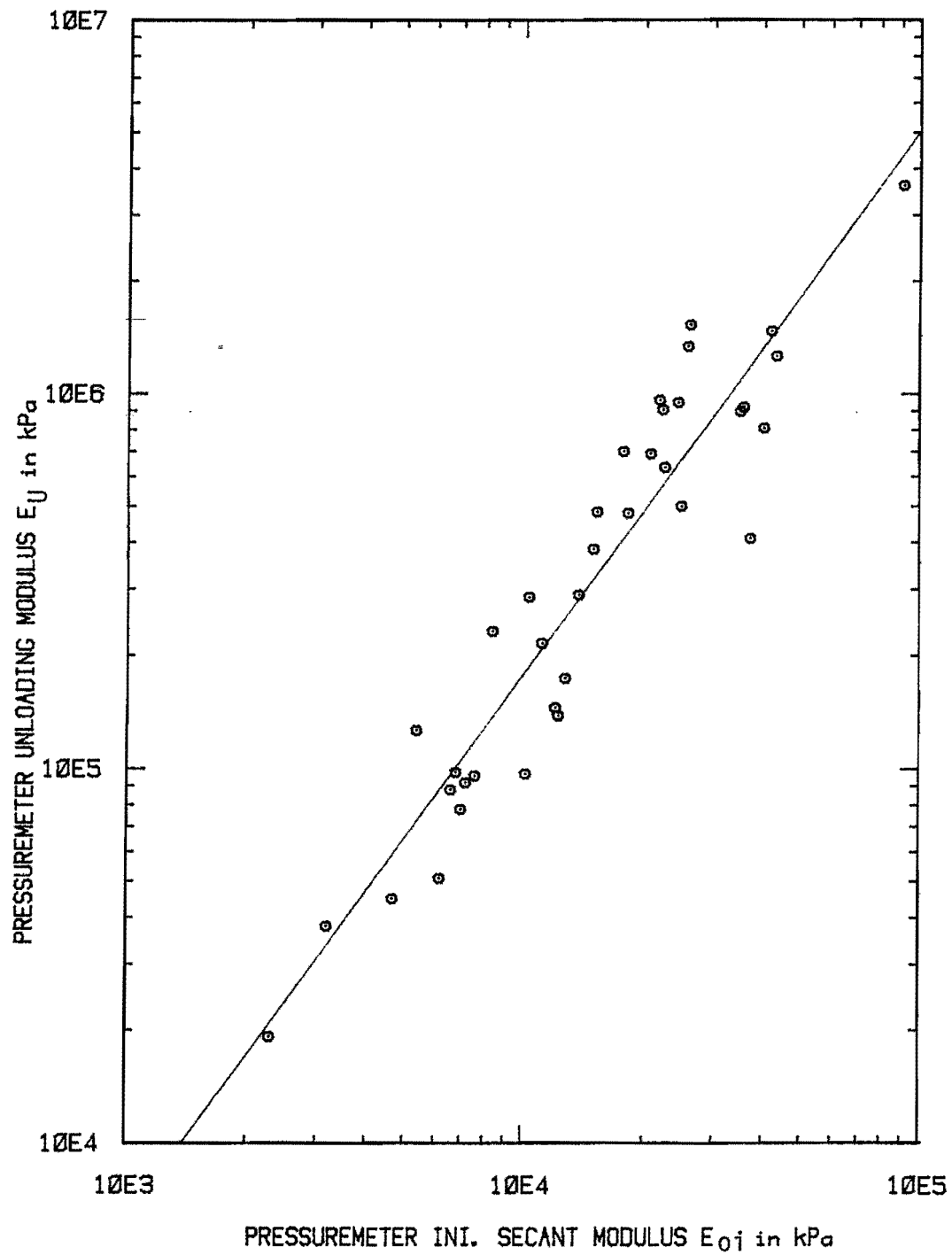


FIG. 17. — Pressuremeter Initial Modulus  $E_{0i}$  versus Pressuremeter Unloading Modulus  $E_U$

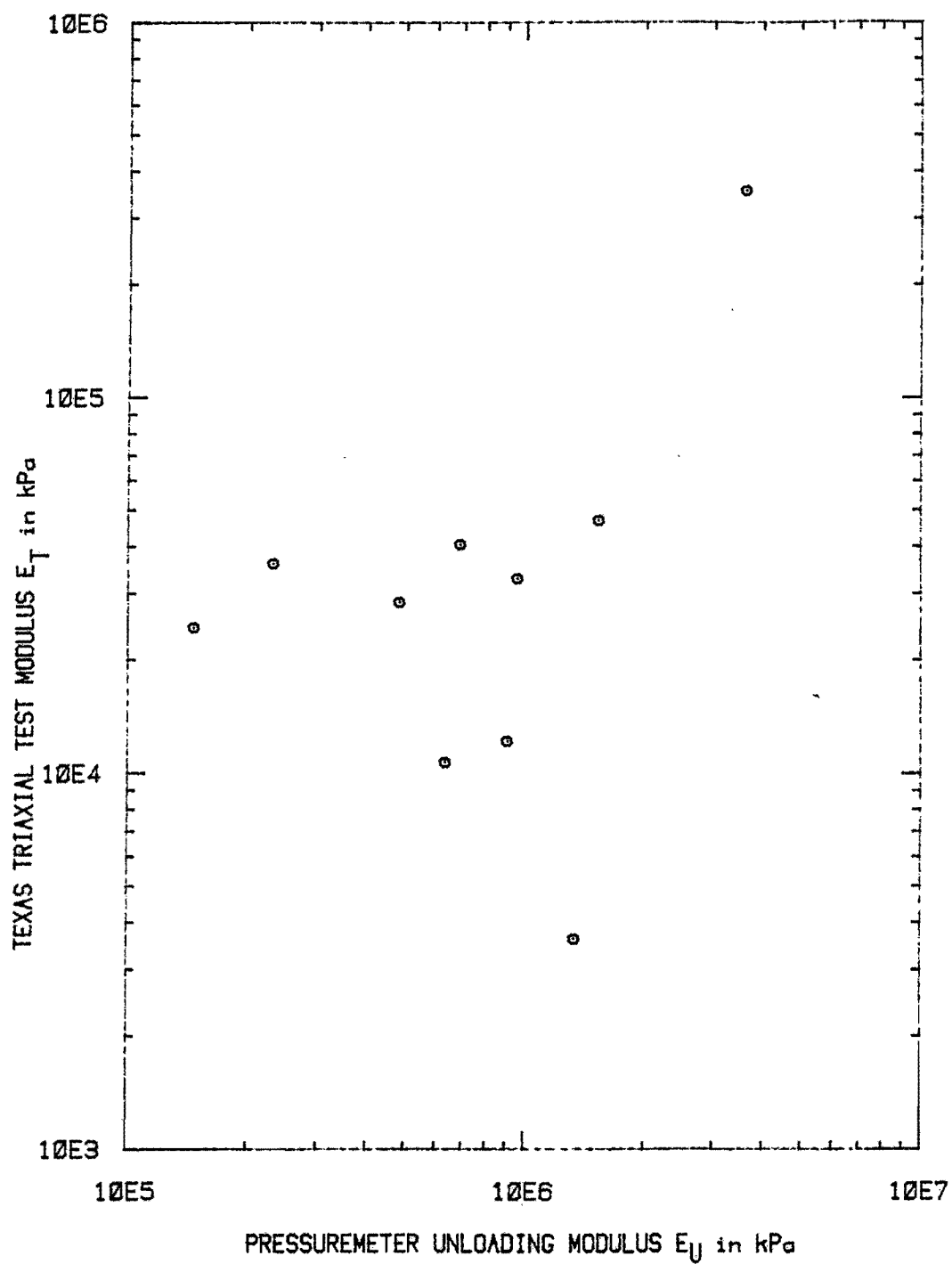


FIG. 18. — Pressuremeter Unloading Modulus  $E_U$  versus  
TTT Modulus  $E_T$

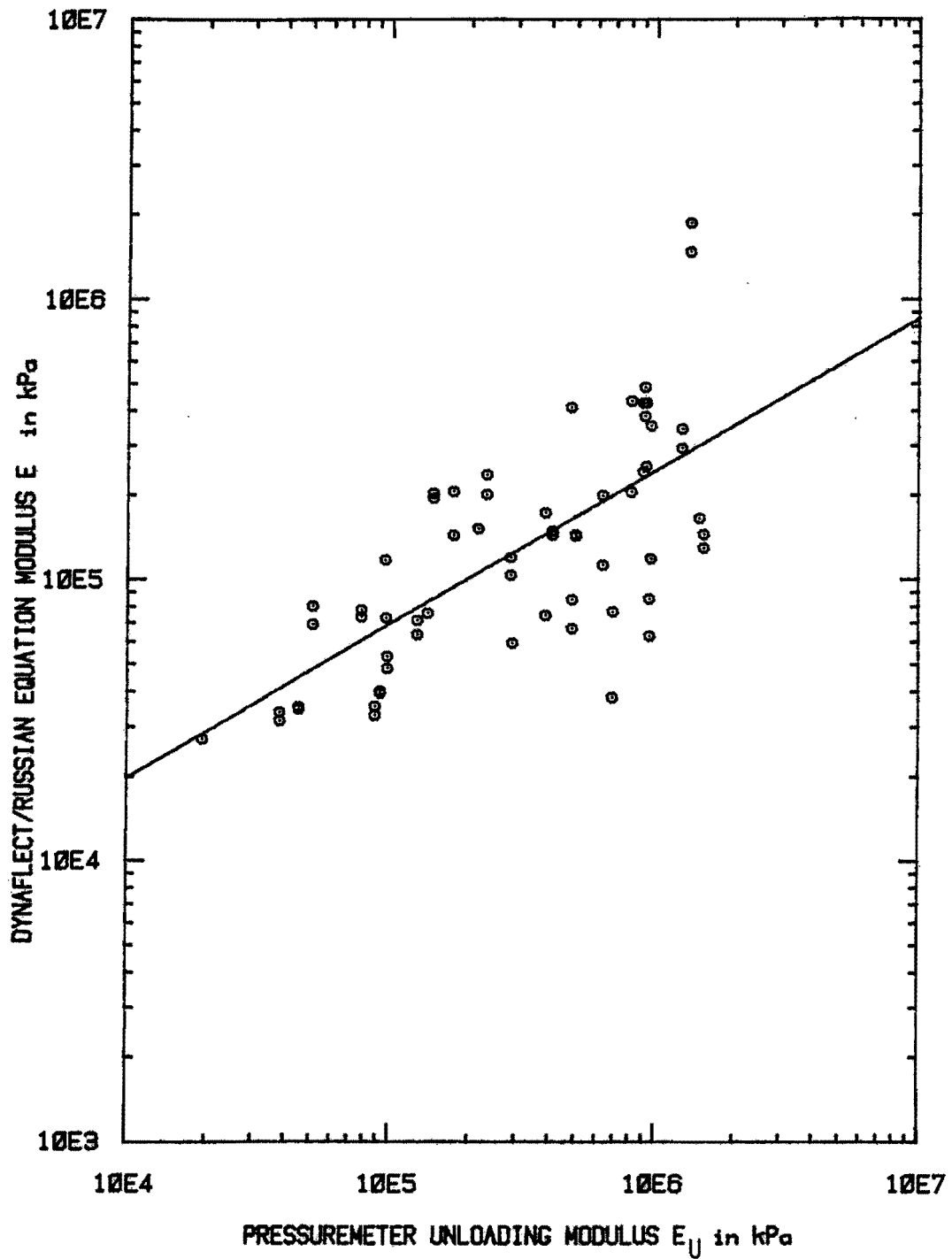


FIG. 19. - Pressuremeter Unloading Modulus  $E_U$  versus  
 Dynaflect/Russian Equation Modulus  $E_D$

in the Russian equation theory, or both. It may also be due to the fact that the stress level is constant for the Dynaflect test while it is not constant for the pressuremeter test. The strain level is constant and small for the Dynaflect test and was chosen as zero for the pressuremeter test. However, the stress level at which the pressuremeter modulus is measured is usually higher than the stress level at which the Dynaflect modulus is obtained. Since higher stress levels give higher moduli, it is not surprising to find that the pressuremeter modulus is consistently higher than the Dynaflect modulus (Fig. 19).

(4) The surface deflections calculated by introducing pressuremeter unloading modulus  $E_U$  into the Russian equation are consistently smaller than the measured deflections as shown on Fig. 20. They range from 10% to 65% of the measured values and average 35%. This suggests that pressuremeter unloading moduli are higher than the ones required to obtain a reasonable calculated deflection under the Dynaflect loading, as was found in the previous correlation.

(5) The limit pressure  $P_1$  versus blow count on the rod used to prepare the pressuremeter hole shows a certain scatter (Fig. 21).

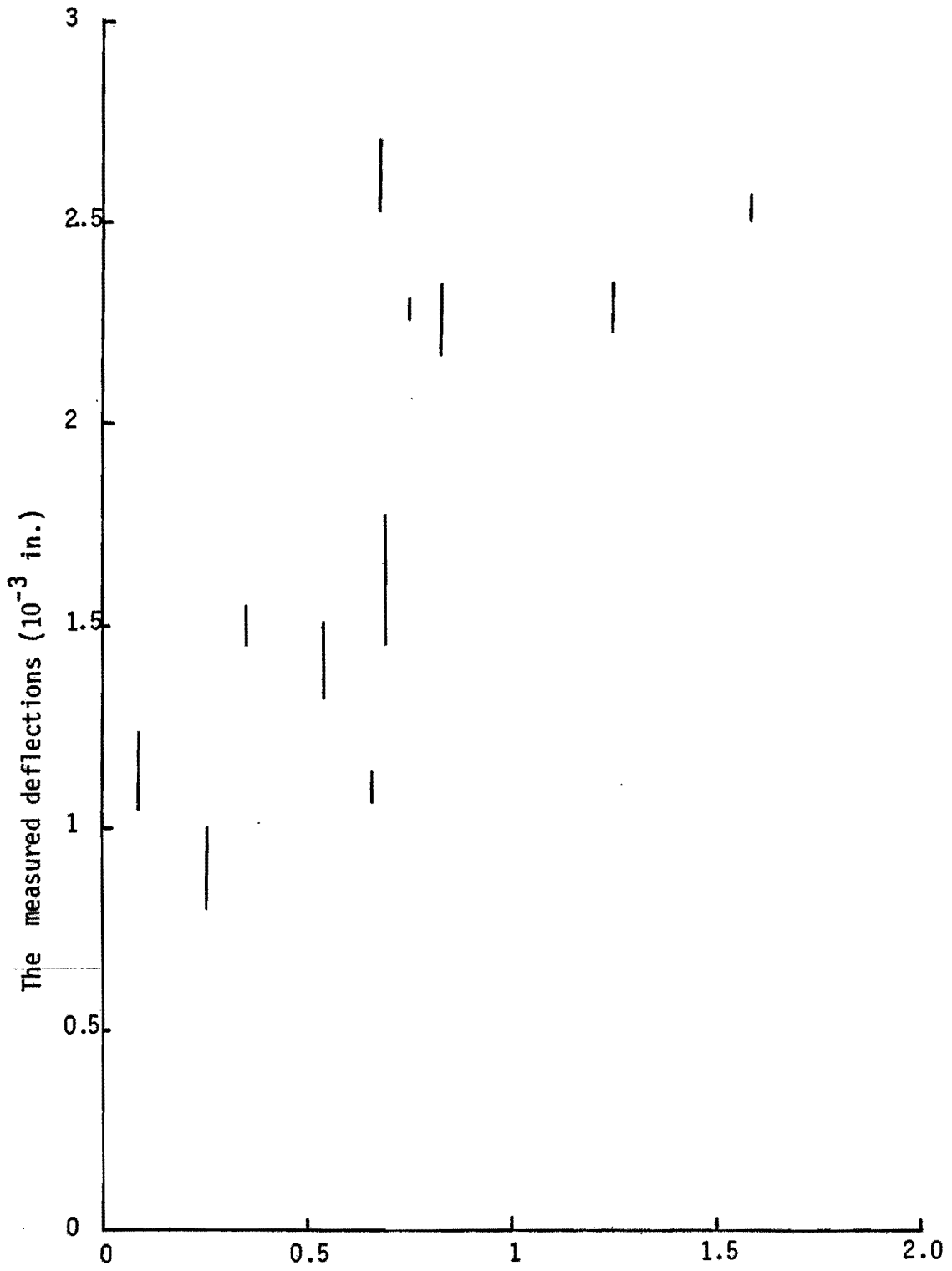
The equation of the straight line on Fig. 21 is

$$P_1 = 74.4 + 57.6 \times N. \quad (59)$$

The scatter is probably due to the imprecisions involved in the rod driving test.

(6) The unloading pressuremeter modulus  $E_U$  versus water content  $w$  (Fig. 22) can be characterized by the following relationship:

$$\log (E_U) = 6.17 - 0.048 \times w, \quad (60)$$



The measured deflections from  $E_U$  ( $10^{-3}$  in.)

The calculated deflections from  $E_U$  ( $10^{-3}$  in.)

FIG. 20. — The Calculated Deflections versus The Measured Deflections

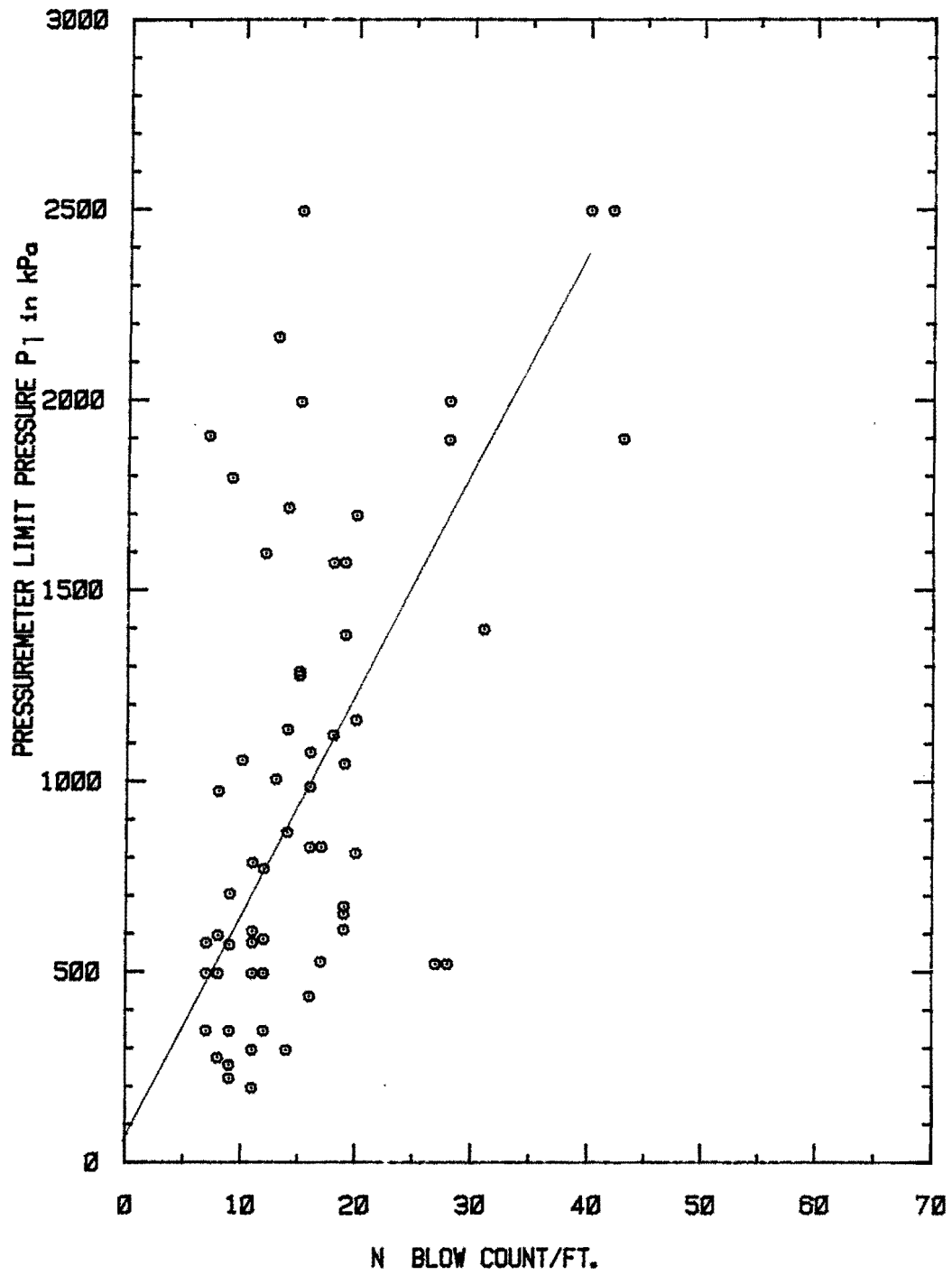


FIG. 21. - The Limit Pressure  $P_1$  versus Blow Count  $N$

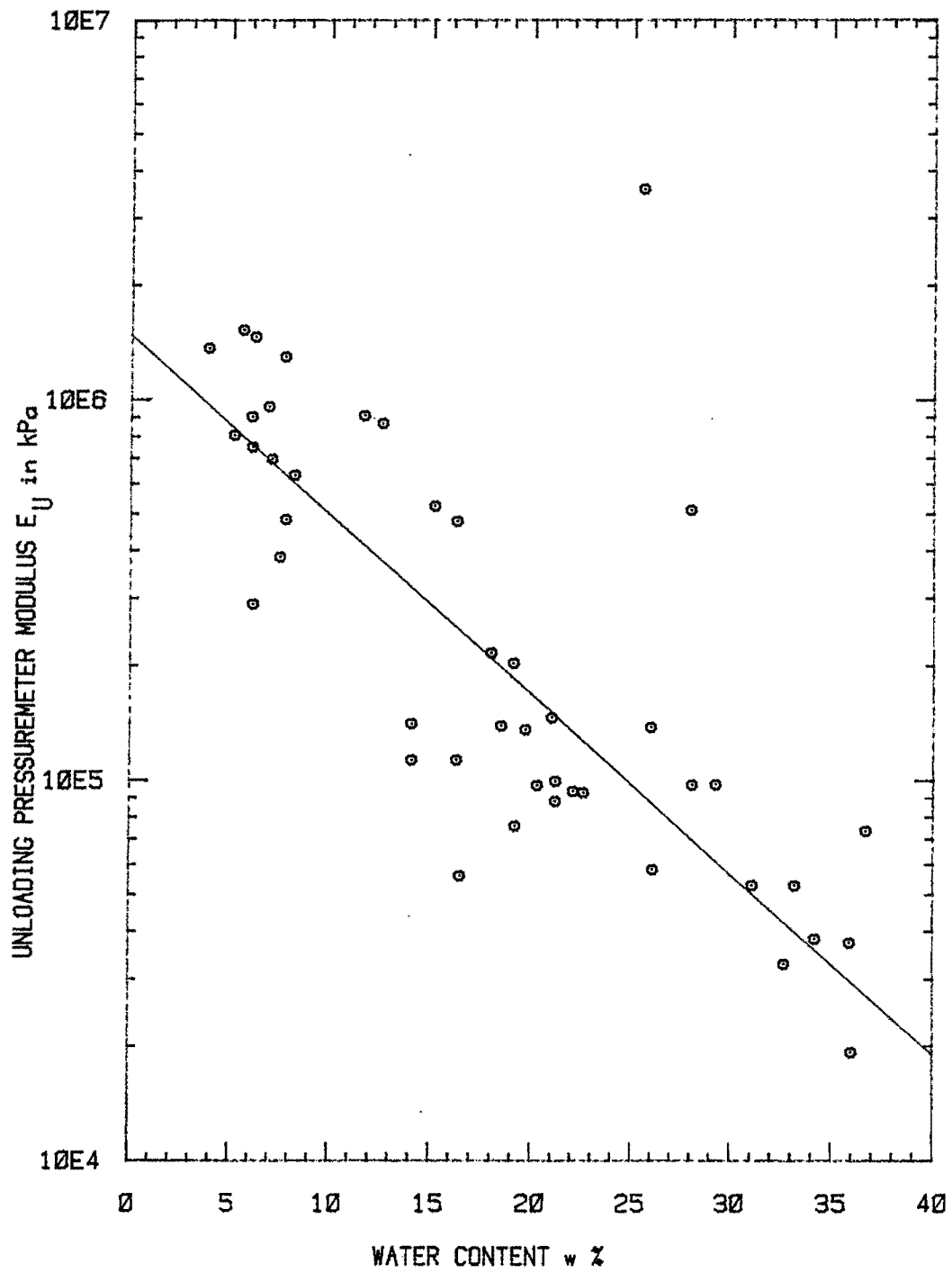


FIG. 22. — Water Content  $w$  versus Unloading Pressuremeter Modulus  $E_U$

where  $E_U$  is in kPa and  $w$  in percentage. The correlation is fairly good and underlines the basic importance of a simple parameter--the water content.

(7) The limit pressure  $P_1$  versus the Texas Triaxial classification TC (Fig. 23) shows a fair correlation:

$$P_1 = 3000 - 460 \times (TC) \text{ with } P_1 \text{ in kPa.} \quad (61)$$

(8) The relationship between the  $n_p$  values obtained from pressuremeter and the  $n_T$  values calculated from the TTT (Fig. 24) is poor.

### The Equivalency Factors

For the calculation of equivalency factors, the Odemark's assumption was made in all cases. This assumption is a reasonable one, especially in the case of unbound base courses (12);

$$\frac{H_B}{H_A} = \left(\frac{E_A}{E_B}\right)^n, \text{ with } n = 0.333. \quad (1)$$

The equivalency factors are calculated and listed in Tables 8(a) - 8(c), and Fig. 25 gives the comparison among these three sets of equivalency factors. The factors have been calculated on the basis of the pressuremeter moduli, of the Dynaflect moduli, and of the TTT moduli leading to three sets of equivalency factors.

The numbers in Columns 8 and 9 in Table 8(b) are calculated by substitution into Eq. 3 so that

$$E.F. = \frac{E_{D(Ref.)}^{n(Ref.)}}{E_{D(i)}^{n(i)}},$$

where  $n_{(Ref.)}$  and  $n_{(i)}$  are values from Russian equation iteration.

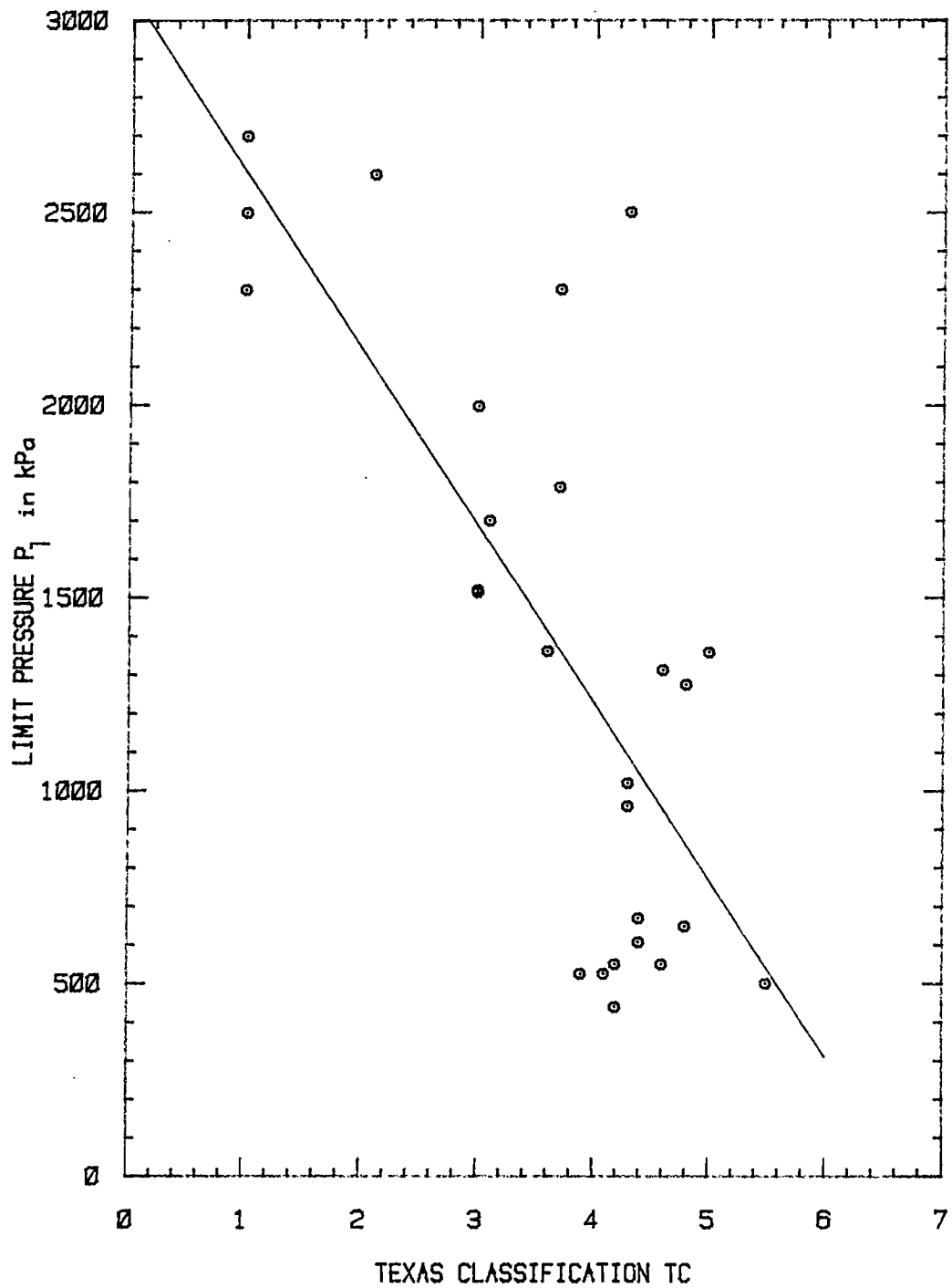


FIG. 23. — The Limit Pressure  $P_l$  versus  
Texas Classification TC

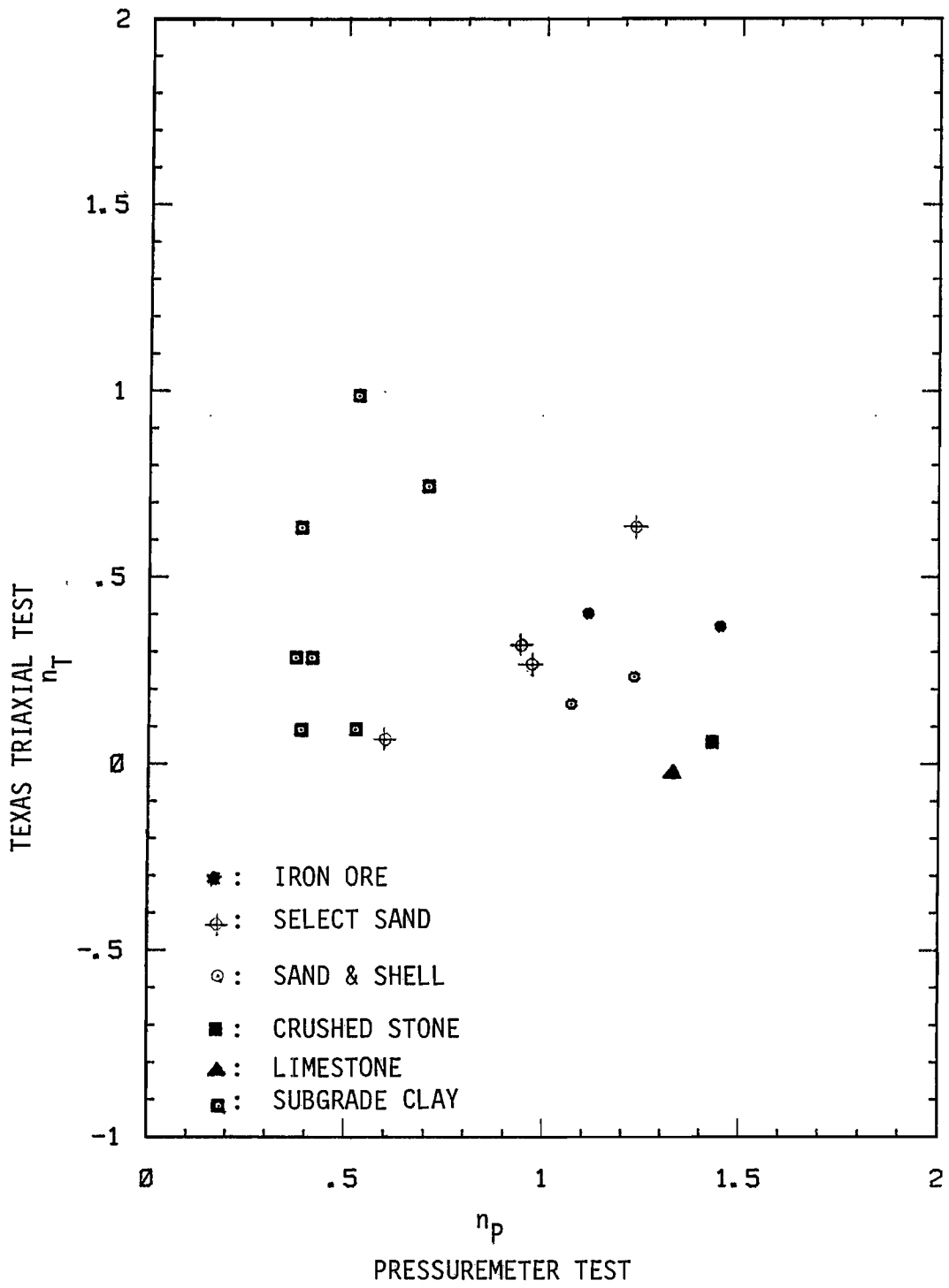


FIG. 24. The  $n_p$  versus The  $n_T$

TABLE 8. - Equivalency Factors

(a) From Pressuremeter Unloading Moduli

Material	Section -Layer	Thickness H (inch)	$E_U$ (kPa)	Average $E_U$	E.F. $p^+$	E.F. $p$
Iron ore	1-2	7.25	961000		1.134	1.027
	11-2	11.0	634000		1.302	1.179
	12-2	9.0	809000		1.201	1.087
					1.212	1.100
Sand and Shell	2-2	12.0	1530000*	1400000 <sup>+</sup>	0.971	0.879
	3-2	12.0	690000	1040000		1.147
	4-2	8.0	1470000*		0.984	0.891
	5-2	5.0	290000			1.531
	6-2	4.0	1260000*		1.036	0.938
	9-3	8.6	1340000*		1.015	0.919
	10-2	6.0	700000			1.141
					1.002	1.064
Select Sand	1-3	4.0	922000		1.149	1.041
	11-3	11.0	907000		1.156	1.047
	3-3	12.0	232000		1.149	1.041
	6-3	10.0	501000		1.409	1.276
	7-3	12.0	485000		1.424	1.290
	10-4	6.0	410000		1.506	1.364
	2-3	6.0	146000		2.124	1.924
	4-3	9.0	139000		2.160	1.956
	5-3	7.5	290000		1.690	1.531
					1.604	1.453
Lime Treated Sandstone	7-2	10.0	3600000		0.730	0.661

Note: + values calculated using the \* numbers to calculate the average  $E_U$ .

TABLE 8. - (Continued)

(b) From the Dynaflect/Russian Equation Moduli

Material	Section -Layer	Thickness H (inch)	$E_D$ (psi)	Average $E_D$	$E.F._D^+$	$E.F._D$	$E.F._D^+$	$E.F._D$
Iron Ore	1-2	7.25	35126		0.858	1.181	1.183	1.548
	11-2	11.0	21749		1.006	1.386	1.204	1.576
	12-2	9.0	39693		0.823	1.134	0.712	0.931
					0.896	1.234	1.033	1.352
Sand and Shell	2-2	12.0	20111*	22159 <sup>+</sup>	1.033	1.422	1.068	1.397
	3-2	12.0	9255	57838		1.842		
	4-2	8.0	24207*		0.971	1.337	0.939	1.228
	5-2	5.0	8726			1.879		1.476
	6-2	4.0	47307			1.069		0.921
	9-3	8.6	237423			0.625		1.074
	10-2	6.0	--		--	--	--	--
					1.002	1.362	1.004	1.219
Select Sand	1-3	4.0	44944		0.790	1.088	1.100	1.435
	11-3	11.0	61129		0.713	0.982	0.866	1.132
	3-3	12.0	32206		0.883	1.216	0.997	1.304
	6-3	10.0	21133		1.016	1.399	0.931	1.218
	7-3	12.0	11539		1.243	1.711	1.286	1.682
	10-4	6.0	--		--	--	--	--
	2-3	6.0	--		--	--	--	--
	4-3	9.0	11168		1.257	1.730	1.222	1.599
	5-3	7-5	8726		1.364	1.879	1.128	1.476
					1.038	1.429	1.076	1.407
Lime Treated Sandstone	7-2	10.0	78010		0.657	0.905	0.679	0.888

Note: + values calculated using the \* numbers to calculate the average  $E_D$ .

TABLE 8. - (Continued)  
(c) From the TTT Moduli

Material	Section - Layer	Thickness H (inch)	$E_T$ (kPa)	Average $E_T$	E.F. $_T^+$	E.F. $_T$
Iron Ore	1-2	7.25	32800		1.100	0.974
	11-2	11.0	10700		1.600	1.415
	12-2	9.0	--		--	--
					1.350	1.195
Sand and Shell	2-2	12.0	46800*	43650 <sup>+</sup>	0.977	0.865
	3-2	12.0	40500*	30307	1.025	0.908
	4-2	8.0	--		--	--
	5-2	5.0	--		--	--
	6-2	4.0	--		--	--
	9-3	8.6	3620			2.030
	10-2	6.0	--		--	--
						1.001
Select Sand	1-3	4.0	--		--	--
	11-3	11.0	12200		1.530	1.354
	3-3	12.0	36100		1.065	0.943
	6-3	10.0	--		--	--
	7-3	12.0	28400		1.154	1.022
	10-4	6.0	--		--	--
	2-3	6.0	24400		1.214	1.075
	4-3	9.0	--		--	--
	5-3	7.5	--		--	--
						1.241
Lime Treated Sandstone	7-2	10.0	355000		0.497	0.440

Note: + values calculated using the \* numbers to calculate the average  $E_U$ .

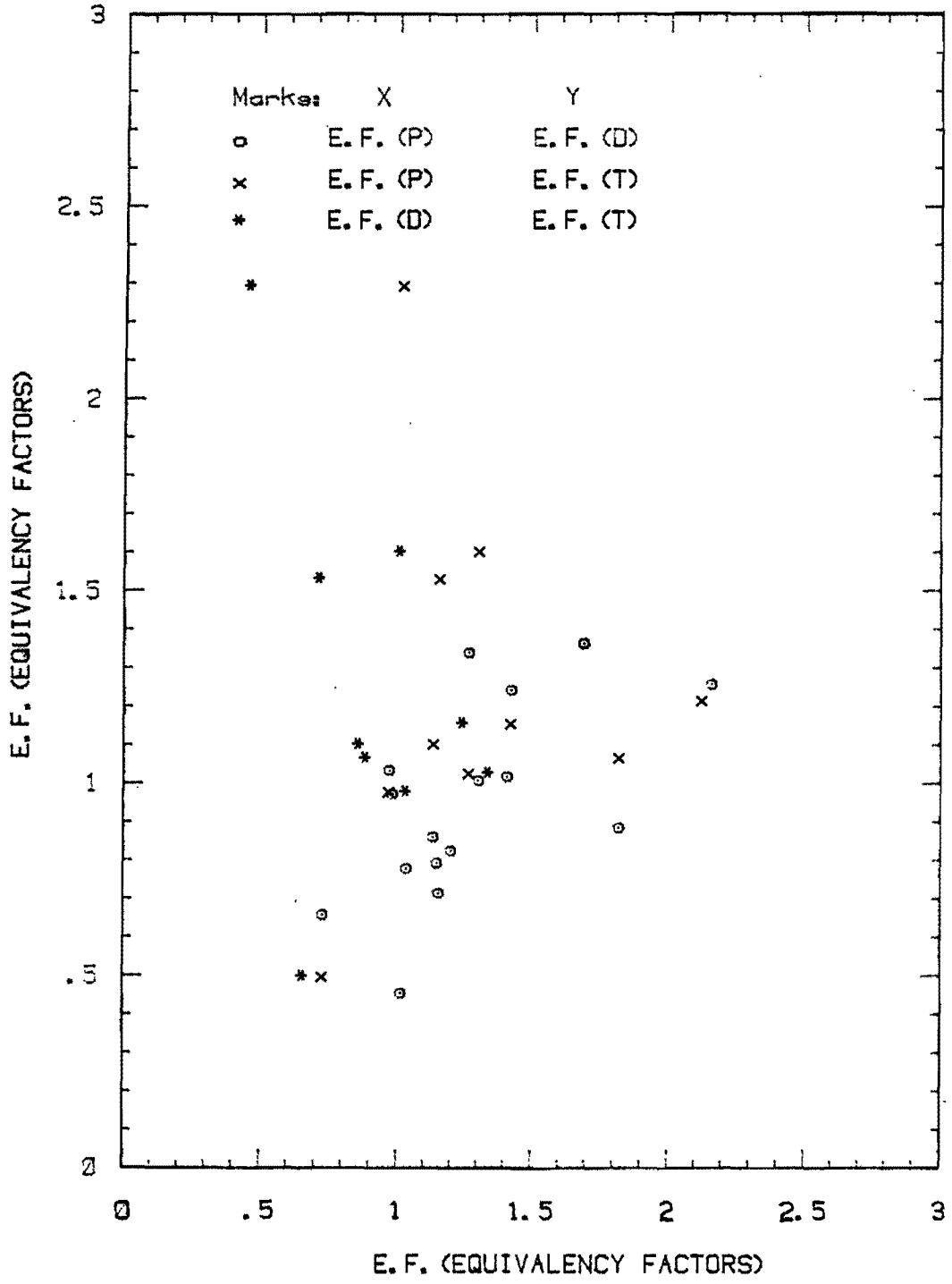


FIG. 25. — Comparisons among Three Sets of Equivalency Factors

The numbers in Columns 7 and 9 in Tables 8(a) - 8(c) are calculated by using the overall average modulus of sand and shell as a reference modulus and using  $n = 0.333$ ;

$$E.F. = \frac{E_{U,D,T(Ref.)}^n}{E_{U,D,T}}$$

Using the Odemark's assumption, the equivalency factors calculated on the basis of the pressuremeter moduli were found to be, on the average: iron ore = 1.21, sand and shell = 1.00 (as reference), select sand = 1.60, and lime treated crushed sandstone = 0.73, as shown in Table 8(a). According to Kuo's charts (9), the equivalency factors for the same materials using pressuremeter moduli  $E_U$  were found to be: iron ore = 1.16, sand and shell = 1.00, select sand = 1.40, and lime treated crushed sandstone = 0.80.

Two conclusions can be reached: (1) a base course, sand and shell for example, does not have a constant equivalency factor (this is probably due to the fact that in the field, factors such as compaction, water content, traffic, and climate influence the behavior of the base course and that these factors vary from one location to the next) and, yet, (2) common trends can be observed between the equivalency factors obtained from the three tests. The Dynaflect, pressuremeter, and TTT all showed that the lime treated crushed sandstone is stronger than the sand and shell, which is stronger than iron ore, and iron ore is stronger than the select sand. Based on the average values from Tables 8(a) - 8(c), the following equivalency factors are recommended:

$$\text{sand and shell} = 1.00,$$

lime treated crushed sandstone = 0.68,  
iron ore = 1.17, and  
select sand = 1.29.

It was not possible to obtain a modulus, and therefore an equivalency factor from the limestone base course in test Sections 9 and 10, because the limestone layer was very thin and very shallow in the pavement sections where it was found.

The scatter of equivalency factors is smallest for the pressuremeter test results. Yet, it is felt that the two other methods lead to reasonable average equivalency factors and, therefore, the method to use for determining equivalency factors becomes a matter of convenience and economy.

#### New Standard Procedure for Cyclic Pressuremeter Test

In light of the pressuremeter tests that have been obtained in this study the following procedure is proposed for performing a cyclic pressuremeter test. The first cycle should be performed by starting to deflate the probe when the raw volumetric strain,  $\frac{\Delta v}{V_0}$ , has reached 10%, at which point the pressure gauge reads  $P_U$ . The unloading should continue, with readings of pressure every 0.5% volumetric strain, until the pressure has decreased to  $0.3P_U$  or the unloading strain has reached 2.5%, whichever comes first. These limits are set so as to avoid a reload curve which exhibits a reverse curvature shape (Fig. 12(b)). During the reloading part of the cycle, readings are taken every 0.5% of volumetric strain. The second cycle should be performed by starting to deflate the probe when the raw

volumetric strain has reached 25% and the third cycle at 50%; otherwise, the same rules apply to the second and third cycles.

The membrane calibration should follow exactly the same procedure as the test with three cycles at 10, 25, and 50% volumetric strain. The volume losses calibration cannot follow the same procedure, since the strain levels of 10, 25, and 50% are not reached during the calibration. Instead the following is recommended: perform three cycles with the first one between 43.5 psi (300 kPa) and 14.5 psi (100 kPa), the second one between 116 psi (800 kPa) and 43.5 psi (300 kPa), the third one between 217.6 psi (1500 kPa) and 72.5 psi (500 kPa).

## PROCEDURE FOR DETERMINING THE EQUIVALENCY FACTOR

### Determination of In-situ Modulus from Texas Triaxial Test Modulus

The pressuremeter unload modulus,  $E_U$ , is believed to be a valid measure of the in-situ modulus; however it is measured at a stress level which is most of the time much higher than the stress level which exists in a pavement loaded by traffic loads. Therefore there is a need to reduce  $E_U$  to the appropriate stress level.

The appropriate stress level depends on the wheel load, but a reasonable average value can be obtained as follows (Fig. 26). The tire pressure  $p$  ranges from 30 psi (206.8 kPa) to 80 psi (551.4 kPa) and the average width of a tire is about 8 in. (20 cm); for the average flexible pavement configuration of Fig. 26 and according to Boussinesq theory the vertical stress at the midheight of the base course is  $0.4p$ , while the horizontal stress is  $0.12p$ . For the above pressures,  $0.12p$  ranges from 3.6 psi (24.8 kPa) to 9.6 psi (66.1 kPa); therefore 5 psi (34.5 kPa) is a reasonable value of the horizontal stress level in the base course of a loaded flexible pavement.

The pressuremeter unloading modulus  $E_U$  was measured in the field at a radial stress,  $P_U$ , (Appendix V); this modulus was reduced to a modulus  $E_{U(5 \text{ psi})}$ , at a radial stress of 5 psi by use of Eq. 55, with  $n_{\text{granular}} = 0.5$  and  $n_{\text{cohesive}} = 0.2$ . These exponent values were selected from the literature because the pressuremeter derived exponents lead to unrealistic results. This modulus,  $E_{U(5 \text{ psi})}$  is considered to be the in-situ modulus. It is obtained from a pavement pressuremeter test; however, the Texas triaxial test is more readily

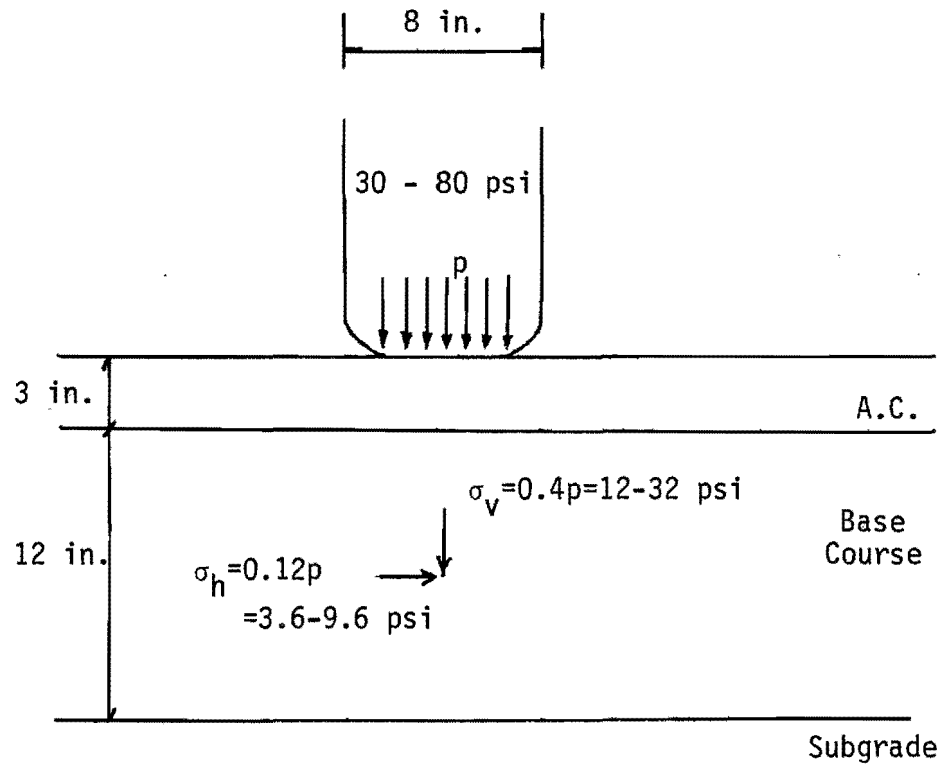


FIG. 26. - Soil Stress in Pavement Due to Wheel Load

available to the Highway Department. Therefore  $E_U(5 \text{ psi})$  needs to be correlated to  $E_T(5 \text{ psi})$  (Fig. 6), obtained from the Texas triaxial tests carried with  $\sigma_3 = 5 \text{ psi}$ . The correlation coefficient is  $f$  and

$$f = \frac{E_U(5 \text{ psi})}{E_T(5 \text{ psi})} \quad (62)$$

The coefficient  $f$  was calculated for the soils with detailed identification properties such as: plasticity index,  $I_p$ ; water content  $w$ , percent passing sieve #200,  $P_p$ ; coefficient of uniformity,  $C_u$ ; and coefficient of curvature  $C_c$ . The  $f$  values are listed in Table 2;  $f$  varied from 2.14 to 29.14. A select multiple regression analysis was carried out in order to select the model which would best describe  $f$  as a function of the simple parameters listed above. The two following models were chosen. For base courses and sands

$$f = 22.08 \times C_u^{0.689} \times w^{-0.282} \times I_p^{-1.632}, \text{ and} \quad (63)$$

For clays

$$f = 5.50. \quad (64)$$

#### Determination of the Equivalency Factor

The following paragraph is a presentation of the proposed step by step procedure for the determination of the equivalency factor of material B with respect to material A.

Step 1. Carry out the following tests on materials A and B: water content, Atterberg limits, and sieve analysis. Calculate the water content,  $w$ , the plasticity index,  $I_p$ , and the coefficient of uniformity,  $C_u$  for materials A and B.

Step 2. Run a Texas triaxial test on materials A and B with a confining pressure of 5 psi. Calculate  $E_T(5 \text{ psi})$  for material A and material B.

Step 3. Calculate the  $f$  values for material A and material B; use Eq. 63 for base courses and sands, and Eq. 64 for clays.

Step 4. Calculate the in-situ modulus,  $E_U(5 \text{ psi})$ , for material A and material B using Eq. 62

Step 5. Calculate the equivalency factor, E.F., of material B with respect to material A as

$$E.F._{B/A} = \frac{H_B}{H_A} = \left( \frac{E_A}{E_B} \right)^{0.333}$$

### Examples

Example 1: A new base course source has been discovered. How does this new base course source compare with sand and shell? More precisely what is the equivalency factor of the new base course with respect to sand and shell?

Step 1. From the files of the Highway Department the following numbers are available for sand and shell:  $w = 7.4\%$ ,  $I_p = 6.4\%$ , and  $C_u = 28.0$ . For the new base course the following numbers are obtained from testing:  $w = 10\%$ ,  $I_p = 7\%$ , and  $C_u = 35$ .

Step 2. From the files of the Highway Department the  $E_T(5 \text{ psi})$  is available for sand and shell:  $E_T(5 \text{ psi}) = 3150 \text{ psi}$ . For the new base course a Texas triaxial test with a confining pressure of 5 psi was performed and the following modulus was obtained:  $E_T(5 \text{ psi}) = 2500 \text{ psi}$ .

Step 3.

$$f \text{ (sand and shell)} = 22.08 \times 28^{0.689} \times 7.4^{-0.282} \times 6.4^{-1.632},$$

$$= 6.03.$$

$$f \text{ (new base course)} = 22.08 \times 35^{0.689} \times 10^{-0.282} \times 7^{-1.632}$$

$$= 5.58.$$

Step 4.

$$\text{Sand and shell } E_{U(5 \text{ psi})} = 6.03 \times 3150 = 18994 \text{ psi.}$$

$$\text{New base course } E_{U(5 \text{ psi})} = 5.58 \times 2500 = 13950 \text{ psi.}$$

Step 5.

$$\text{E.F. new base course/sand \& shell} = \left( \frac{18994}{13950} \right)^{0.333} = 1.11.$$

Examples 2. Three base courses are feasible for a job site:

sand and shell, iron ore, and lime treated crushed sandstone. It has been determined that a thickness of 9 in. would be required for the sand and shell base course. What thickness of iron ore and lime treated crushed sandstone would be equivalent to the 9 in. of sand and shell ?

Step 1: The following data has been collected from the laboratory identification tests:

	w(%)	I <sub>p</sub>	C <sub>u</sub>
sand & shell	7.4	6.4	28.0
iron ore	6.1	9.2	38.6
lime treated crushed sandstone	25.5	7	18.3

Step 2. The following moduli,  $E_T(5 \text{ psi})$ , have been calculated from the results of Texas triaxial tests with 5 psi of confining pressure on the three base courses.

	sand & shell	iron ore	lime treated crushed sandstone
$E_T(5 \text{ psi})$	3150 psi	2382 psi	25750 psi

Step 3. The  $f$  values are calculated.

	$f$
sand & shell	6.03
iron ore	4.39
lime treated crushed sandstone	2.74

Step 4. The in-situ moduli,  $E_U(5 \text{ psi})$ , can then be obtained.

	$E_U(5 \text{ psi})$
sand & shell	18994 psi
iron ore	10457 psi
lime treated crushed sandstone	70555 psi

Step 5. The following symbols are used: sand & shell = SS, iron ore = IO, lime treated crushed sandstone = LT. The equivalency factors are

$$E.F._{IO/SS} = \left( \frac{18994}{10457} \right)^{0.333} = 1.22 \text{ and}$$

$$E.F._{LT/SS} = \left( \frac{18994}{70555} \right)^{0.333} = 0.65.$$

Then the layer thicknesses are determined

	H (in.)
sand & shell	9
iron ore	11
lime treated crushed sandstone	6

## CONCLUSIONS AND RECOMMENDATIONS

The equivalency factors found in this study were calculated according to the following equation,

$$\text{Equivalency Factor E.F.} = \frac{H_B}{H_A} = \left( \frac{E_A}{E_B} \right)^{\frac{1}{3}} . \quad (1)$$

The base course which was chosen as a reference for calculating all other equivalency factors was sand and shell, since it is widely used in the area where the tests were performed.

The moduli required in Eq. 1 were obtained from pressuremeter tests, from Dynaflect tests, and from existing records of Texas triaxial tests. On the average, the iron ore base course gave an equivalency factor of 1.17, the selected sand subbase gave an equivalency factor of 1.29, and the lime treated crushed sandstone base course gave an equivalency factor of 0.68. These equivalency factors were calculated with reference to sand and shell (i.e.: E.F. sand and shell = 1). The equivalency factors obtained for the same base course by each of the three methods (pressuremeter, Dynaflect, Texas triaxial test) were reasonably close; it is therefore concluded that the three methods are equally satisfactory and that the choice of method is essentially a matter of convenience, efficiency, and economy.

The Russian equation method is a very efficient approximate method capable of extracting the individual moduli of the pavement layers from a measured Dynaflect deflection basin. It is most accurate in the determination of the subgrade modulus. The comparison between the moduli measured in the different layers by the pressuremeter and the moduli back calculated from measured Dynaflect basins, using the

Russian equation, shows some scatter. This scatter may be due to the fact that the pressuremeter moduli were obtained at different stress levels in the soil, while the Dynaflect derived moduli were obtained at a consistent stress level.

In addition, this study leads to an improved understanding of the pressuremeter test on several aspects.

1. It is now possible to obtain a pressuremeter modulus at any strain level including zero strain, both for the unloading and reloading moduli, by performing one unload/reload cycle during the test.
2. It is also now possible to get an idea of the stress level dependency of the pressuremeter modulus by performing one unload/reload cycle during the test.
3. It was found that the unload/reload cycle procedure must be standardized so that consistent and comparable results can be obtained from one test to the next. A standard procedure has been proposed.
4. Since base courses are often thinner than 9 in. (22.9 cm) (the present length of the probe), a 5 in. (12.7 cm) long 1 in. (2.54 cm) diameter probe would enable the testing of thinner layers.
5. A borehole preparation method which creates less disturbance to the soil is needed.

It is felt that the pavement pressuremeter test can replace advantageously the Texas triaxial test for evaluating base course materials in place. The major advantage of the pressuremeter is that

it tests the soil in the field in its natural environment. The Dynaflect test does not give the same detailed information on the mechanical properties of the subgrade and pavement layers; however, the Dynaflect test is much shorter and easier to run than the other two tests.

Finally, a detailed step by step procedure has been developed to obtain the equivalency factor of any soil with respect to any other soil. The method is based on the determination of the water content, the plasticity index, the coefficient of uniformity and a modulus obtained from the Texas triaxial test. Two examples of the use of the procedure were included.



## APPENDIX I. - REFERENCES

1. Baguelin, F., Jezequel, J. F., and Shields, D. H. "The Pressuremeter and Foundation Engineering", 1st Ed., 1978, Trans Tech Publications, Clanspaal, Germany.
2. Briaud, J. L. "The Pressuremeter: Application of Pavement Design", Ph.D. Dissertation, University of Ottawa, Ottawa, Ontario, Canada.
3. Briaud, J. L. and Shields, D. H. "A Special Pressuremeter and Pressuremeter Test for Pavement Evaluation and Design", ASTM, Geotechnical Testing Journal, Vol. 2, No. 3, 1979.
4. Briaud, J. L. and Shields, D. H. "Use of a Pressuremeter Test to Predict the Modulus and Strength of Pavement Layers", to be published in the Transportation Research Record, 1981.
5. Crossley, R. W. and Beckwith, G. H. "Subgrade Elastic Modulus for Arizona Pavements -- Final Report", Sergent, Hauskins & Beckwith, Inc., Phoenix, Arizona, January 1978.
6. Duncan, J. M. and Chang, C. Y. "Nonlinear Analysis of Stress and Strain in Soils", Journal of the Soil Mechanics and Foundations Division, ASCE, No. SM5, Proc. Paper 7513, 1970.
7. Irwin, L. H. "Equipment and Methods for Deflection-Based Structural Evaluation of Pavements", An Informal Representation made at the 1979 Forest Service Geotechnical Workshop, held in Ames, Iowa, November 1979.
8. Kondner, R. L. "Hyperbolic Stress-Strain Response: Cohesive Soils", Journal of the Soil Mechanics and Foundations Division, ASCE, Vol. 89, No. SM1, Proc. Paper 3429, 1963.
9. Kuo, S. S. "Development of Base Layer Thickness Equivalency", Research Report No. R-1119, Research Laboratory Section, Testing and Research Division, Michigan Department of Transportation, Lansing, Michigan, June 1979.
10. Lytton, R. L., Moore, W. M., and Mahoney, J. P. "Pavement Evaluation Phase I, Pavement Evaluation Equipment", FHWA-RD 75-78, Texas Transportation Institute, Texas A&M University, College Station, Texas March 1975.
11. Lytton, R. L. and Michalak, C. H. "Flexible Pavement Deflection Equation using Elastic Moduli and Field Measurements", Research Report 207-7F, Texas Transportation Institute, Texas A&M University, College Station, Texas, September 1979.

12. Lytton, R. L. "Layer Equivalents", A Project Report Submitted to Texas Industries, Incorporated, 1980, Arlington, Texas.
13. "Manual of Testing Procedures -- Soil Section", Materials and Tests Division, Texas Highway Department, Austin, Texas.
14. Michalak, C. H., Lu, D. Y., and Turman, G. W. "Determining Stiffness Coefficients and Elastic Moduli of Pavement Materials from Dynamic Deflections", Research Report 207-1, Texas Transportation Institute, Texas A&M University, College Station, Texas, November 1976.
15. Odemark, N. "Investigations as to the Elastic Properties of Soils Design of Pavements According to The Theory of Elasticity", Staten Vaeginstitut, Stockholm, 1949.
16. Scrivner, F. H. and Moore, W. M. "An Empirical Equation for Predicting Pavement Deflections", Research Report 32-12, Texas Transportation Institute, Texas A&M University, College Station, Texas, October 1968.
17. Scrivner, F. H. and Michalak, C. H. "Linear Elastic Theory as a Model of Displacements Measured within and beneath Flexible Pavement Structures Loaded by the Dynaflect", Research Report 123-25, Texas Transportation Institute, Texas A&M University, College Station, Texas, August 1974.
18. Selvadurai, A. P. S. "Elastic Analysis of Soil-Foundation Interaction", Elsevier Scientific Publishing Co., New York, 1979.
19. Terzaghi, K. and Peck, R. B. "Soil Mechanics in Engineering Practice", 2nd Ed., 1967, John Wiley & Sons, Inc., New York.
20. "Texas Highway Department Pavement Design System -- Part I -- Flexible Pavement Designer's Manual", Highway Design Division, Texas Highway Department, Austin, 1972.
21. Timoshenko, S. P. and Goodier, J. N. "Theory of Elasticity", 3rd Ed., 1970, McGraw-Hill, New York.
22. Vlasov, V. Z. and Leont'ev, N. N. "Beams, Plates, and Shells on Elastic Foundation", (Translated from Russian), Israel Program for Scientific Translations, Jerusalem, Israel, 1966.
23. Yoder, E. J. and Witczak, M. W. "Principles of Pavement Design", 2nd Ed., 1975, Wiley, New York.

## APPENDIX II. - NOTATION

- A = base -course material A;
- a = constant of regression analysis;
- $a_o$  = the distance to the origin in X direction;
- $a_c$  = the inverse of  $E_c$ ;
- $a_M$  = the inverse of  $E_M$ ;
- $a_R$  = the inverse of  $E_R$ ;
- $a_V$  = the inverse of  $E_V$ ;
- $a_{CU}$  = the inverse of  $E_{CU}$ ;
- $a_{CR}$  = the inverse of  $E_{CR}$ ;
- B = base course material B;
- B' = experimental test constant of repeated load triaxial test;
- b = constant of regression analysis;
- $b_o$  = the distance to the origin in X direction;
- $b_c$  = the inverse of  $\sigma_{ult}$  after correction;
- $b_M$  = the inverse of  $\sigma_{ult}$  from the membrane calibration curve;
- $b_R$  = the inverse of  $\sigma_{ult}$  from the pressuremeter test curve;
- $b_{CR}$  = the inverse of  $\sigma_{ult}$  after correction;
- C = an experimental test constant;
- $C_c$  = coefficient of curvature;
- $C_u$  = uniformity coefficient;
- CBR = the value of California bearing ratio;
- D = diameter of the rigid plate;
- $D_{calculated}$  = the calculated deflection;

- $D_{\text{measured}}$  = the measured deflection;  
 $E$  = the secant modulus;  
 $E_A$  = elastic modulus of material A;  
 $E_B$  = elastic modulus of material B;  
 $E_C$  = the corrected value of modulus;  
 $E_D$  = the Dynaflect/Russian equation modulus;  
 $E_M$  = secant modulus on membrane calibration curve;  
 $E_R$  = raw value of modulus in pressuremeter test;  
 $E_T$  = the Texas triaxial test modulus;  
 $E_U$  = the pressuremeter unloading modulus;  
 $E_V$  = secant modulus on volume losses curve;  
 $E_{CU}$  = the corrected pressuremeter unloading modulus;  
 $E_{CR}$  = the corrected pressuremeter reloading modulus;  
 $E_d$  = subgrade deformation modulus from triaxial test;  
 $E_e$  = elastic modulus;  
 $E_f$  = the secant modulus at failure;  
 $E_i$  = the elastic modulus of layer  $i$ ;  
 $E_o$  = the modulus of the datum modulus;  
 $E_s$  = subgrade elastic modulus;  
 $E_t = \frac{E_e}{(1 - \nu_e)^2}$  ;  
 $E_3$  = subgrade elastic modulus from dynamic triaxial test;  
 $E_{it}$  = the initial tangent modulus;  
 $E_{oi}$  = the pressuremeter initial secant modulus;  
 E.F. = the equivalency factor;  
 $f$  = an experimental test constant;

$H$  = an elastic layer of depth  $H$ ;  
 $H'$  = the transformed depth of all layers;  
 $H_A$  = the thickness of layer A;  
 $H_B$  = the thickness of layer B;  
 $h_i$  = the thickness of layer  $i$ ;  
 $I_p$  = plasticity index;  
 $K$  = constant;  
 $k$  = modulus of subgrade reaction;  
 $k'$  = the number of layers;  
 $k_v$  = parameter in Vlasov model;  
 $K_1$  = experimental test constant;  
 $K_2$  = experimental test constant;  
 $K_1'$  = experimental test constant;  
 $K_2'$  = experimental test constant;  
 $K_0(\alpha r) = K_0$  the modified Bessel function with argument,  $\alpha r$ ;  
 $l$  = the number of the layer in which  $Z$  falls;  
 $m$  = experimental test constant;  
 $M_R$  = resilient modulus;  
 $N$  = the blow count;  
 $n$  = Odemark's assumption ( $\frac{1}{3}$ ) in transforming layer thickness;  
 $n_A$  = experimental test constant of material A;  
 $n_B$  = experimental test constant of material B;  
 $n_p$  = an experimental test constant;  
 $n_T$  = an experimental test constant;  
 $n_a$  = an experimental test constant;

$P$  = a concentrated load;  
 $p$  = unit load on the plate;  
 $P_p$  = percentage of passing #200 sieve;  
 $P_R$  = the radial stress at C on the pressuremeter curve;  
 $P_U$  = the radial stress at A on the pressuremeter test curve;  
 $P_l$  = the limit pressure;  
 $P_{AM}$  = the pressure reading at A in membrane calibration curve;  
 $P_{AR}$  = the pressure reading at A in pressuremeter test curve;  
 $P_{BM}$  = the pressure reading at B on membrane calibration curve;  
 $P_{BR}$  = the pressure reading at B on pressuremeter test curve;  
 $P_{CM}$  = the pressure reading at C on membrane calibration curve;  
 $P_{CR}$  = the pressure reading at C on pressuremeter test curve;  
 $P$ - $V$  = pressure versus volume curve for pressuremeter test;  
 $P_{corrected}$  = the corrected ultimate strength;  
 $q$  = distributed load acting on the rigid plate;  
 $q_0$  = the uniform distributed load;  
 $q(\xi)$  = a distributed load;  
 $R$  = material resistance value (from stabilometer test);  
 $r$  = the distance to the Z axis in cylindrical coordinates;  
 $r_0$  = the radius of a rigid circular plate;  
 $S$  = subgrade support value;  
 $s$  = settlement of the rigid plate under the distributed circular load;  
 $t$  = parameter in Vlazov model;  
 $TC$  = the Texas classification;  
 $u$  = displacement component in X direction;

- $v$  = the volume reading at desired point on pressuremeter test curve;
- $V_A$  = volume injected at A on pressuremeter test curve;
- $V_B$  = volume injected at B on pressuremeter test curve;
- $V_C$  = initial volume of the probe;
- $V_m$  = mean volume in the probe of two stress level readings of pressuremeter test;
- $V_0$  = the deflated volume of the probe;
- $V_{AR}$  = the volume reading at A on pressuremeter test curve;
- $V_{AV}$  = the volume reading at A on volume losses curve;
- $V_{BR}$  = the volume reading at B on pressuremeter test curve;
- $V_{BV}$  = the volume reading at B on volume losses curve;
- $w$  = water content;
- $w'$  = displacement component in Z direction;
- $w_l$  = liquid limit;
- $w_p$  = plastic limit;
- $x$  = the variable for distance in X direction;
- $z$  = the depth of concerned point below the surface;
- $\bar{z}$  = the transformed depth to the point at depth  $z$ ;
- $\alpha = \sqrt{\frac{k_v}{2t}}$  : a transformed parameter;
- $\epsilon_a$  = the recoverable axial strain;
- $\epsilon_{\text{uncorrected}}$  = uncorrected strain of pressuremeter test;
- $\theta$  = bulk stress or first stress invariant;
- $\nu$  = Poisson's ratio of the soil;
- $\nu_0$  = Poisson's ratio for the elastic material;

$v_e$  = Poisson's ratio for the elastic material;

$v_t = v_e(1-v_e)$ ;

$\xi$  = the distance to the origin in X direction;

$\sigma$  = stress;

$\sigma_d$  = the repeated axial deviator stress;

$\sigma_1$  = the major principal stress;

$\sigma_3$  = the confining pressure in triaxial test;

$\sigma_{1f}$  = the applied axial pressure at failure;

$\sigma_{3f}$  = the confining pressure at failure;

$\psi_k$  = an integral equation for the variation of displacement;

$\psi_t$  = an integral equation for the variation of displacement;

$$\psi_\alpha = \frac{\psi_k}{\psi_t}$$

$\Delta$  = deflection of the plate;

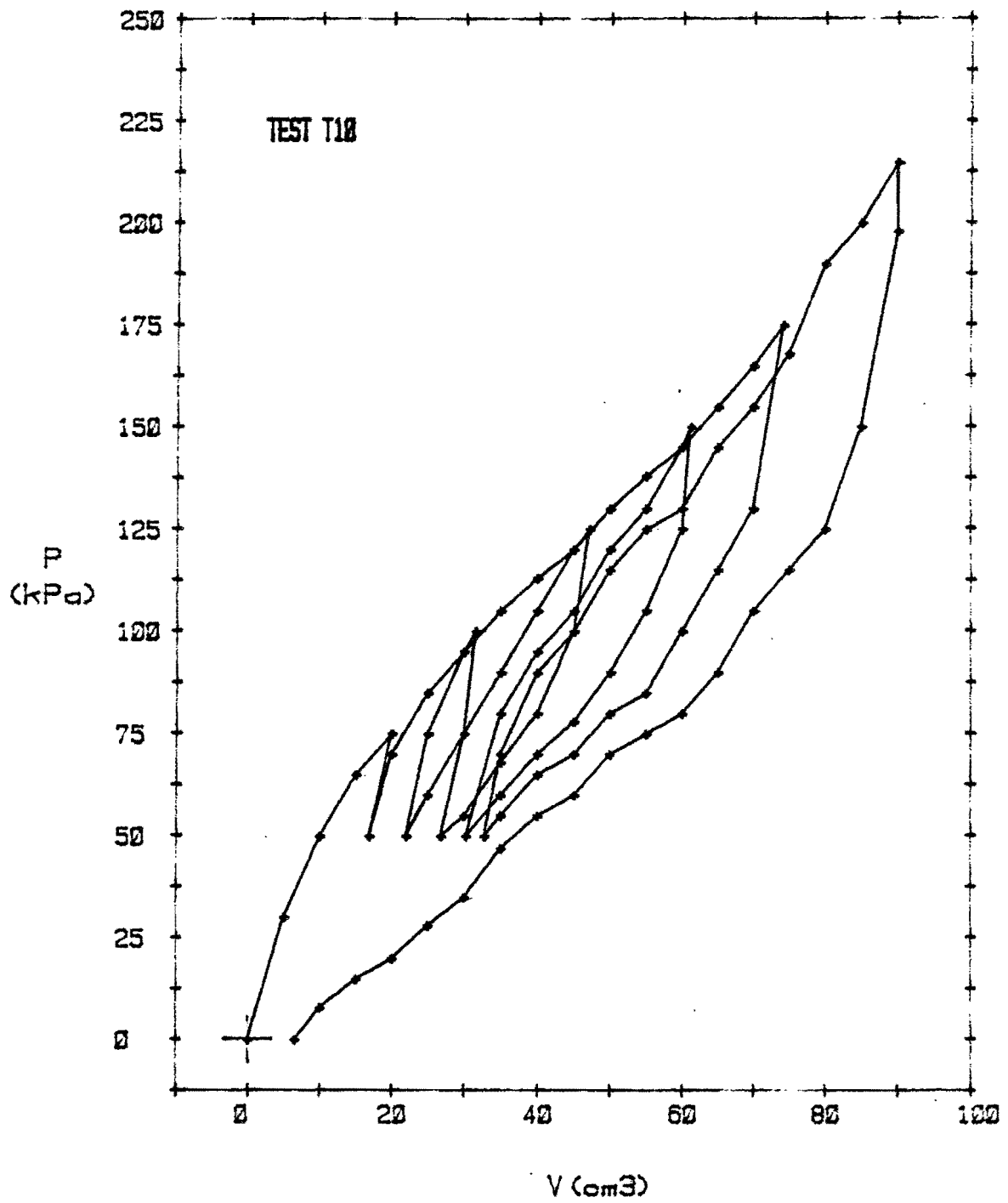
$\Delta v$  = the volume difference between two points on pressure-meter test curve;

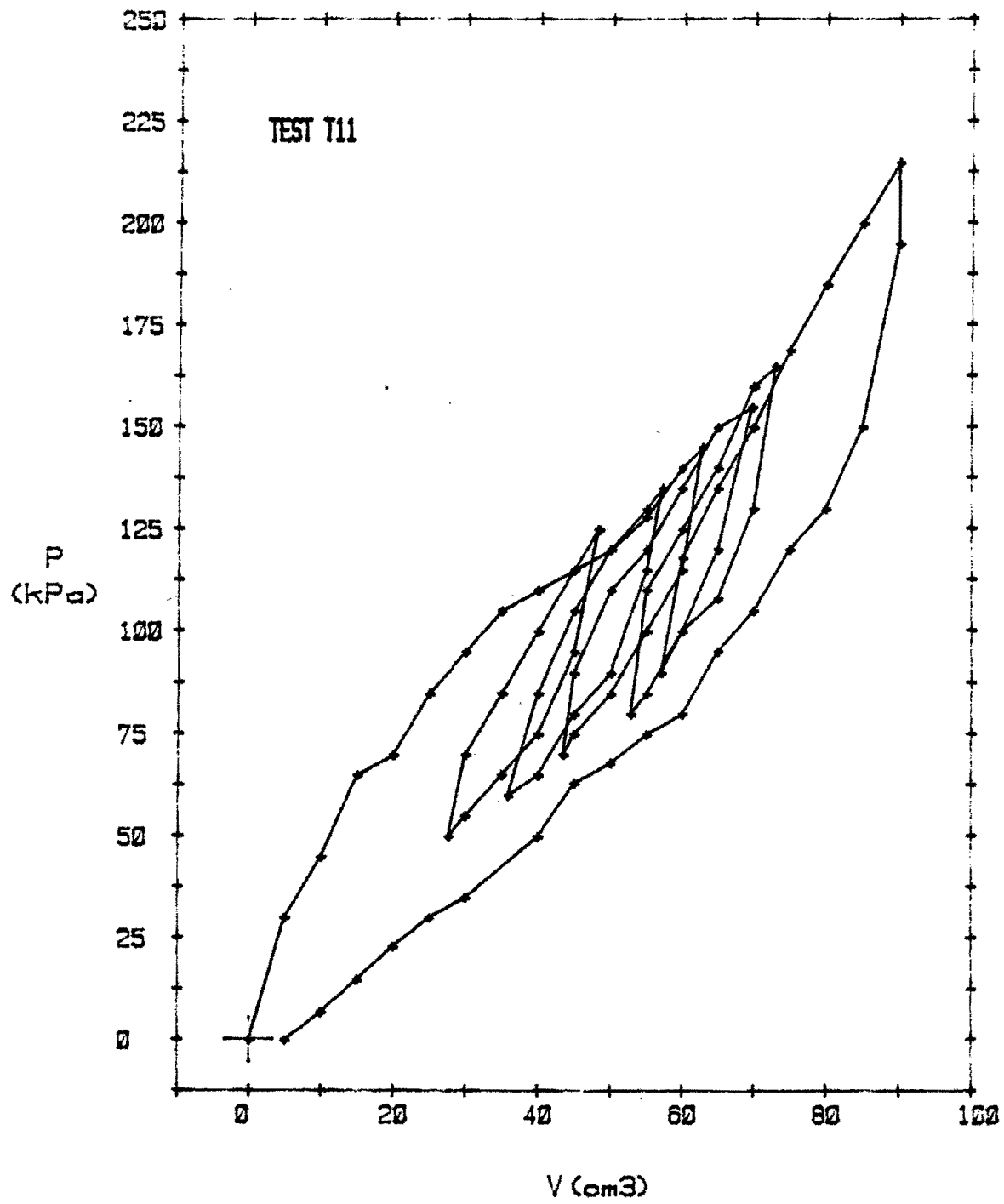
$\Delta P_{AB}$  = the pressure difference between stress levels A and B;

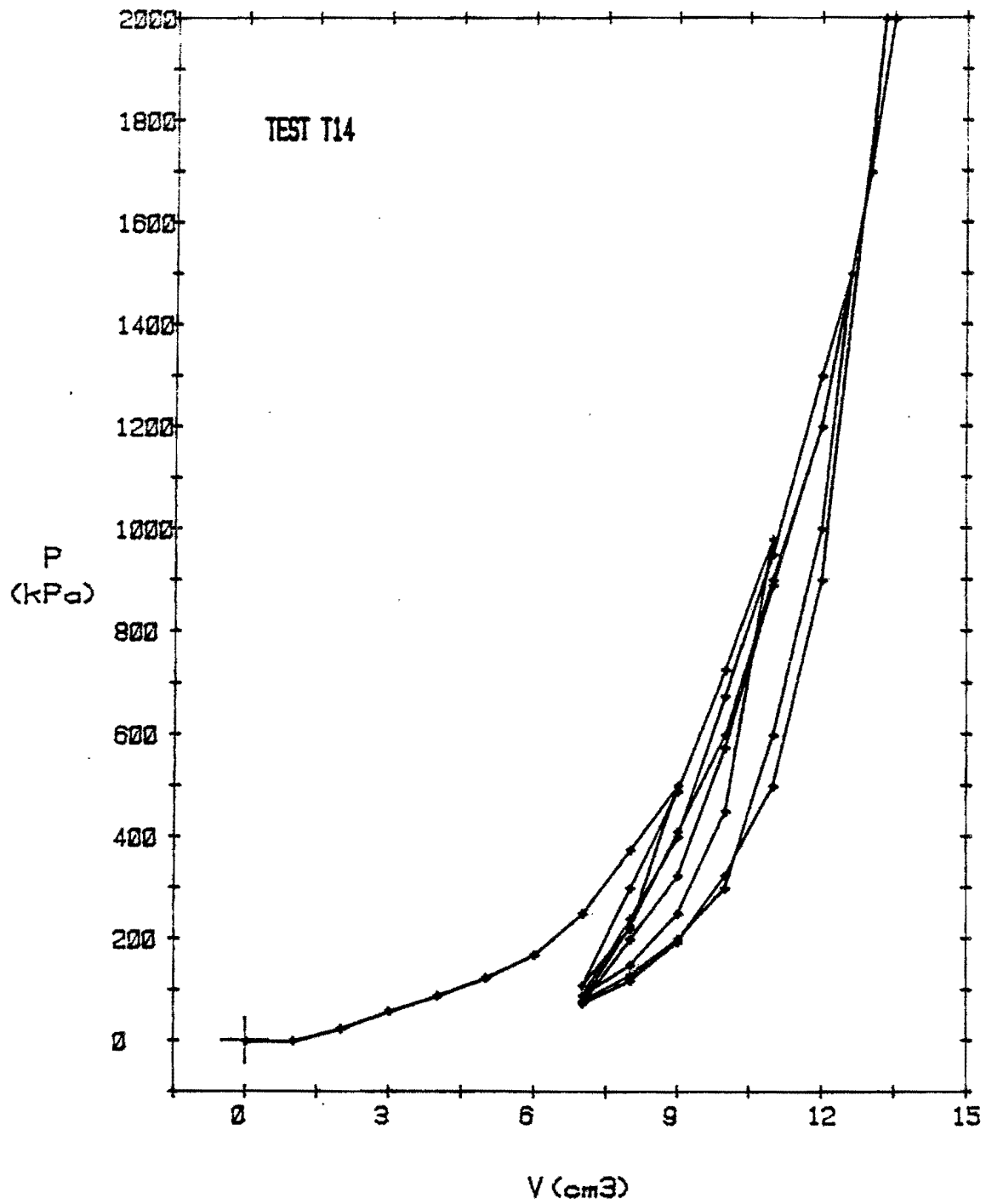
$\Delta V_{AB}$  = the volume difference between stress levels A and B;

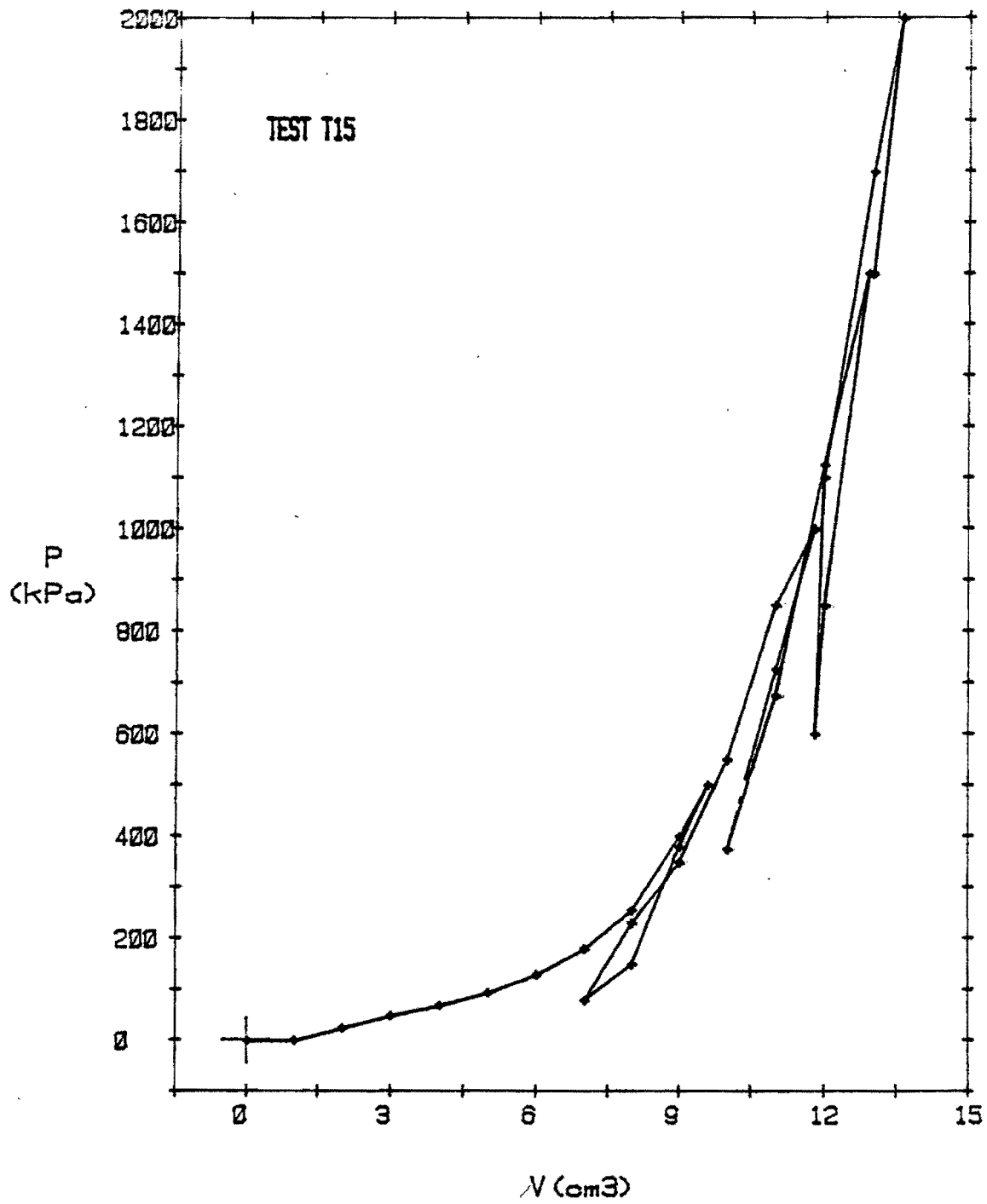
APPENDIX III. - CALIBRATION CURVES FOR PRESSUREMETER TESTS

1. Membrane Calibration Curves : Tests 10 and 11
2. Volume Losses Curves : Tests 14 and 15











APPENDIX IV. - MEASURED DEFLECTIONS FROM DYNAFLECT TEST



## SECTION 1

TEST NO.	SENSOR 1	SENSOR 2	SENSOR 3	SENSOR 4	SENSOR 5
T111	.8750	.4800	.2715	.1860	.1335
T112	.7900	.4750	.2820	.1920	.1380
T113	.9900	.5500	.2925	.1905	.1410
T114	.9450	.5200	.2835	.1830	.1320
T115	.8800	.5100	.2805	.1845	.1365
AVERAGE	.8960	.5070	.2820	.1872	.1362

## SECTION 2

TEST NO.	SENSOR 1	SENSOR 2	SENSOR 3	SENSOR 4	SENSOR 5
T 58	2.3400	1.6200	1.1700	.9000	.7350
T 59	2.2950	1.6200	1.1550	.8900	.7400
T 60	2.2200	1.5900	1.1550	.8950	.7450
T 61	2.2500	1.6200	1.1550	.8900	.7400
T 62	2.2500	1.5900	1.1550	.8800	.7300
AVERAGE	2.2710	1.6080	1.1580	.8910	.7380

## SECTION 3

TEST NO.	SENSOR 1	SENSOR 2	SENSOR 3	SENSOR 4	SENSOR 5
T 35	1.5900	1.2600	.8050	.5350	.3650
T 36	1.7700	1.2900	.8300	.5500	.3750
T 37	1.6200	1.3200	.9200	.6250	.4050
T 38	1.4400	1.2000	.8350	.5800	.3800
T 39	1.5300	1.2600	.8400	.5900	.4000
AVERAGE	1.5900	1.2660	.8460	.5760	.3850

## SECTION 4

TEST NO.	SENSOR 1	SENSOR 2	SENSOR 3	SENSOR 4	SENSOR 5
T 73	1.4400	.8500	.5700	.3850	.3100
T 74	1.5300	.9200	.5400	.4050	.3200
T 75	1.4700	.8900	.5400	.4000	.3150
T 76	1.4400	.9000	.5450	.4000	.3200
T 77	1.4700	.9100	.5450	.4000	.3150
AVERAGE	1.4700	.8940	.5480	.3980	.3160

## SECTION 5

TEST NO.	SENSOR 1	SENSOR 2	SENSOR 3	SENSOR 4	SENSOR 5
T 99	2.5200	1.5300	.9000	.6150	.5550
T100	2.7000	1.5900	.9050	.6100	.4600
T101	2.7000	1.5900	.8600	.5800	.4350
T102	2.7000	1.5300	.8300	.5850	.4600
T103	2.5950	1.5000	.8200	.5800	.4600
T104	2.6850	1.5600	.8200	.5950	.4700
AVERAGE	2.6500	1.5500	.8558	.5942	.4733

## SECTION 6

TEST NO.	SENSOR 1	SENSOR 2	SENSOR 3	SENSOR 4	SENSOR 5
T 42	2.2950	1.5000	.9800	.6650	.4850
T 43	2.2950	1.5000	.9700	.6500	.4900
T 44	2.2500	1.4700	.9650	.6600	.5000
T 45	2.2650	1.4700	.9800	.6600	.5000
T 46	2.2650	1.5000	.9950	.6750	.5050
AVERAGE	2.2740	1.4880	.9780	.6620	.4960

## SECTION 7

TEST NO.	SENSOR 1	SENSOR 2	SENSOR 3	SENSOR 4	SENSOR 5
T152	1.0800	.8650	.5900	.4000	.2655
T153	1.0800	.8500	.5850	.4050	.2730
T154	1.1250	.8650	.5800	.4050	.2640
T155	1.0800	.8550	.5800	.3900	.2595
T156	1.0800	.8400	.5800	.3950	.2610
T157	1.0650	.8150	.5500	.3800	.2520
AVERAGE	1.0850	.8483	.5775	.3958	.2625

## SECTION 8

TEST NO.	SENSOR 1	SENSOR 2	SENSOR 3	SENSOR 4	SENSOR 5
T105	1.7100	1.2450	.8550	.6600	.5400
T106	1.6050	1.1850	.8150	.6400	.5300
T107	1.6350	1.1850	.8250	.6450	.5100
T108	1.6500	1.2000	.8300	.6450	.5220
T109	1.7850	1.2750	.8500	.6570	.5300
T110	1.7850	1.2600	.8300	.6350	.5000
AVERAGE	1.6950	1.2250	.8342	.6470	.5220

## SECTION 9

TEST NO.	SENSOR 1	SENSOR 2	SENSOR 3	SENSOR 4	SENSOR 5
T175	2.5200	2.0400	1.4400	1.1250	.8850
T176	2.5500	2.0400	1.4700	1.1250	.8750
T177	2.5200	1.9950	1.4550	1.1250	.8750
T178	2.5050	2.0100	1.4550	1.1250	.8700
T179	2.4900	2.0250	1.4850	1.1550	.9000
AVERAGE	2.5170	2.0220	1.4610	1.1310	.8810

## SECTION 10

TEST NO.	SENSOR 1	SENSOR 2	SENSOR 3	SENSOR 4	SENSOR 5
T157	2.3100	1.8150	1.3800	1.2150	1.0800
T158	2.3100	1.8300	1.4400	1.2600	1.0350
T159	2.2650	1.8000	1.3950	1.2000	1.0650
T160	2.1600	1.7700	1.3500	1.2000	1.0200
T161	2.3100	1.8600	1.3500	1.2000	1.0500
AVERAGE	2.2710	1.8150	1.3830	1.2150	1.0500

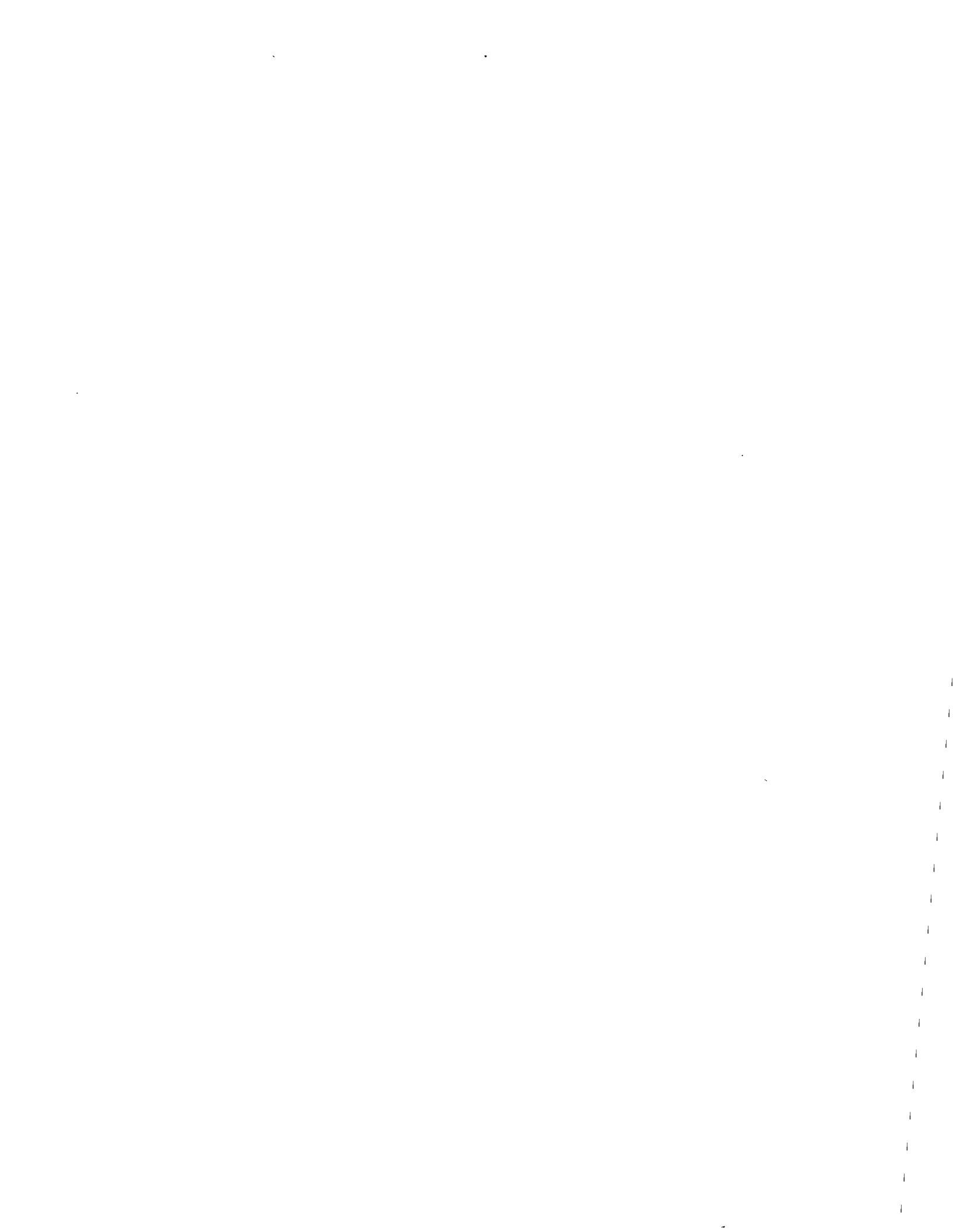
## SECTION 11

TEST NO.	SENSOR 1	SENSOR 2	SENSOR 3	SENSOR 4	SENSOR 5
T129	1.3050	.8000	.5130	.3850	.2895
T130	1.4250	.8700	.5500	.4000	.2925
T131	1.5000	.9100	.5600	.4050	.2955
T132	1.4250	.9000	.5550	.3950	.2835
T133	1.4610	.8880	.5520	.3900	.2835
AVERAGE	1.4232	.8736	.5460	.3950	.2889

## SECTION 12

TEST NO.	SENSOR 1	SENSOR 2	SENSOR 3	SENSOR 4	SENSOR 5
T189	1.1850	.8950	.6450	.4900	.3750
T190	1.2300	.9150	.6500	.4850	.3450
T191	1.1550	.8050	.5370	.4000	.3050
T192	1.0800	.7150	.4750	.3500	.2625
T193	1.0500	.6800	.4300	.3150	.2310
AVERAGE	1.1400	.8020	.5474	.4080	.3037

APPENDIX V. - THE CALCULATED RESULTS OF THE PRESSUREMETER TEST DATA



TEST NO.	CYCLE NO.	$E_U$ (kPa)	$E_R$ (kPa)	$E_o$ (kPa)	$\frac{1}{b_R}$ (kPa)	$\frac{E_U}{E_R}-1$	$P_U$ (kPa)	$P_R$ (kPa)	$n_p$
12	1	169000	203000	11700	760	-0.1658	525	203	-0.1903
	2	91000	44200	11700	242	1.0592	525	53	--
13	1	306000	308000	12700	608	-0.0064	655	210	-0.0057
	2	358000	382000	12700	884	-0.0640	702	226	-0.0586
	3	363000	295000	12700	1008	0.2303	754	252	0.1891
25	1	135000	51800	6500	765	1.6065	473	57	0.4509
26	1	196000	64700	14200	2970	2.0268	818	122	0.5808
28	1	514000	42500	15500	4450	10.9754	1070	113	1.1023
29	1	59600	34200	7180	712	0.7424	368	57	0.2963
30	1	152000	89900	11300	2180	0.6898	795	98	0.2500
31	1	223000	44900	8800	2370	3.9677	675	108	0.8725
33	1	242000	38600	7900	2390	5.2735	560	90	1.0045
34	1	870000	77400	26100	295	10.2368	1380	135	1.0407
47	1	67600	38900	7400	820	0.7365	360	80	0.3669

TEST NO.	CYCLE NO.	$E_U$ (kPa)	$E_R$ (kPa)	$E_o$ (kPa)	$\frac{1}{b_R}$ (kPa)	$\frac{E_U}{E_R}-1$	$P_U$ (kPa)	$P_R$ (kPa)	$\eta_p$
48	1	93500	39200	5900	684	1.3846	325	75	0.5927
49	1	138000	34900	11400	1560	2.9524	550	70	0.6667
50	1	338000	179000	20900	2690	0.8852	1125	250	0.4215
52	1	79300	141000	8560	624	-0.4379	395	73	-0.3398
53	1	81500	37000	4960	869	1.2005	340	70	0.4990
54	1	88400	58400	6650	556	0.5132	300	73	0.2917
55	1	1260000	857000	43200	28640	0.4673	1605	490	0.3232
56	1	100000	68000	5300	718	0.4724	405	98	0.2717
	2	134000	58500	5300	871	1.2974	403	97	0.5819
	3	142000	45900	5300	998	2.0957	410	95	0.7728
	4	68200	45600	5300	1010	0.4958	411	88	0.2612
57	1	664000	209000	28900	4270	2.1834	1390	355	0.8484
	2	525000	133000	28900	6300	2.9663	1388	274	0.8492
	3	1040000	148000	28900	7520	5.9826	1434	302	1.2475
	4	1020000	206000	28900	3750	3.9611	1442	376	1.1915
	5	768000	168000	28900	9490	3.5704	1440	365	1.1072

TEST NO.	CYCLE NO.	$E_U$ (kPa)	$E_R$ (kPa)	$E_o$ (kPa)	$\frac{1}{b_R}$ (kPa)	$\frac{E_U}{E_R}-1$	$P_U$ (kPa)	$P_R$ (kPa)	$n_p$
63	1	40000	15000	4150	509	1.6704	255	88	0.9183
64	1	53400	36200	6220	522	0.4748	295	91	0.3288
65	1	162000	92200	12400	1740	0.7540	795	185	0.3854
66	1	944000	81500	25200	10800	10.5816	1455	208	1.2576
67	1	37400	24000	3990	368	0.4457	215	85	0.3972
68	1	53200	31700	4520	454	0.6754	226	75	0.4650
69	1	130000	60800	11800	2020	1.1408	685	98	0.3904
70	1	1470000	138000	26000	6070	9.6734	1420	218	1.2620
71	1	2160000	221000	27100	7570	8.7728	1649	235	1.1688
	2	1330000	135000	27100	16900	97.7645	1668	199	2.1602
	3	2070000	177000	27100	10800	10.6975	1622	241	1.2899
	4	835000	145000	27100	26500	4.7812	1659	242	0.9115
79	1	207000	116000	10100	1050	0.7850	530	85	0.3166
80	1	536000	194000	18400	3060	1.7670	1080	158	0.5286

TEST NO.	CYCLE NO.	$E_U$ (kPa)	$E_R$ (kPa)	$E_o$ (kPa)	$\frac{1}{b_R}$ (kPa)	$\frac{E_U}{E_R}-1$	$P_U$ (kPa)	$P_R$ (kPa)	$n_p$
81	1	152000	93200	12400	1300	0.6254	680	215	0.4219
82	1	1270000	219000	43200	11300	4.8159	1760	260	0.9206
83	1	254000	108000	10600	1260	1.3595	575	90	0.4629
84	1	423000	150000	18200	2690	1.8206	1018	199	0.6353
85	1	126000	96600	12300	1300	0.3029	667	164	0.1882
86	1	1450000	165000	41400	18500	7.8218	1588	229	1.7243
87	1	186000	100000	12800	1210	0.8569	516	86	0.3443
	2	204000	105000	12800	1230	0.9410	513	84	0.3665
	3	226000	63900	12800	1700	2.5285	516	78	0.6674
	4	199000	53900	12800	2220	2.6876	507	81	0.7115
	5	196000	71700	12800	1730	1.7304	508	74	0.5214
88	1	1680000	418000	41000	6120	3.0243	1688	389	0.9486
	2	1130000	193000	41000	18300	4.8433	1705	328	1.0700
	3	1080000	210000	41000	27700	4.1354	1727	381	1.0826
	4	1450000	240000	41000	14900	5.0294	1731	361	1.1451
	5	2440000	229000	41000	16100	9.6498	1730	365	1.5203

TEST NO.	CYCLE NO.	$E_U$ (kPa)	$E_R$ (kPa)	$E_o$ (kPa)	$\frac{1}{b_R}$ (kPa)	$\frac{E_U}{E_R}-1$	$P_U$ (kPa)	$P_R$ (kPa)	$n_p$
90	1	105000	106000	10400	1190	-0.0042	764	267	-0.0040
91	1	104000	68500	10100	1130	0.5193	594	132	0.2781
92	1	352000	108000	13900	2970	2.2519	1010	265	0.8814
93	1	115000	52900	8760	1390	1.1805	655	165	0.5654
94	1	82800	59800	10100	1010	0.3843	559	137	0.2313
95	1	248000	56300	13700	6850	3.3988	927	199	0.9612
96	1	77600	49000	6400	795	0.5847	430	140	0.4103
	2	83600	47900	6400	844	0.7469	428	139	0.4960
	3	70300	39900	6400	990	0.7598	426	133	0.4855
	4	55800	40700	6400	996	0.3712	429	127	0.2593
	5	81300	46800	6400	920	0.7384	428	142	0.4996
97	1	269000	101000	13900	2420	1.6584	890	220	0.6996
	2	250000	60400	13900	9980	3.1283	888	224	1.0294
	3	343000	80800	13900	4800	3.2489	906	228	1.0485
	4	304000	77600	13900	7990	2.9124	893	227	0.9944

TEST NO.	CYCLE NO.	$E_U$ (kPa)	$E_R$ (kPa)	$E_o$ (kPa)	$\frac{1}{b_R}$ (kPa)	$\frac{E_U}{E_R}-1$	$P_U$ (kPa)	$P_R$ (kPa)	$n_p$
118	1	344000	82800	10500	3230	3.1495	828	199	0.9981
119	1	359000	75900	10200	2850	3.7297	782	196	1.1229
120	1	786000	110000	37200	30200	6.1509	1575	253	1.0746
121	1	961000	132000	21900	6670	6.2852	1373	349	1.4499
122	1	237000	81200	12300	3250	1.9177	788	99	0.5162
123	1	203000	41800	8500	2650	3.8552	605	93	0.8413
124	1	1010000	127000	32700	9560	6.9385	1478	199	1.0332
125	1	1130000	123000	36700	23000	8.2291	1565	223	1.1393
126	1	--	--	34700	--	--	--	--	--
	2	4640000	866000	34700	2950	4.3632	1505	728	2.3105
	3	842000	370000	34700	6630	1.2762	1330	603	1.0387
	4	832000	341000	34700	5500	1.4410	1355	428	0.7736
	5	713000	109000	34700	--	5.5614	1305	188	0.9696

TEST NO.	CYCLE NO.	$E_U$ (kPa)	$E_R$ (kPa)	$E_o$ (kPa)	$\frac{1}{b_R}$ (kPa)	$\frac{E_U}{E_R}-1$	$P_U$ (kPa)	$P_R$ (kPa)	$n_p$
136	1	97400	38400	5730	1180	1.5319	373	95	0.6766
137	1	53700	17900	3300	630	2.0022	189	45	0.7601
138	1	728000	183000	23600	4980	2.9826	1388	302	0.9051
139	1	478000	67900	19000	7000	6.0406	943	162	1.1061
140	1	166000	44300	7540	2160	2.7380	524	90	0.7461
141	1	112000	32200	4070	1230	2.4636	308	54	0.7135
142	1	1120000	201000	21900	4640	4.5876	1378	257	1.0234
143	1	722000	110000	25800	5860	5.5636	1178	219	1.1183
144	1	159000	166000	5730	283	-0.0467	403	209	-0.0728
	2	69000	27600	5730	2180	1.5032	401	73	0.5386
145	1	174000	114000	5870	449	0.5266	383	199	0.6461
	2	120000	42800	5870	1370	1.8164	381	53	0.5249
146	1	873000	470000	21400	1440	0.8583	1188	629	0.9744
	2	510000	70700	21400	11300	6.2201	1187	74	0.7106

TEST NO.	CYCLE NO.	$E_U$ (kPa)	$E_R$ (kPa)	$E_o$ (kPa)	$\frac{1}{b_R}$ (kPa)	$\frac{E_U}{E_R}-1$	$P_U$ (kPa)	$P_R$ (kPa)	$n_p$
147	1	702000	779000	22900	972	-0.0992	1028	519	-0.1529
	2	276000	51600	22900	20400	4.3441	957	84	0.6872
148	1	77300	41600	6780	794	0.8594	405	133	0.5552
149	1	79500	39400	7180	758	1.0152	424	107	0.5089
150	1	485000	226000	15300	3770	1.1431	1305	365	0.5983
151	1	3640000	186000	90800	--	--	1894	237	1.4304
	2	4770000	199000	90800	--	--	1794	197	2.4809
	3	5850000	152000	90800	--	--	1993	157	1.4356
	4	--	132000	90800	--	--	--	--	--
	5	--	118000	90800	--	--	--	--	--
	6	2390000	106000	90800	--	--	1991	96	1.0248
164	1	44000	26800	3860	630	0.6440	285	78	0.3837
165	1	103000	62500	7620	1380	0.6556	650	188	0.4056
166	1	626000	174000	38400	9770	2.5861	1643	194	0.5991
167	1	572000	99600	16400	7920	4.7411	1385	300	1.1425

TEST NO.	CYCLE NO.	$E_U$ (kPa)	$E_R$ (kPa)	$E_o$ (kPa)	$\frac{1}{b_R}$ (kPa)	$\frac{E_U}{E_R}-1$	$P_U$ (kPa)	$P_R$ (kPa)	$n_p$
168	1	37700	18100	3100	545	1.0889	225	78	0.6911
169	1	73400	45100	5650	1030	0.6269	478	124	0.3607
170	1	1260000	390000	41900	5310	2.2225	1752	296	0.6581
171	1	827000	99100	18800	12100	7.3498	1231	216	1.2178
172	1	33300	16200	2570	468	1.0533	204	85	0.8163
	2	29600	13800	2570	584	1.1423	201	70	0.7223
	3	34200	16800	2570	536	1.0365	199	74	0.7190
	4	37700	20000	2570	475	0.8846	200	73	0.6288
173	1	478000	196000	31300	7650	1.4322	1687	294	0.5082
	2	805000	190000	31300	7960	3.2328	1707	231	0.7214
	3	912000	223000	31300	7880	3.0897	1688	279	0.7824
	4	981000	237000	31300	8360	3.1448	1731	283	0.7851
	5	974000	254000	31300	7920	2.8313	1705	258	0.7106
180	1	19600	9960	2230	308	0.9631	137	39	0.5314
181	1	58300	35400	4910	870	0.6478	442	136	0.4238
182	1	57200	44600	7180	1000	0.2819	477	109	0.1677

TEST NO.	CYCLE NO.	$E_U$ (kPa)	$E_R$ (kPa)	$E_o$ (kPa)	$\frac{1}{b_R}$ (kPa)	$\frac{E_U-1}{E_R}$	$P_U$ (kPa)	$P_R$ (kPa)	$n_p$
183	1	1300000	126000	25200	12200	9.3027	1543	224	1.2086
184	1	19200	11600	2450	273	0.6568	174	92	0.7922
	2	24800	14200	2450	261	0.7525	170	83	0.7825
	3	18700	15200	2450	271	0.2281	166	83	0.2965
	4	22300	13600	2450	294	0.6363	165	83	0.7105
	5	26400	13800	2450	279	0.9045	162	79	0.8971
185	1	35500	27700	4070	672	0.2809	380	130	0.2308
186	1	54800	44500	8510	1100	0.2314	477	121	0.1513
187	1	1370000	129000	26300	14600	9.5622	1573	309	1.4485
	2	1820000	137000	26300	17000	12.2901	1589	317	1.6049
	3	1580000	149000	26300	14100	9.6015	1592	321	1.4744
	4	926000	164000	26300	12500	4.6604	1610	320	1.0729
	5	955000	155000	26300	16600	5.1615	1588	319	1.1329
196	1	724000	201000	23900	7500	2.6061	1854	352	0.7720
197	1	345000	113000	11700	2640	2.0525	944	165	0.6387
198	1	518000	128000	39300	15900	3.0625	1597	249	0.7535

TEST NO.	CYCLE NO.	$E_U$ (kPa)	$E_R$ (kPa)	$E_o$ (kPa)	$\frac{1}{b_R}$ (kPa)	$\frac{E_U}{E_R}-1$	$P_U$ (kPa)	$P_R$ (kPa)	$\eta_p$
199	1	--	--	--	--	--	--	--	--
	2	1030000	108000	20500	7130	8.5455	1844	257	1.1449
200	1	1090000	143000	28800	7950	6.6488	1739	205	0.9505
	2	12000000	2200000	28800	3100	4.4875	1736	908	2.6269
201	1	425000	114000	18400	4540	2.7463	1101	181	0.7304
	2	136000	599000	18400	1340	-0.7726	1079	605	-2.5560
202	1	1100000	209000	41200	10200	4.2528	1668	309	0.9838
	2	1580000	223000	41200	7440	6.0943	1616	278	1.1132
	3	915000	219000	41200	11900	3.1773	1693	317	0.8526
	4	1790000	183000	41200	31400	8.8114	1702	306	1.3308
	5	1220000	250000	41200	9860	3.9093	1691	326	0.9657
	6	1000000	162000	41200	66300	5.1635	1758	269	0.9688



APPENDIX VI. - TEXAS TRIAXIAL TEST DATA



Section No.	Material	$\sigma_3$ psi (kPa)	Modulus $E_T$ psi (kPa)	$(\sigma_1 - \sigma_3)_f$ psi	$\frac{1}{3}(\sigma_1 + 2\sigma_3)$ psi	$\epsilon_f$
1	Iron Ore	0 ( 0 )	1884 (12990)	37.30	84.9	0.0198
		5 ( 34.47)	2381 (16410)	61.68	174.9	0.02591
		10 ( 68.94)	2761 (19030)	91.40	277.0	0.03311
		15 (103.41)	3728 (25690)	115.44	366.2	0.03096
		20 (137.89)	4018 (27690)	144.04	465.8	0.03585
2	Sand & Shell	0 ( 0 )	1546 (10660)	50.10	114.0	0.0324
		3 ( 20.68)	3358 (23140)	100.08	248.5	0.0298
		10 ( 68.94)	3625 (24980)	162.42	438.7	0.0448
		15 (103.41)	3427 (23620)	187.12	529.4	0.0546
		20 (137.89)	5123 (35310)	223.36	646.4	0.0436
	Select sand	0 ( 0 )	1378 ( 9500)	35.28	80.3	0.0256
		0 ( 0 )	1165 ( 8030)	31.00	70.6	0.0266
		3 ( 20.68)	1520 (10480)	48.02	130.0	0.0316
		5 ( 34.47)	1766 (12170)	53.34	155.9	0.0302
		10 ( 68.94)	2698 (18600)	82.30	256.3	0.0305
		15 (103.41)	2814 (19400)	98.78	328.3	0.0351
		20 (137.89)	3614 (24910)	118.52	407.7	0.0328

Section No.	Material	$\sigma_3$ psi (kPa)	Modulus $E_T$ psi (kPa)	$(\sigma_1 - \sigma_3)_f$ psi	$\frac{1}{3}(\sigma_1 + 2\sigma_3)$ psi	$\epsilon_f$
2	Clay Subgrade	0 ( 0 )	616 ( 4250)	15.60	35.5	0.0253
		0 ( 0 )	546 ( 3760)	14.46	32.9	0.0265
		3 ( 20.68)	608 ( 4190)	16.80	58.9	0.0276
		5 ( 34.47)	658 ( 4540)	23.18	87.2	0.0352
		10 ( 68.94)	732 ( 5050)	31.46	140.6	0.0430
		15 (103.41)	694 ( 4780)	37.30)	188.4	0.0538
		20 (137.89)	800 ( 5510)	44.36	238.9	0.0554
3	Sand & Shell	0 ( 0 )	2859 (19710)	68.90	156.8	0.0241
		0 ( 0 )	2252 (15520)	62.82	143.0	0.0279
		3 ( 20.68)	4004 (27600)	101.70	252.2	0.0254
		5 ( 34.47)	2938 (20250)	119.60	306.7	0.0407
		10 ( 68.94)	3659 (25220)	162.82	439.6	0.0445
		20 (137.89)	4434 (30560)	225.70	651.7	0.0509
		Select Sand	0 ( 0 )	355 ( 2450)	6.60	15.0
	3 ( 20.68)		497 ( 3430)	9.84	43.1	0.0198
	5 ( 34.47)		534 ( 3680)	13.28	64.7	0.0249
	10 ( 68.94)		604 ( 4650)	19.36	113.0	0.0287
	15 (103.41)		699 ( 4820)	25.16	160.7	0.0360
	20 (137.89)		856 ( 5900)	30.92	208.3	0.0361

Section No.	Material	$\sigma_3$ psi (kPa)	Modulus $E_T$ psi (kPa)	$(\sigma_1 - \sigma_3)_f$ psi	$\frac{1}{3}(\sigma_{1f} + 2\sigma_3)$ psi	$\epsilon_f$
3	Clay Subgrade	0 ( 0 )	1824 (12570)	34.10	77.6	0.0187
		0 ( 0 )	1788 (12320)	31.10	70.8	0.0174
		3 ( 20.68)	2826 (19480)	52.86	141.0	0.0187
		5 ( 34.47)	2620 (18060)	65.50	183.6	0.0250
		10 ( 68.94)	3455 (23810)	91.90	278.2	0.0266
		15 (103.41)	4805 (33120)	114.36	363.8	0.0238
		20 (134.89)	4628 (31900)	138.84	454.0	0.0300
7	Crushed Sandstone	0 ( 0 )	16004(110310)	140.84	329.7	0.0088
		5 ( 20.68)	25742(177420)	257.42	620.5	0.0100
		10 ( 34.47)	30072(207270)	264.64	671.4	0.0088
		15 (103.41)	26034(179440)	294.18	773.1	0.0113
		20 (134.89)	29361(202370)	331.78	893.2	0.0113
	Select Sand	0 ( 0 )	1344 ( 9260)	16.26	37.0	0.0121
		5 ( 20.68)	2060 (14200)	38.32	121.7	0.0186
		10 ( 34.47)	2528 (17420)	62.18	210.5	0.0246
		15 (103.41)	1867 (12870)	84.02	294.7	0.0450
		20 (134.89)	2614 (18020)	115.28	400.4	0.0441

Section No.	Material	$\sigma_3$ psi (kPa)	Modulus $E_T$ psi (kPa)	$(\sigma_1 - \sigma_3)_f$ psi	$\frac{1}{3}(\sigma_1 + \sigma_3)$ psi	$\epsilon_f$
7	Clayey Sand	5 ( 34.47)	512 ( 3530)	32.54	110.4	0.0635
		10 ( 68.94)	1568 (10810)	39.84	159.7	0.0254
	Subgrade	15 (103.41)	1508 (10390)	45.98	208.1	0.0305
		20 (134.89)	1213 ( 8360)	52.40	257.2	0.0432
9	Limestone Base	0 ( 0 )	1844 (12710)	23.78	54.1	0.0129
		3 ( 20.68)	1838 (12670)	68.54	176.7	0.0373
		5 ( 34.47)	1812 (12490)	96.22	253.5	0.0531
		10 ( 68.94)	1746 (12030)	138.12	383.4	0.0791
		15 (103.41)	1850 (12750)	184.02	522.4	0.0995
		20 (134.89)	1658 (11430)	194.52	580.7	0.1173

Section No.	Material	$\sigma_3$ psi (kPa)	Modulus $E_T$ psi (kPa)	$(\sigma_1 - \sigma_3)_f$ psi	$\frac{1}{3}(\sigma_{1f} + 2\sigma_3)$ psi	$\epsilon_f$
11	Iron Ore	0 ( 0 )	10291( 70930)	103.94	236.6	0.0101
		5 ( 34.47)	7759( 53480)	136.56	345.3	0.0176
		10 ( 68.94)	9817( 67660)	172.78	462.0	0.0176
		15 (103.41)	11736( 80890)	206.56	573.7	0.0176
	Select Sand	0 ( 0 )	705 ( 5000)	23.78	54.1	0.0328
		5 ( 34.47)	883 ( 6090)	45.84	138.8	0.0519
		10 ( 68.94)	954 ( 6580)	50.38	183.7	0.0528
		15 (103.41)	1222 ( 8420)	82.58	291.4	0.0676
	Sandy Clay	0 ( 0 )	392 ( 2700)	24.68	56.2	0.063
		15 (103.41)	890 ( 6130)	47.42	211.4	0.0533
		20 (137.89)	1114 ( 7680)	52.14	256.6	0.0468

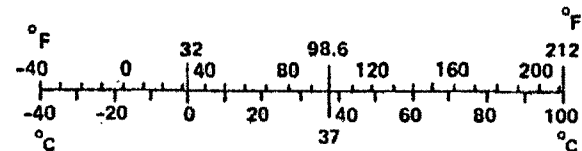
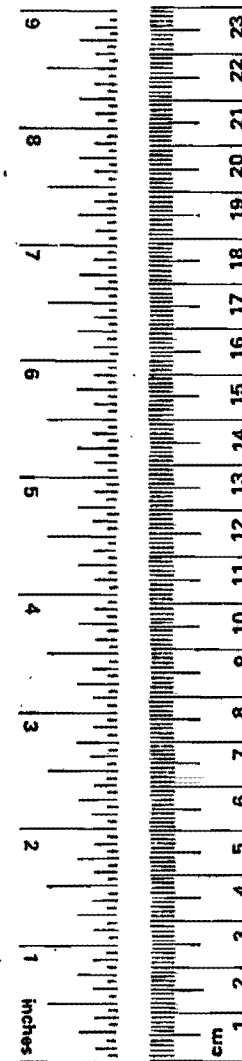
## METRIC CONVERSION FACTORS

### Approximate Conversions to Metric Measures

Symbol	When You Know	Multiply by	To Find	Symbol
<b>LENGTH</b>				
in	inches	*2.5	centimeters	cm
ft	feet	30	centimeters	cm
yd	yards	0.9	meters	m
mi	miles	1.6	kilometers	km
<b>AREA</b>				
in <sup>2</sup>	square inches	6.5	square centimeters	cm <sup>2</sup>
ft <sup>2</sup>	square feet	0.09	square meters	m <sup>2</sup>
yd <sup>2</sup>	square yards	0.8	square meters	m <sup>2</sup>
mi <sup>2</sup>	square miles	2.6	square kilometers	km <sup>2</sup>
	acres	0.4	hectares	ha
<b>MASS (weight)</b>				
oz	ounces	28	grams	g
lb	pounds	0.45	kilograms	kg
	short tons (2000 lb)	0.9	tonnes	t
<b>VOLUME</b>				
tsp	teaspoons	5	milliliters	ml
Tbsp	tablespoons	15	milliliters	ml
fl oz	fluid ounces	30	milliliters	ml
c	cups	0.24	liters	l
pt	pints	0.47	liters	l
qt	quarts	0.95	liters	l
gal	gallons	3.8	liters	l
ft <sup>3</sup>	cubic feet	0.03	cubic meters	m <sup>3</sup>
yd <sup>3</sup>	cubic yards	0.76	cubic meters	m <sup>3</sup>
<b>TEMPERATURE (exact)</b>				
°F	Fahrenheit temperature	5/9 (after subtracting 32)	Celsius temperature	°C

### Approximate Conversions from Metric Measures

Symbol	When You Know	Multiply by	To Find	Symbol
<b>LENGTH</b>				
mm	millimeters	0.04	inches	in
cm	centimeters	0.4	inches	in
m	meters	3.3	feet	ft
m	meters	1.1	yards	yd
km	kilometers	0.6	miles	mi
<b>AREA</b>				
cm <sup>2</sup>	square centimeters	0.16	square inches	in <sup>2</sup>
m <sup>2</sup>	square meters	1.2	square yards	yd <sup>2</sup>
km <sup>2</sup>	square kilometers	0.4	square miles	mi <sup>2</sup>
ha	hectares (10,000 m <sup>2</sup> )	2.5	acres	
<b>MASS (weight)</b>				
g	grams	0.035	ounces	oz
kg	kilograms	2.2	pounds	lb
t	tonnes (1000 kg)	1.1	short tons	
<b>VOLUME</b>				
ml	milliliters	0.03	fluid ounces	fl oz
l	liters	2.1	pints	pt
l	liters	1.06	quarts	qt
l	liters	0.26	gallons	gal
m <sup>3</sup>	cubic meters	35	cubic feet	ft <sup>3</sup>
m <sup>3</sup>	cubic meters	1.3	cubic yards	yd <sup>3</sup>
<b>TEMPERATURE (exact)</b>				
°C	Celsius temperature	9/5 (then add 32)	Fahrenheit temperature	°F



\* 1 in = 2.54 (exactly). For other exact conversions and more detailed tables, see NBS Misc. Publ. 286, Units of Weights and Measures, Price \$2.25, SD Catalog No. C13.10:286.